Development of polyaspartic coating with improved adhesion on metallic surfaces by using nanosilica

Assarian, Arezoo

University of Zagreb

FACULTY OF CHEMICAL ENGINEERING AND TECHNOLOGY

Arezoo Assarian

DEVELOPMENT OF POLYASPARTIC COATING WITH IMPROVED ADHESION ON METALLIC SURFACES BY USING NANOSILICA

DOCTORAL THESIS

Zagreb, 2019

Sveučilište u Zagrebu

FAKULTET KEMIJSKOG INŽENJERSTVA I TEHNOLOGIJE

Arezoo Assarian

RAZVOJ POLIASPARTATNOG PREMAZA S POBOLJŠANOM PRIONJIVOŠĆU UPORABOM NANOČESTICA SILICIJEVA DIOKSIDA

DOKTORSKI RAD

Zagreb, 2019.

University of Zagreb

FACULTY OF CHEMICAL ENGINEERING AND TECHNOLOGY

Arezoo Assarian

DEVELOPMENT OF POLYASPARTIC COATING WITH IMPROVED ADHESION ON METALLIC SURFACES BY USING NANOSILICA

DOCTORAL THESIS

Supervisor:
Prof. Sanja Martinez, Ph.D.

Zagreb, 2019

Sveučilište u Zagrebu

FAKULTET KEMIJSKOG INŽENJERSTVA I TEHNOLOGIJE

Arezoo Assarian

RAZVOJ POLIASPARTATNOG PREMAZA S POBOLJŠANOM PRIONJIVOŠĆU UPORABOM NANOČESTICA SILICIJEVA DIOKSIDA

DOKTORSKI RAD

Mentor:
Prof. dr. sc. Sanja Martinez

Zagreb, 2019.

Bibliographic facts:

- UDK: 620.197.6:549.514.5(043.3)=111
- Znanstveno područje: tehničke znanosti
- Znanstveno polje: temeljne tehničke znanosti
- Znanstvena grana: materijali
- Institution: Sveučilište u Zagrebu, Fakultet kemijskog inženjerstva i tehnologije, Zavod za elektrokemiju
- Voditelj rada: prof. dr. sc. Sanja Martinez
- Broj stranica: 99
- Broj slika: 70
- Broj tablica: 18
- Broj priloga: 0
- Broj literaturnih referenci: 159
- Datum obrane: 20.03.2019.

- Sastav povjerenstva za obranu:

1. Prof. dr. sc. Mirela Leskovac, Fakultet kemijskog inženjerstva i tehnologije Sveučilišta u Zagrebu
2. Prof. dr. sc. Emi Govorčin Bajsić, Fakultet kemijskog inženjerstva i tehnologije Sveučilišta u Zagrebu
3. Prof. dr. sc. Vesna Alar, Fakultet strojarstva i brodogradnje Sveučilišta u Zagrebu

- Rad je pohranjen u:
    1. Nacionalnoj i sveučilišnoj knjižnici u Zagrebu, Hrvatske bratske zajednice bb;
    2. Knjižnici Fakulteta kemijskog inženjerstva i tehnologije Sveučilišta u Zagrebu, Marulićev trg 20;
    3. Knjižnici Sveučilišta u Rijeci, Dolac 1
    4. Knjižnici Sveučilišta u Splitu, Livanjska 5 i
    5. Knjižnici Sveučilišta u Osijeku, Europska avenija 24.

Tema rada prihvaćena je na 180. sjednici Fakultetskog vijeća Fakulteta kemijskog inženjerstva i tehnologije u Zagrebu, održanoj dana 28. studenoga 2016., te odobrena na sjednici Senata Sveučilišta u Zagrebu 17. siječnja 2017.

Acknowledgements

I wish to express my appreciation to the following people for their help, support and guidance to make this work and to fulfill my wishes to use my knowledge and valuable experience for the better world.

Prof. Sanja Martinez, Ph.D. for the effective supervision of my career and this work, for the numerous helpful discussions in the last six years, and for giving me the opportunity to perform the research.

Prof. Marko Rogošić, Ph.D. for his extensive help and critics during this work.

Prof. Emi Govorčin Bajsić, Ph.D. and prof. Mirela Leskovac, Ph.D. for great cooperation on the analytical methods.

Many thanks to Mrs. Elizabeta Šlezak for the help and kindness.

Marina Mrđa Lalić, dipl. kem. ing., Denis Sačer, mag. ing. cheming. and Marija Lukić, mag. ing. cheming., who helped me in many ways for the success of this research.

Thanks to all the professors, staff and my classmates at the Faculty of Chemical Engineering and Technology of the University of Zagreb.

My friends Marina Čengić, Ivan Dabro, Radovan Karabaić, Jana Ivandić, Aida and Monem for their support.

The people at the Brodarski Institute for their cooperation, Mrs. Nevenka Bodulijak, representative of BYK company, Mr. Srba Tasić and Mr. Predrag Knežević from Covestro Company for their help and advice during this research.

My mother Fatemeh and my father Mohammad Mehdi, my sister Azadeh and my brother Amir for love and support.

Last but not least, my husband Motalleb and my son Kasra for love, support, understanding and always being there for me. I love you.

Abstract

The aim of this thesis was to investigate and develop polyaspartic coatings with nanosilica fillers modified with amino groups (NH_2-) in order to enhance adhesion of coating on metallic surfaces and increase the productivity of the protective coating.

The idea was to develop polyaspartic coating formulations for applying directly to metal surfaces (DTM). For this purpose, seven samples of polyaspartic coatings with different amounts of nanosilica filler of 20–30 nm in size were prepared. The coatings were applied on 2 mm thick low carbon steel panels prepared according to surface preparation standard Sa 2.5. The samples were characterized by mechanical testing with respect to hardness, adhesion, bending and impact resistance. The results showed that only 2% of the nanosilica per total mass of formulation improved adhesion of the coating to the surface of the substrate and that it was possible to apply the coating directly to the metal surface. Also, nanosilica filler changed the functionality of other particles or fillers, increased hydrophobic and oleophobic coating characteristics, altered rheology and thixotropy properties of coatings.

After finalizing the formulation, degradation of coatings was analyzed by the electrochemical impedance spectroscopy (EIS), scanning electron microscopy (SEM) and Fourier-transform infrared spectroscopy (FTIR) methods as well as by exposure of applied coatings to salty atmosphere in a salt spray chamber.

No agglomeration and excellent compatibility of nanoparticles with other components in the formulation was observed. The main advantages of the modified polyaspartic coating were fast curing, fast drying time, excellent mechanical and chemical resistance and high film build which made it possible to reduce the number of coats in a coating system. The polyaspartic coating system with improved coating adhesion increased the durability of coating system and reduced volatile organic compounds (VOC) emissions and overall cost of the coating application process.

Keywords: *polyaspartic coatings, nanosilica fillers, adhesion, corrosion, protective coatings*

Sažetak

Cilj ove disertacije bio je istražiti i razviti poliaspartatne premaze s punilima na osnovi nanočestica silicijeva dioksida modificiranih amino-skupinama (NH_2-) kako bi se poboljšala adhezija premaza na metalnim površinama i povećala produktivnost zaštitnog premaza.

Ideja je bila razviti formulacije poliaspartatnih premaza za izravno nanošenje na metalne površine (DTM, engl. *directly to metal*). S tom je svrhom pripremljeno sedam uzoraka poliaspartatnog premaza s različitim udjelima nanočestica SiO_2 dimenzija od 20 do 30 nm kao punila. Premazi su naneseni na ploče od niskougljičnog čelika debljine 2 mm uz pripremu površine prema standardu Sa 2.5. Uzorci su karakterizirani mehaničkim testovima s obzirom na tvrdoću, adheziju, savijanje i otpornost na udar. Rezultati su pokazali da samo 2 % nanočestica SiO_2 po ukupnoj masi formulacije poboljšava adheziju premaza na površinu supstrata i da je moguće nanošenje premaza izravno na metalnu površinu. Također, nanočestice SiO_2 mijenjaju funkcionalnost ostalih čestica ili punila, povećavaju hidrofobna i oleofobna svojstva premaza, mijenjaju njena reološka i tiksotropna svojstva.

Nakon finaliziranja formulacije, degradacija premaza analizirala se metodama elektrokemijske impedancijske spektroskopije (EIS), pretražne (engl. *scanning*) elektronske mikroskopije (SEM) i infracrvene (engl. *infrared*) spektroskopije s Fourierovom transformacijom signala (FTIR), kao i izlaganjem primijenjenih premaza atmosferi u slanoj komori.

Uočeno je da nema aglomeracije nanočestica te je utvrđena njihova izvrsna kompatibilnost s ostalim komponentama u formulaciji. Glavne prednosti modificiranog poliaspartatnog premaza bile su brzo očvršćivanje, brzo sušenje, izvrsna mehanička i kemijska otpornost i velika debljina mokroga premaza što omogućava smanjenje broja premaza u zaštitnom sustavu. Sustav poliaspartatnog premaza s poboljšanim prianjanjem povećava trajnost zaštitnog premaza i snižava emisiju hlapivih organskih spojeva i ukupni trošak procesa nanošenja premaza.

Ključne riječi: poliaspartatni premazi, čestice nanopunila, adhezija, korozija, zaštitni premazi

Contents

List of Tables:

List of Figures:

1. INTRODUCTION

Color is one of the most beautiful phenomena of nature. Almost meaningless and boring the world would be without colors. Colors, as applied to materials in the form of paints and coatings give them nice, eye-pleasing look. Nevertheless, coatings have other important roles in the world that surrounds us. One of these important roles is in the creation of protective films on surfaces of materials, in order to protect them against the corrosive and aggressive environment.

The history of paints dates back to about 40,000 years ago, when cave dwellers started painting the walls of caves to mark and decorate their habitats [1-3]. Nowadays the paint is everywhere, from skyscrapers to microchips. The effect of paints in our life is very important as they serve not only as a decoration but also as a protection of different surfaces made of metal, plastic, wood, construction materials, textiles, leather and glass.

The term coating is used primarily in industries, although it is more general and encompasses the paints, lacquers, varnishes, etc. The term paint is primarily used in architecture and households to cover the approximate meaning of the term coating as used in industries [2].

Paints and coatings are among the significant materials common to different industries. Today, many kinds of paints and coatings are used with different advantages including their low mass, chemical stability and resistance to different atmospheric conditions. Once applied on a substrate, they allow the retention and improvement of bulk properties of a material, protecting it against the environmental exposure.

Components of the environment, water and oxygen for example, can diffuse through the coating, often via microcracks, and may cause material damage, mechanical degradation or delamination of the coating. When a painted surface is damaged by mechanical and/or chemical agents, not only the beauty of the surface disappears, but its acoustical, electrical and thermal properties are also altered at the microscopic level. Damage caused by penetration of dust particles, moisture, grease and contamination into the coating layers affects the rate of corrosion on material surfaces by increasing it, which naturally leads to the failure of structures.

The repair and maintenance of damaged painted surfaces of industrial or architectural constructions is one of the largest and most expensive issues, especially when damage occurs on such a small scale as micro-cracks. Repairing damaged painted surfaces always requires time, manpower and is often associated with high costs. Therefore, ideal repair measures should be quick and effective, and applied directly on the damaged site, thus eliminating the need for

removing the damaged component [4].

One of the important roles of a coating is to protect surfaces against chemical and mechanical damage. Metal surfaces are extremely important to protect because of corrosion. Corrosion is the deterioration of metals as a consequence of (primarily) the (chemical) reaction between the metal and the environment [5].

There are some important methods of corrosion control which include suitable selection of material, application of coatings, use of inhibitors, cathodic protection… [6] Among the mentioned methods, the application of coatings is quite common and very practical, but it is difficult to select a suitable protective coating for each particular metal surface. A protective coating is one of the solutions to increase the lifetime of surfaces. There are many solutions to improve or increase the productivity of materials but applying a suitable protective coating is efficient in comparison to other solutions [6].

A coating is a complex system. Main components of common coating formulations are shown in figure 1. The type of coating is determined primarily by the type of the resin and so are the many properties of the coating [7].

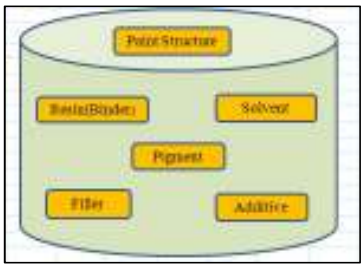

Figure 1: The main components of coating formulation

Based on the binder type, protective coatings can be divided into two wide groups: metallic and nonmetallic (inorganic and organic) coatings. Based on the application, paints and coatings can be divided into automotive paints, decorative paints and industrial paints (protective coatings).

A serious concern in the field of paints and coatings lies the fact that the product life can very often exceed the coating life, and all coatings manufacturers are trying to extend the lifetime of their coatings. From the preparation of surfaces to the application of coatings, there are many factors which are very important and involved in the improvement of the lifetime of coatings.

Some of the problems which may decrease the lifetime of coatings are listed below [8]:

- There is a lack of adhesion between the surfaces and coating films
- There is a low resistance of coating films against exposure to sunlight

- There is a weak stability of many coating films in humid, corrosive and abrasive environments
- There are difficulties in preparation of stable coating films in case of two-component coatings, multi-layered coatings and the lack of control during the application process which leads to non-uniform and inhomogeneous coating films [9]
- There are difficulties in production of environmentally friendly coatings with high-performance properties, because many of the coating properties are improved significantly using organic and inorganic components which are hazardous and harmful for the environment
- The application of coatings is in many cases associated with extensive use of energy, manpower and money
- There is a need for the regular maintenance and re-application of coatings onto surfaces because of the polymer aging
- There is a lack of customer satisfaction related to quality, stability, performance and overall cost of coatings

As shown in figure 2, China had the largest share of the world coating production in 2014. About 45% of the coatings produced around the world are used and applied in decoration and protection of new constructions as well as in maintenance of existing constructions, including residential places, public buildings, and industries. A large share of the coatings is used for decoration and/or protection of industrial products.

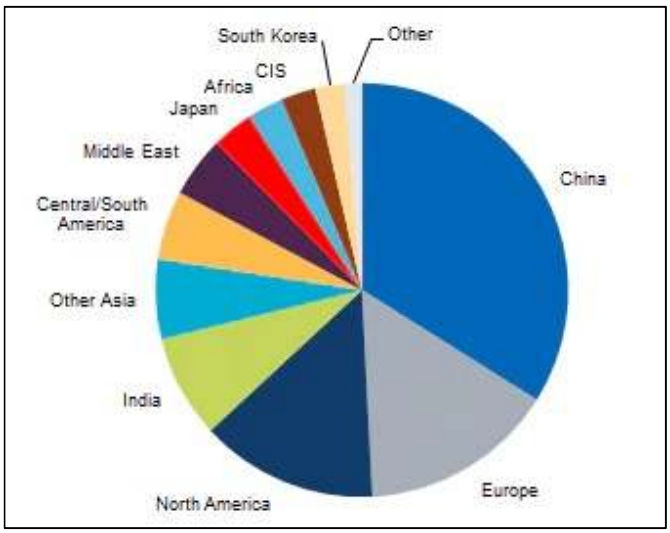

Figure 2: World production of paints and coatings in 2014 [10]

Without coatings, product lifetimes would decrease extremely. A large group of coatings is commonly applied on site and in ambient conditions [10], such as road marking coatings (traffic paints), refinishing of vehicles, heavy duty and industrial equipment, shipbuilding and vessels. Those coatings have to be designed to withstand the harsh environment.

The important ingredients of solvent-borne paints and coatings are solvents, resins, pigments, fillers, and additives. The so-called vehicle is the major part of paint and coating formulations; it is a combination of the accurate amounts of resin (binder) and solvent. The other components such as pigments, fillers and additives are dispersed in the vehicle [11]. The amount of each component is different and related to the type of paint and its application but generally, the amounts of solvent for solvent-borne paints are approximately 60% including toluene, xylene, methyl ethyl ketone (MEK) and methyl isobutyl ketone (MIBK). Resin amounts are up to 30%, pigments or fillers contribute to 7 to 8%, and additives to 2 to 3%. The important subjects of environmental concern are about organic solvents and heavy metals which are used in the pigments. Resins and other additives may affect the toxicity of the paints and coatings, too.

Figure 3 shows the process of coating from the preparation of a surface to the application of the coating up to the final inspection of the coating. y

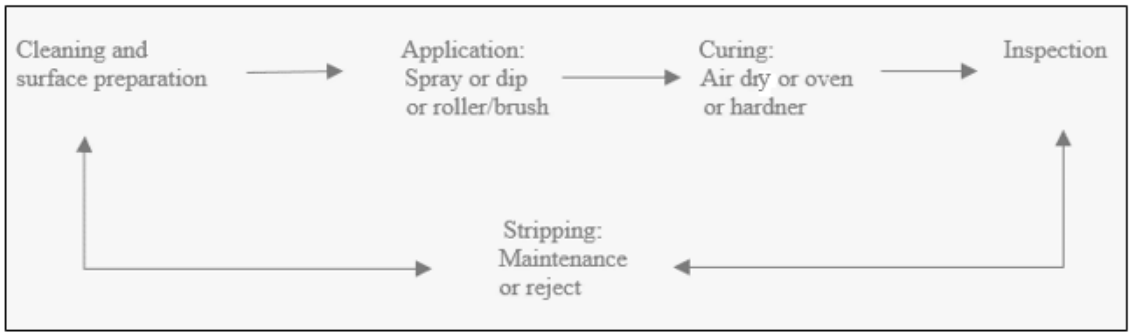

Figure 3: Coating process

Total demand for coatings will increase from 2014 to 2019 at the average annual rates of 3% in the United States and 1.5–2.5% in Western Europe. In Japan, the demand for paints and coatings will grow relatively slowly at the annual rate of 0.5%. Total consumption of paints and coatings worldwide will increase at the rate of about 6% per year. The fastest growths are expected in Asia Pacific (5%), Eastern Europe (6%), and Latin America (8%); the expected annual growth rates are 8% in China, 11% in India and 4–5% in Indonesia [10].

The global industry of coatings moves forward to environmentally friendly technologies. Figure 4 shows recent yearly consumption of coatings by technology.

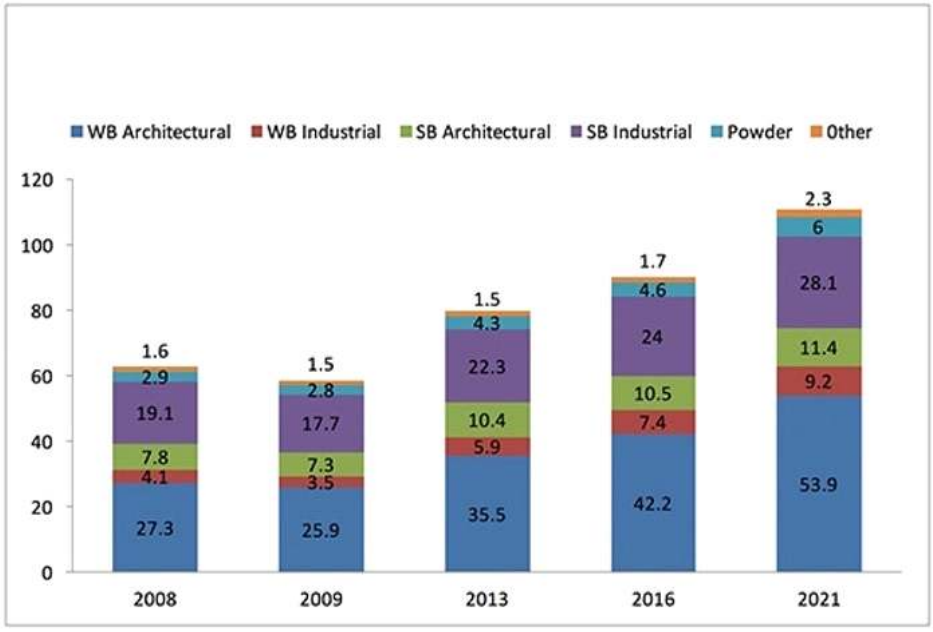

Figure 4: Annual consumption of coatings by technology, in billion dry Lb. [12].

WB and SB stand for water-borne and solvent-borne coatings

One of the new subjects interesting for paints and coatings manufacturers as well as for the consumers is nanotechnology, with many types of research and patents issued in the field of paints and coatings. The new technology has created opportunity to change or modify or improve many specific properties such as scratch resistance, hardness, flexibility, bending, wear, corrosion and UV resistance with adding very small particles of ceramic or metallic materials [13].

The new technology is usually slowly diffusing to major applications because of the high costs. It is difficult and costly to reduce the size of particles to nanodimensions. Moreover, special additives are required to improve film build properties and special dispersing agents and surface modifiers are needed to prevent the coating structure of agglomerating. In the following years, air pollution legislation will remain to be a driving force behind the admission of new coating technologies [14].

Coatings applied to the material serves as an interface to protect surfaces from any deterioration which is caused by environmental conditions [15]. Recently, paint and coating technologies are improved in order to suit the individual purposes. Here again, the use of nanocoatings is gradually paving its way towards applications.

A characteristic feature of nanocoatings is the dimension of dispersed particles which is in the range of nanometers. Nanocoatings may provide better protection of surfaces and in some cases

they may be classified as multipurpose materials. They have the ability to contribute simultaneously to different properties, e.g. unlike the conventional coatings, they can provide better mechanical and chemical resistance at the same time [16].

Nanoparticle fillers for nanocoatings are manufactured by two main classes of methods: vapor phase methods and liquid phase methods. Vapor phase methods include plasma arc, laser ablation, chemical vapor deposition, flame synthesis processes, and vapor condensation, whereas liquid phase methods include sol-gel, electrolysis, precipitation, hydrothermal processes, and microemulsion processes. Nanocoatings are expected to meet higher demand in industrial segments because of high range of erosion and corrosion problems occurring in harsh industrial environments [17].

The polyaspartic coating is a solvent-based protective coating with distinct and improved properties contributed by the nanoadditives. Prior to the research described here, all the information about conventional solvent-based protective coatings was collected, in particular with respect to the main problems found in their application as well as in their durability.

Polyaspartic coatings are a new generation of protective coatings for protecting metal surfaces against many defects including corrosion, mechanicals and chemicals damage and weathering problems. Importantly, they may be formulated in a way that allow for their direct application on metal surfaces. However, they may suffer from poor adhesion onto substrates. In order to eliminate this problem, nanosilica particles were investigated as potential filler, with an aim to improve the adhesion as well as rheology and thixotropy parameters. On the other hand, nanosilica is an excellent additive that can alter the functionality of other particles or fillers and it can increase hydrophobic or oleophobic coating characteristics.

The aim of this research was to produce a polyaspartic coating with excellent adhesion by using nanosilica in the formulation.

The degradation of prepared polyaspartic coatings was analyzed by the method of electrochemical impedance spectroscopy (EIS) and by the complementary methods of coating analysis – scanning electron microscopy (SEM) and Fourier-transform infrared spectroscopy (FTIR). The exposure in a salt spray chamber was used as well. Mechanical testing methods such as hardness test, adhesion, bending and impact testing provided the additional parameters to be included in the assessment of new coatings.

The expected main advantages of the modified polyaspartic coating were the fast curing, fast drying, excellent mechanical and chemical resistance, as well as the high film build which may

reduce the number of coats in a coating system. The polyaspartic coating system with improved coating adhesion might increase the durability of coating system and reduce the overall costs of the coating process.

The other aim of the research was to increase the productivity of coatings along with decreasing emission of the volatile organic compounds from the coating formulation.

2. THEORETICAL BACKGROUND

2.1. The electrochemistry of corrosion

The surfaces of all metals in contact with the air are protected by oxide films (gold is an exception). When such a metal is immersed in an aqueous solution, the oxide film tends to dissolve. If the solution is acidic, the oxide film may dissolve completely, leaving bare metal surface, free of any contaminants.

When a clean metal surface without oxide layer is exposed to the solution, positively charged metal ions tend to migrate from the metal into the solution [18].

$$\mathrm{M} \rightarrow \mathrm{M}^{n+} + n\mathrm{e}^{-} . \tag{1}$$

The accumulation of negative charge on the metal surface due to remaining electrons leads to a potential difference between the metal surface and the solution. This potential difference is known as the electrode potential or the metal potential.

A prolonged dissolution and deposition of metal ions would result in the metal obtaining a stable potential as soon as the rate of dissolution becomes equal to the rate of deposition:

$$\mathrm{M}^{n+} + n\mathrm{e}^{-} \rightarrow \mathrm{M} . \tag{2}$$

This potential is called the reversible potential, E_r, and its value is related to the concentration of dissolved metal ions and $E°$ which is the standard reversible potential for the unit activity of dissolved metal ions, $a_{M^{n+}}$, [18], i.e.:

$$E_{\mathrm{r},\mathrm{M}^{n+}/\mathrm{M}} = E^{\mathrm{o}}_{\mathrm{M}^{n+}/\mathrm{M}} + RT/nF \ln a_{\mathrm{M}^{n+}} , \tag{3}$$

where R is the gas constant, F is the Faraday constant, T is the absolute temperature, a is the activity of dissolved ions and n is the number of electrons transferred per ion. Once the potential has reached the reversible potential, no additional dissolution of metal occurs. The amount of metal which dissolves via this process is normally very low.

The reversible potential is generally not reached by contacting metal and solution. Rather it becomes more positive due to the fact that electrons can be removed from the metal by a number of alternative reactions. In acidic solutions, electrons can react with hydrogen ions adsorbed on the metal surface producing the hydrogen gas [18, 19].

$$2\mathrm{H}^{+} + 2\mathrm{e}^{-} \rightarrow \mathrm{H}_2 . \tag{4}$$

The appearance of reaction (4) allows for the continued process of transferring metal ions into solution, i.e. to corrosion of the metal. Reaction (4) is reversible as well and has a reversible potential given by:

$$E_{\mathrm{r,H^+/H_2}} = E^{\mathrm{o}}_{\mathrm{H^+/H_2}} + RT/F \ln\left(\frac{p^{\mathrm{l/2}}_{\mathrm{H_2}}}{p^{\mathrm{ol/2}} a_{\mathrm{H^+}}}\right), \tag{5}$$

Where p_{H2} is the partial pressure of hydrogen gas and $p°$ is the standard pressure, commonly set to 1 bar. If the partial pressure of hydrogen is allowed to build up, the reversible potential of reaction (4) could occur. The situation of equilibrated reaction (4) might arise with no further evolution of hydrogen gas and the net dissolution of metal ions would eventually cease. Typically, hydrogen outflows from the system, the potential remains more negative than the reversible one and the corrosion goes on.

The concentration of hydrogen ions in neutral solutions is too low to allow for reaction (4) to take place at a significant rate. However, the electrons may react with oxygen molecules, which are coming from the air, dissolve in the solution and then adsorb on the metal surface, thus producing hydroxyl ions.

$$\mathrm{O_2 + 2H_2O + 4e^- \rightarrow 4OH^-}. \tag{6}$$

The potential of the metal stays again more negative than the reversible potential for reaction (6)

$$E_{\mathrm{r,O_2/OH^-}} = E^{\mathrm{o}}_{\mathrm{O_2/OH^-}} - RT/4F \ln\left(\frac{p^{\mathrm{o}} a^4_{\mathrm{OH^-}}}{p_{\mathrm{O_2}}}\right), \tag{7}$$

For this reason, corrosion can proceed through the coupling of reactions (1) and (6).

In electrochemical language, an electrode at which an oxidation reaction happens is termed an anode. The procedure of oxidation involves electrons leaving the reacting species, as in the metal dissolution reaction (1). As a result, the local area of a corroding metal where its dissolution occurs is the anode and metal dissolution is the anodic reaction of corrosion.

The term cathode is used for an electrode at which a reduction reaction takes place. Reduction involves a gain of electrons, as is the case for reactions (4) and (6). The reduction of hydrogen ions and oxygen are accordingly the cathodic reactions of corrosion and the local area of a corroding metal where those reactions happen is the cathode [19].

2.2. 1 Cathodic reactions

Within the cathodic reduction process, hydrogen ions or oxygen molecules need to be adsorbed on the metal surface. The hydrogen ions or oxygen molecules must be transported from the bulk of solution to the metal/solution interface. This transport takes place by the processes of diffusion and convection. Because the potential of the metal may be kept at values more negative that the equilibrium one (negative overpotential region of the Tafel plot), the rate of reduction of hydrogen ions and oxygen molecules may exceed the rate at which these species may be transported to the metal surface. Then the rate of transport of the species to be reduced controls the rate of reduction reactions:

$$2H^+(aq) + 2e^- \rightarrow H_2(g), \tag{8}$$

$$O_2(g) + 2H_2O + 4e^- \rightarrow 4OH^-(aq). \tag{9}$$

The process is illustrated in Figure 5 [20].

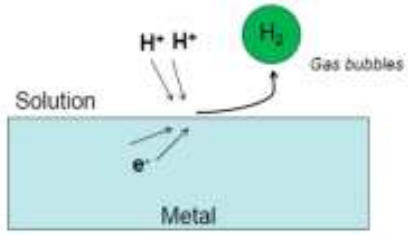

Figure 5: Cathodic reaction – evolution of hydrogen gas

2.2.1. Anodic reactions

On anodic polarization of a metal (positive overpotential region in the Tafel plot), the cathodic polarization curves for reduction of hydrogen ions or oxygen molecules do not change greatly for different metals. The reversible potentials for those reactions will not change, however, the exchange currents and the Tafel slopes of the polarization curves can differ considerably.

The corrosion process is present everywhere and known to everyone. It is widely understood that the corrosion process converts bare metal into a less-valued material which eventually may result in a critical failure of a component or system. The rust which forms on the surface of steel is the common consequence of the corrosion [20].

The major component of steel, iron (Fe) at the surface of an element undergoes a number of transformations. Firstly, the iron atom can lose some electrons and become a positively charged

ion:

$$\mathrm{Fe} \rightarrow \mathrm{Fe}^{n+} + n\mathrm{e}^{-} \quad (10)$$

This positively charged ion may bind to different elements or groups of atoms which can be negatively charged. The other half-reaction of conversion of steel immersed in water into rust involves water and dissolved oxygen and is described by Equation (9). By summing the two half-reactions the equation for the oxidation of iron is formed:

$$2\mathrm{Fe} + \mathrm{O}_2 + 2\mathrm{H}_2\mathrm{O} \rightarrow 2\mathrm{Fe}(\mathrm{OH})_2 \quad (11)$$

Oxygen dissolves quite easily in water and reacts with iron hydroxide because there is usually an excess of it. The common red-colored rust involving trivalent iron is formed:

$$4\mathrm{Fe}(\mathrm{OH})_2 + \mathrm{O}_2 \rightarrow 2\mathrm{H}_2\mathrm{O} + 2(\mathrm{Fe}_2\mathrm{O}_3 \cdot \mathrm{H}_2\mathrm{O}) \quad (12)$$

The schematic of metal oxidation (anodic reaction) is given in Figure 6 [20].

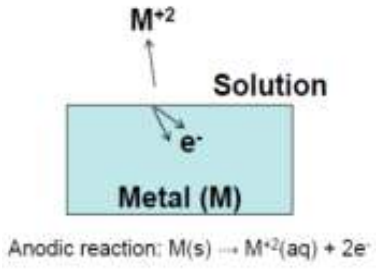

Figure 6: Anodic reaction – dissolution of metal

2.2.1. Corrosion protection

Corrosion and corrosion protection represents one of the biggest challenges in all worldwide industries and therefore, corrosion-resistant coatings and their development are critical for the protection of metals and metallic components. Metal constructions, machines, pipelines, tanks and similar equipment are all in danger of suffering from corrosion effects unless they are regularly controlled and maintained. Metals and metallic structures can be protected from corrosion in many different ways such as by using corrosion inhibitors, cathodic protection and protective coatings [21].

Generally, corrosion inhibitors are used in a controlled environment for corrosion protection. However, many inhibitors are not green materials or environmentally friendly. They are leached from the coating and become available to come into direct contact with the metal and block the

active corrosion site on the metal surface [22]. Corrosion inhibitors may have numerous negative aspects such as the loss of the coating integrity because of the leaching process or the inhibitor deactivation because of adverse interactions with some of the components of the coating formulation. Encapsulation of corrosion inhibitors is a promising technique to impede both the side interactions of the inhibitor with the coating components and the degradation of the coating integrity because of leaching [23].

Cathodic protection is another way of protecting metal constructions. It is commonly used method for protection of underground and undersea metallic structures, such as oil and gas pipelines, cables, utility lines and structural foundations [24]. The idea is to induce polarization of a metal construction with respect to the environment (soil, water…) which may be done actively, by the external current sources or passively, by using sacrificial anode to be dissolved or degraded instead of the construction metal.

Protective coatings serve as a barrier between the metal surface and corrosive environment and they can be the organic or metallic type. Organic coatings are usually in a form of a liquid and are applied over the surface to be protected [25, 26].

Metallic coatings are applied through plating or bonding two metal components together – the substrate and a protective thin layer of metal over the substrate surface. Together they provide a film that changes the surface properties of the substrate and of the metal being applied. The substrate then becomes a composite material exhibiting properties generally not achievable by either of the materials if used alone. Together, they add specific properties to the surface, such as resistance to corrosion or oxidation, electrical and wear resistance, more attractive appearance, or thermal protection [27].

Given that the corrosion of the metal substrate is an electrochemical process, electrochemical testing techniques and strategies should provide effective tools for measuring of corrosion protection efficiency of various kinds of protective coatings.

The electrochemical techniques for studying corrosion protection may involve measurements in bulk solution or under atmospheric conditions. The techniques which can be performed in atmospheric situations are mostly global techniques that assess the net performance of the complete coated substrate at the same time; the techniques utilized in bulk solution may be either global techniques or local techniques that assess the coating performance at one particular place.

The typically used electrochemical techniques for analysis of coating performance include

cyclic potentiodynamic polarization (CPDP), open circuit potential (OCP), scanning electrochemical microscope (SECM), electrochemical impedance spectroscopy (EIS), scanning ion-selective electrode technique (SIET), localized electrochemical impedance spectroscopy (LEIS), scanning Kelvin probe (a nondestructive method, SKP), electron probe microanalysis (EPMA), hydrogen evolution reaction tests (HERT), linear polarization resistance (LPR) and others [28].

Some of the mentioned techniques are being used for evaluation and quantification of the effects of environmental and metallurgical parameters on the corrosion behavior of metals and metal composites, while others are being used for studying the protection mechanism and surface analysis.

These methods fall short of providing details of the local reactions occurring directly at the damage site. On the other hand, the processes occurring locally at the solid or liquid interfaces may prove to be the key to exploring the mechanisms of the respective electrochemical reactions and of the active species included.

2.2. Coating formulation

There are five main elements of a coating formulation: binder (resin), pigment, solvent, extender (filler) and additive(s). The number of their combinations is practically limitless. Different combinations of each element are used as depending on the application. The binder (resin) will very probably determine the main field of application of the coating and pigment may enhance the ability of the coating to be applied in corrosion protection, give color, etc. [29]

2.2.1. Binder (resin) type

The binder provides a physical structure of a coating; it is the suitable medium for supporting and settling pigments and additives. Binder adheres to all coating components and forms a uniform coating film that may bind to surfaces. The binder governs and controls the wide range of properties of the coating film. Generally, organic polymers are used as binders in anticorrosion coatings. For improving the characteristics of a coating, resins from different groups may be blended to take some advantages of each component [30].

2.2. 1.1. Epoxies

Epoxies are the most important group of binders that are used in anticorrosive coatings because

of their excellent properties such as chemical resistance, adhesion to surfaces, hardness, and strength. The epoxide group (Figure 7) has a ring structure and it can supply a crosslinking place to react with proton-containing groups, such as acids, amines, alcohols or phenols. In the crosslinking reaction esters, secondary amines, aliphatic or aromatic ethers are produced, respectively (Figure 8). Most commonly, epoxy is a thermosetting polymer that is produced by a reaction between an epoxide as a resin and a hardener such as a polyamine [31]

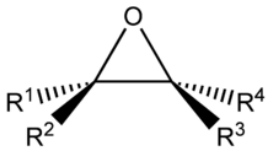

Figure 7: Epoxide group

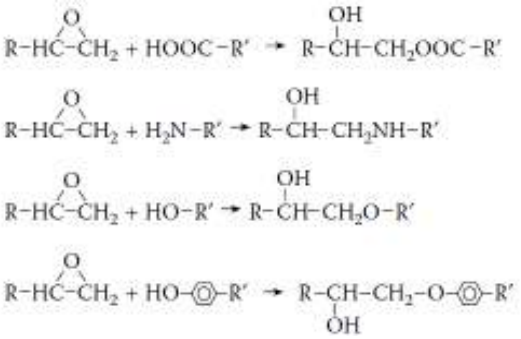

Figure 8: Usual reactions of epoxide group to form epoxies

The most usually used epoxy resins are those based on diglycidyl ether of bisphenol A (DGEBA or Bis A epoxies), those based on diglycidyl ether of bisphenol F (DGEBF or Bis F epoxies), epoxy phenol or cresol novolac multifunctional resins, resins based on polyamine adducts, ketimines, polyamides/amidoamines, aromatic amines, cycloaliphatic amines or polyisocyanates [32, 33].

Regardless of the excellent properties of epoxy resin, there are some disadvantages. Epoxy resin is vulnerable to UV rays. The sunlight contains enough energy to break covalent bonds of epoxy resins. The polymer backbone will break down if the epoxy film is exposed to sunlight for a long time and UV degradation will accrue. The UV degradation in the epoxy coating film is exhibited by a loss of gloss and occurrence of chalk dust (chalking). On the other hand, epoxy resins are very brittle which results in low flexibility of epoxy coatings. Those disadvantages are not directly related to corrosion but they may result in a damage of a coating film. A damaged protective layer is ready to crack easily by mechanical or chemical forces which may deteriorate the anti-corrosion properties of the coating later on [34, 35].

2.2.1.2. Acrylics

Acrylics are the other large group of binders that are used for producing anti-corrosive coatings. In principle, acrylic binders are based on methacrylate and acrylate monomers and they are formed by radical polymerization (Figure 9).

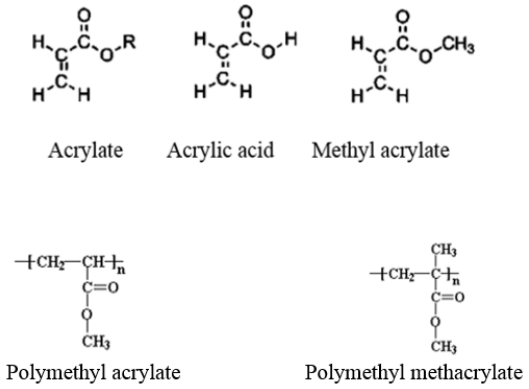

Figure 9: Basic acrylic monomers and polymers

The resin produces coatings with good UV resistance (especially in exterior applications) and good weather resistance; acrylics are glossy and resistant to hydrolysis. Acrylic resins are thermosetting polymers or thermoplastics which can be formulated into water-borne, solvent-borne and powdered UV-curable coatings [36].

Acrylic resins are often resistant to alkaline saponification. Polymethyl acrylates exhibit lower resistance to saponification in comparison with polymethyl methacrylates. However, coating formulation may include a proper monomer for copolymerization and excellent results can be achieved in terms of avoiding saponification [37]. Copolymers may be used to improve the properties of acrylic resins. For example, acrylates are soft and suitable for improving flexibility and bending properties of a coating whereas methacrylates provide resistance to alkalis and increase hardness. So, a combination of those monomers may be used to improve the acrylic coating properties in more directions [38].

Generally, the initiator is a compound with a peroxy or azo group which forms two free radicals upon decomposition of the central bond (Table 1). Monomers may combine with those free radicals to create larger free radical molecules [39].

Table 1: Commonly used initiators and monomers of acrylic resins

Initiators	Unsaturated acrylic monomers
Azobisisobutyronitrile (AIBN)	Methacrylic acid
Dibenzoyl peroxide	Methyl methacrylate
Tert-butyl perbenzoate	Butyl methacrylate
Di-tert-butyl peroxide	Ethyl acrylate
	2-Ethyl hexyl acrylate

2.2.1.3. Polyurethanes

When hydroxyl groups, amines or water react with isocyanate, polyurethane resins are formed (Figure 10). Regarding the mechanisms of curing, polyurethane resins are divided into chemical curing and moisture curing resins. Regarding the type of isocyanate, they are divided into those derived from aromatic or aliphatic isocyanates. The limitations of application of aromatic polyurethanes as coatings include short recoat time between multiple coats and sensitivity to UV radiation. In relation to the last limitation, aromatic polyurethanes are a suitable choice for internal parts or as an intermediate coats because they have better chemical and solvent resistance, they are fast curing and less expensive. Obviously, aliphatic polyurethanes are used for outdoor applications because of higher UV resistance, better resistance to weathering and mechanical stress and gloss or color retention [40].

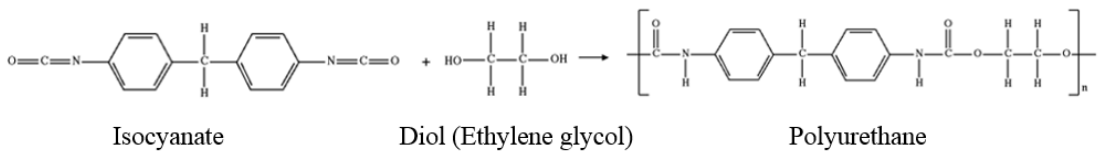

Figure 10: Reaction of polyurethane resin formation

Polyurethane coatings are cured in two ways: by action of moisture or by action of chemicals. The main difference between them lies in the fact that moisture-cure polyurethanes are one-component coatings with two isocyanate functional groups which are cured with ambient water, whereas chemical-cure polyurethanes are two-component coatings with a relatively short pot life which are cured by reactants (curing agents). Two-component polyurethanes are formed as a combination of a liquid binder (A component) with a hardener or crosslinker (B component). Generally, polyurethane coatings tolerate damp surfaces, which is particularly true for moisture-cure polyurethanes. Since isocyanates react very easy with water, this may lead to adhesion problems at the metal/coating interface. The reaction between isocyanate and water produces carbon dioxide which is responsible for creating pinholes, voids, and bubbles in the coating film. With chemical-cure polyurethanes, the properties of the coating may be improved by selecting proper reactant in order to achieve desired results. For instance, polyester-cured polyurethanes demonstrate high chemical resistance, polyurethanes cured with polyether polyols show high hydrolysis resistance and acrylic-cured urethanes have superior resistance to UV radiation.

There are various coatings available for protecting metal surfaces against corrosion but polyurethane coatings are the best choice generally for several reasons. Polyurethane coating films create a smooth and hard surface. The coating films exhibit fair resistance to humidity, oxidation, weathering and consequently corrosion. They perform well in heavy-duty industries and they do not require often maintenance. Anti-corrosive polyurethane coatings have adequate flexibility and good resilience as well as chemical and abrasion resistance. Their strong adhesion to metal surfaces contributes in forming coating layers resistant to penetration of steam and contaminants. Polyaspartic coatings are relatively new type of polyurethane coatings which could be one of the best solutions to prevent corrosion of metallic surfaces. There are other binders that are commonly used in protective coatings such as polyesters, alkyd resins, chlorinated rubber etc. Nevertheless, this work is focused on polyaspartic coatings [41, 42].

2.2.1.4. Polyaspartics

Polyaspartics were discovered in early1990s and introduced as a relatively new generation of coatings. Actually, polyaspartics may be regarded as aliphatic polyurea derivatives. One of the reactants in producing polyaspartics is the sterically hindered aliphatic secondary amine derived from aspartic acid, Figure 11.

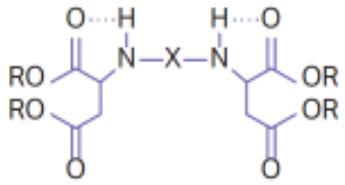

Figure 11: General structure of aspartic acid derivatives used in production of polyaspartics

The other reactant is an aliphatic polyisocyanate. The reaction involved in curing of polyaspartics is schematized in Figure 12) [43].

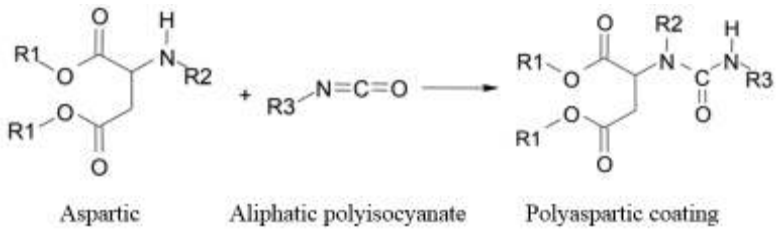

Figure 12: Basic reaction of formation of polyaspartic coatings

A part of aspartic structure marked by X in Figure 11 can affect the reactivity of aspartic with polyisocyanates and its variation may be used in adjusting some parameters such as pot life and drying time. There is a wide range of polyisocyanates that are used as hardeners (co-reactants) and each one may influence the properties of a polyaspartic-based coating. The polyaspartic esters as components used in reaction with polyisocyanates (co-reactants) produce coatings with low or near-zero volatile organic compounds (VOC) emissions, they are characterized by fast curing, abrasion (and consequently) corrosion resistance, increased productivity and possibility of high build application. Once can conclude, therefore, that polyaspartic resins demonstrate many benefits in comparison with conventional resins that used for producing protective coatings, such as higher abrasion, chemical and mechanical resistance, faster applying and higher overall performance. [44]

2.2.2. Pigments

The anti-corrosive pigments are commonly divided into three main types: inhibitive, sacrificial and barrier ones. The action of inhibitive pigments includes a release of soluble pigments into water; the pigments will then penetrate through the coating to the metal surface to protect it against corrosion. Solubility and reactivity are the important factors for selecting an inhibitive pigment. The sacrificial pigments act as sacrificial anodes; the typical sacrificial pigment consists of zinc particles; galvanic cells are formed at the surface of metal where zinc film plays anode role and the metal surface to be protected acts as cathode in the electrical contact with zinc particles. It is important to note that both inhibitive and sacrificial pigments may be introduced in the layer in direct contact with the metal surface (e.g. primer layer). Barrier pigments have flake-like or plate-like shape of particles; unlike the inhibitive and sacrificial pigments, they may be used in primer, intermediate coat, and topcoat [45, 46].

2.2.2.1. Inhibitive pigments

The best known inhibitive pigment is the red lead, Pb_3O_4, used for a long time. Lead pigments are usually formulated within a resin system to be applied as primer, but this pigment is not recommended anymore because of its toxicity.

Phosphates are used as inhibitive pigments as well. There are many pigments containing functional groups composed of phosphorus and oxygen. The common phosphate pigments

which are used in the structure of protective coatings include zinc phosphate, aluminum zinc phosphate, zinc molybdenum phosphate, aluminum zinc hydroxyphosphate, zinc hydroxymolybdate phosphate, zinc silicophosphate, zinc aluminum polyphosphate, aluminum phosphate, dihydrogen tripolyphosphates, dihydrogen aluminium triphosphate, strontium aluminum polyphosphate, calcium aluminum polyphosphate silicate, zinc calcium strontium polyphosphate silicate, laurylammonium phosphate, hydroxyphosphates of iron, barium, chromium, cadmium, and magnesium. Among the mentioned pigments, zinc phosphate is used in a wide range of binders, from epoxies to those based on alkyds. Actually, it is a multipurpose pigment because of its low activity and solubility as well as non-toxicity, but zinc phosphate pigment is susceptible to fungi attack. Zinc phosphate pigment may hydrolyze itself and it cannot be used alone in long time exposure; gradually it will disappear from the coating film and therefore it should be used with other anti-corrosive pigments.

Another anti-corrosive pigment is ferrite which is formed by calcination of metal oxide. Ferrite pigment in reaction with fatty acids of binders creates an alkaline environment at the interface metal/coating by forming metal soaps that will protect consequently the metal surface against corrosion.

There are other inhibitive pigments as well, such as zinc potassium chromate, strontium chromate, zinc tetroxychromate, calcium-exchanged silica, barium metaborate, molybdates, and silicates [47].

2.2.2.2. Sacrificial pigments

Zinc dust is used for long time in zinc-rich paints (ZRP) for the protection of metal constructions (especially those made of steel) against surface deterioration. Zinc dust is produced by condensing purified zinc vapors; it protects metal surface by scarifying itself. There are two types of zinc dust: granules and flakes. Flakes are highly effective and show good performance in comparison with granules. Zinc dust protects metal surfaces against corrosion by four mechanisms.

- Zinc dust as a sacrificial anode acts in cathodic protection of the metal surface, but only shortly after applying the coating onto metal surfaces (high amount of zinc dust is necessary for this mechanism to be active)
- Zinc dust forms insoluble zinc salts in the coating film via reacting between zinc ions and other substances. Thus formed zinc salts will fill in the holes in the coating, which

will consequently reduce the coating film permeability (high amount of zinc dust is necessary for this mechanism to be active)

- Zinc dust consumes oxygen molecules that diffuse through the coating film toward the metal surface, i.e. oxygen reduction takes place.
- Upon corrosion of zinc dust, alkaline conditions are formed on metal surfaces [48, 49]

2.2.2.3. Barrier pigments

Barrier coatings act by the reduction of the permeability of liquid and vapor through a coating film. Barrier pigments are commonly divided into two main groups: nonmetallic and metallic pigments.

Mica, talc and micaceous iron oxide (MIO) all belong to the nonmetallic group whereas aluminum, zinc flakes, stainless steel, nickel, and cupronickel are classified into the metallic group. The barrier pigments should be insoluble in water but it is the shape of pigment particles that is important. Most of them are flake-shaped or laminar; when a coating layer is formed, their particles are oriented in parallel to each other and to the protected surface. The particle size affects the protecting properties of coating against surface corrosion; the smaller is the size of particles, the more layers of pigment will form in the dried film of coating. In that case, water or contaminants have to travel longer distances within the coating film to reach the metal surface. This is the main reason why the barrier coatings are used primarily as topcoats to increase weathering resistance of the coating.

Effective barrier properties can be increased by:

- Applying thicker coating films composed of multiple layers
- Selecting a binder with a higher degree of crosslinking
- Using higher pigment volume fractions
- Using pigments with smaller particle size (and with suitable particle shape)

In addition to the mentioned properties of barrier pigments, the metallic pigments reflect UV radiation and withstand higher ambient temperatures.

The role of pigment is important in selection of a proper pigment for the coating system under consideration. The formulator has to know if the pigment will play an active role or a passive role in protection. The other factors important for manufacturers include the price of pigment,

its compatibility with the binder of the coating system and ease of its mixing or blending with the binder [50, 51].

2.2.3. Additives

For improving the performance of the selected binder and anti-corrosive pigment in the protective coating, proper additives need to be used. Additives do not play a key role in the anti-corrosive system, but without them it is impossible to achieve a desirable result of using a protective coating. The amount of additives is very small (less than 5% in a total formulation) but their effect is very huge. Additives have to be admixed in the certain stage of coating production in adequate quantities. The goal of manufacturer of protective coatings is to produce a coating with excellent performance, cost-effective price, easy to apply, with zero or near-to-zero VOC emission and great appearance with longtime durability, so it will be possible just with adding the proper additive for each goal [52].

There are the different classifications of additives, e.g. based on application, based on type of the system: aqueous/solvent borne, based on binder… According to their application they are divided into the following main groups.

- Rheology modifiers

Rheological additives are primarily thickeners; without them the pigments would settle on the bottom of the coating container to form a hard layer or sediment. In addition, the coatings without thickeners would sag and run down upon application on the surface.

- Flow and dispersion agents

Flow and dispersion agents control the behavior of the wet film of a coating during mixing, application or curing. This category includes surfactants, dispersants, anti-floating/antiflooding and thixotropic additives. Dispersing agents promote the dispersion of pigment particles during the coating production. Dispersing agents bind to the surface of the pigment particles thus reducing the attractive force between the particles and separating them as far as possible. The separation of pigment particles by dispersing agents remains stabilized in the final coating formulation (Figure 13).

Figure 13: The dispersion of nanoparticles in liquid matrices

- Catalysts and driers

Driers, inhibitors and catalysts agents control the process of drying during formation of a coating film. Drying or curing control agents are classified into crosslinkers, auxiliary additives and catalysts/initiators. All three types of drying control additives modify and improve the drying process by adding or activating groups to reduce the curing time.

- Defoamers

There is a distinction between defoamers and anti-foam agents. Defoamers are used for breaking the bubbles and removing the foam which is created during the application process (e.g. by brush, rollers or spray). On the other hand, anti-foam agents prevent the formation of foam during mixing or blending components of the coating formulation. Defoamers are commonly surfactants; they reduce the volume of bubbles created in the application of an aqueous based coating due to high surface energies at the liquid/air interface [53].

- Adhesion promoters

Adhesion promoters will increase adhesion between the film coating and the metal surfaces. They should be compatible both with the binder and the surface on which the coating is applied. In the industrial sector the lack of adhesion is a critical point. Typically, the coating system consists of primer, medium coat and topcoat and adhesion between those layers is important, too. In some situations, e.g. for immersed constructions or in corrosive environments, the adhesion between primer (first coating layer) and the metal substrate is even more important. Generally, the first layer of coating (primer) is applied on the metal surface to provide a smooth surface and increase adhesion for the next layer, but the adhesion at the primer/metal interface should be supported by adhesion promoters in some applications such as offshore or onshore industries. Silanes, titanates, chromates, zircoaluminates are examples of adhesion promoters.

Silanes are commonly used in the protective coating systems, especially those based on urethanes, acrylics and epoxies [54].

- Additives for protection against destructive influences of environment

This category of additives reduces destructive effects of the environment on the coating films and increases the stability of the coating on surfaces. Antioxidants, anti-fouling agents, UV stabilizers, corrosion inhibitors and biocides are the examples of those compounds. The regulation on their use is very strict and attempts to control toxicity of those additives and their effect on the natural ecosystems and living beings. For example, Tributyltin ($C_{12}H_{27}Sn$, TBT) was used for 40 years as a biocide in the anti-fouling coatings for preventing of adhering fungi, barnacles, algae, and shellfish on the hulls of ships, vessels and all marine constructions. Nevertheless, TBT poisoned sea organisms at the bottom of the food chain and proved to be harmful to the ecosystems. The amount of 1 ng of TBT per liter of water demonstrated toxic effects. The usage of TBT is forbidden in all the waters of the world since 2008 [55, 56].

2.2.4. Nanomaterials in coatings

Surfaces are coated by protective coatings, from small parts on electrical instruments to huge parts on ships, planes, automobiles etc. As a global forecast, the production of industrial coatings is estimated to about 54.7 million metric tons in 2020 [57].

According to extreme demand of coating by industries, it is necessary to improve their properties. Nanotechnology has recently shown a key role in the development of so-called smart coatings. Innovative and new nano-based coatings are being extensively used for many reasons. They protect the surface against corrosion and contamination, they provide a self-cleaning and self-healing surface, limit biological soiling and are used in creating special designs which are very important in automotive and airplane industry and construction [58].

The amount of nanomaterial that is used in the coating depends on the desired function [59]. Nanomaterials which are commonly used today in the nano-based coatings include titanium dioxide, silicon dioxide, carbon black, iron oxide, zinc oxide, and silver.

Nanomaterials improve many characteristics of the coatings; they may increase adhesion between the coating and the surface and thus enhance the durability of the coating. Also, nanomaterials may be used to achieve a combination of contradictory properties such as simultaneous hardness and flexibility, low thickness and high coverage etc. In general,

nanomaterial-containing coatings demonstrate better properties than conventional coatings. Nanocoatings may be applied directly to metal, wood, plastic, glass and concrete surfaces [60].

Nanomaterials find their applications in nanobiotechnology, nanoelectronics, nanocoatings, nanoplasmonics, food and agriculture, energy, furniture, space, cosmetics, automotive industry, cement industry, construction, displays, medicine, fight against Alzheimer's disease, HIV/AIDS treatment, fight against cancer, surgery, environment protection, disaster relief and development cooperation, green industries and sports equipment (see example in Figure 14) [61, 62].

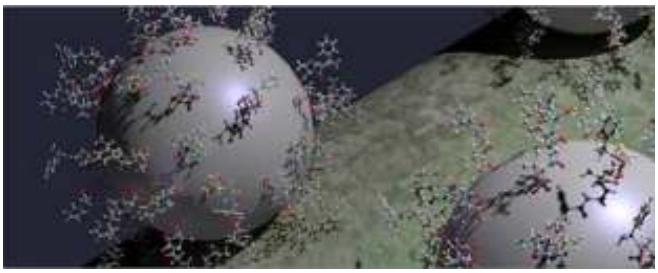

Figure 14: Silver-silica nanoparticles with an ampicillin coating are safe for human cells and lethal to antibiotic-resistant microorganisms. [61]

2.2.5. Producing nanomaterials to be used in coatings

Nanomaterials are not only found in nature (volcano emissions), but can be produced also by human activities (tobacco smoke, diesel exhaust fumes). Nanomaterials may be manufactured intentionally as well, and they are already used in many products such as food, construction materials, and composites. There is a wide range of nanomaterials that were discovered only recently, for instance, nano-silver, carbon nanotubes and nano-titanium. The market for the new generation nanomaterials is predicted to grow rapidly.

Dispersion of particles is the important issue in producing coatings that contain nanomaterials. The dispersion will be affected by particle distribution. There is a possibility of agglomeration of particles in the coating if the nanomaterials were not distributed properly. There are three steps for using nanoparticles in the liquid coating: wetting, dispersing and stabilizing. It is not just simply mixing nanoparticles in a coating, because it has to integrate into a resin matrix and it is evident that the matrix of the resin must have ability to hold the nanoparticles. Nanoparticles will sink to the bottom of container in case of incompatibility between nanoparticles surface and coating vehicle. There is a big difference between dispersing a nanoparticle and a conventional micron-sized particle. The nanoparticles have high surface

energy so they require higher energy for dispersing in comparison to conventional particles. The nanoparticles which are strongly embedded in the resin matrix will not release from the coating layer on the surfaces easily even in a harsh weathering [63].

2.2.5.1. Applications of nanocoatings

Nanocoating creates a compatible network of molecules on a surface. Nanocoatings are the nanoscale thin films that are applied to surfaces to create higher corrosion protection, better antifouling and antibacterial properties, excellent thermal shock, heat and radiation resistance, self-cleaning or self-healing, water resistance and other properties. The following applications are some top applications of nanocoatings: anti-corrosive coatings, waterproof and non-stick coatings, antibacterial coatings, thermal barrier coatings, anti-abrasion coatings, self-healing coatings, anti-reflection coatings, and anti-graffiti coatings.

2.2.5.2. Anti-corrosive coatings

One of the main uses of nanocoatings is as an anti-corrosive layers to protect surfaces (for example metals) against degradation due to moisture, contaminants, salt, radiation, oxidation and harsh environment. Nano coating as an anti-corrosive coating is applied on a metal surface to inhibit the contact between corrosive materials and surface and acts as a barrier layer that helps to increase the lifetime of metal. There are many studies in this field to progress and improve the application of nanomaterials in the nanocoatings [64].

2.2.5.3. Waterproof and non-stick coatings

Water repellent nanocoatings are one of the main targets in the field of manufacturing nanocoatings. The manufacturers of the hydrophobic coatings were inspired by the “lotus effect” to produce a water repellent coating (Figure 15). The droplets of water roll off on the surface of these coatings and collect dirt and contamination in the same way as on the lotus leaves. These properties keep a surface cleaner continuously and reduce the cost, time and energy of cleaning the surfaces. The wide range of applications includes clothing, shoes, furniture, glass, electronics etc.

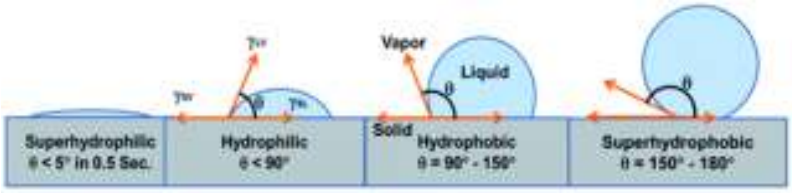

Figure 15: Comparison of hydrophobic and hydrophilic contact angles [66]

Non-stick coatings have the similar properties as waterproof coatings but they are able to repel oil, dirt, water and almost any liquid. They are particularly interesting for food packaging industries because they have many problems to design packaging for some food products, for example mayonnaise and ketchup sauce. Those products stick on the packaging and could not come out of it smoothly so the last portion of the products remains in the bottles and containers which have to be thrown away by customers [65, 66].

2.2.5.4. Antibacterial coatings

Antibacterial coatings prevent and reduce the growth of microorganisms on surfaces. Application of these coatings is very important in public places, healthcare industries, and public transport as well as in kitchens, air conditioning, sanitary facilities, food packaging and pharmaceutical industries for reducing the risk of infectious diseases [67].

2.2.5.5. Thermal barrier coatings

Thermal barrier coatings are being taken into consideration in the aircraft industry and aviation sector. Those coatings are applied on the metallic parts of aero engine parts and gas turbines exposed the high temperatures. The coatings increase thermal tolerance and decrease oxidation as well as thermal fatigue of metallic surfaces. Also, thermal barrier coatings are applied in engine exhausts systems of cars [68].

2.2.5.6. Anti-abrasion coatings

Friction is a main reason of abrasion on surfaces which is created by regular use of a part. Abrasion can reduce the lifetime of surfaces and increase the maintenance costs. Anti-abrasion coatings act by reducing or in some part eliminating wear and rub on surfaces which produce the mechanical damages and eventual failure of parts. Those coatings can be applied to surfaces which are not suitable for using lubricants [69].

2.2.5.7. Self-healing coatings

In nature, self-healing phenomenon is actually a commonplace. There is a wide range of self-healing systems since living organisms have intrinsic self-healing capabilities. If, for example, some of the branches are cut off from a tree, the tree will still have the ability to grow. If a man accidentally cuts himself, his body will initiate an emergency response, in order to repair the wound.

Inspired by nature's self-healing systems, a new progress has been made in developing synthetic materials in the recent decade, the materials possessing the ability to self-repair after sensing damage. Following the nature´s concept of self-healing, the term "self-healing" in materials science today refers to a self-recovery property of the mechanical integrity and original properties of the material, after destructive actions of the external environment (for example scratches) or under the influence of internal stresses. Such self-recovery properties have been incorporated into a new generation of smart materials, called self-healing coatings, which appeared on the market quite recently. Since these smart materials possess the self-reparation ability when damage occurs without the need for detection or repair by manual intervention of any kind, it is believed that these self-healing coatings will gradually replace the conventional coatings systems, given their multiple advantages of application. They can be used in wide range of industrial and non-industrial applications, from electronics, chemical production, furniture production, automotive, spacecraft, interior design, energy, construction, or in basically in any industry or production which could benefit from self-healing materials. Self-healing batteries, ceramics and plastics, tires which seal themselves, the fabric which does not fade – all of them have potential applications for self-healing concepts.

Given that the research and development of smart materials and their applications, represent a new area in research (globally recognized field of study in the 21st century), the advancements made in the field are expectedly leading to an accelerated interest, efforts, and progress in materials science to be made in formulation and development of functional materials which can imitate nature's self-healing ability (biomimetic materials). These materials will ideally enable self-healing from macroscopic or microscopic damage, similar to how living organisms behave (Figure 16) [70, 71].

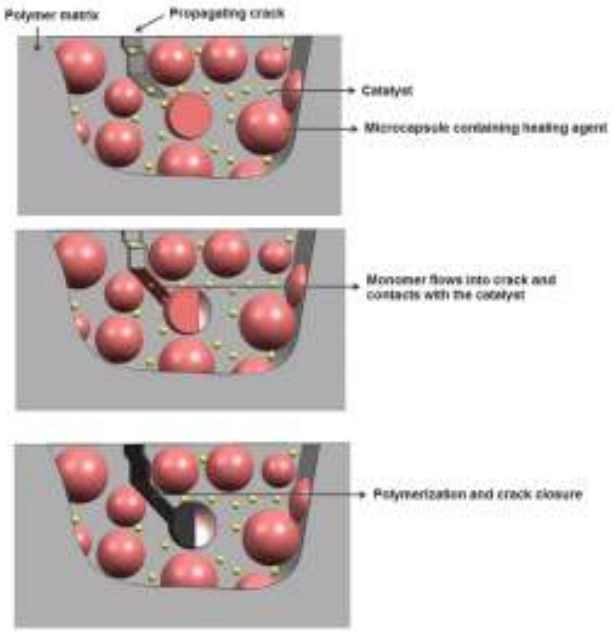

Figure 16: Schematic representation of the self-healing concept using embedded microcapsules [71]

2.2.5.8. Anti-reflective coatings (ARC)

Certainly, the fundamental part of efficient solar cells is antireflective coating. The ARC influence is demonstrated by increasing the amounts of the short-circuit current and the efficiency of solar cells. When applied at the solar cells surface, anti-reflective coatings improve the efficiency of panels. The reflection of sunlight from the front of solar panel surfaces may diminish the efficiency of a solar cell. By applying ARC as a topcoat on the solar cell surface, the reflection coefficient can be reduced (Figure17).

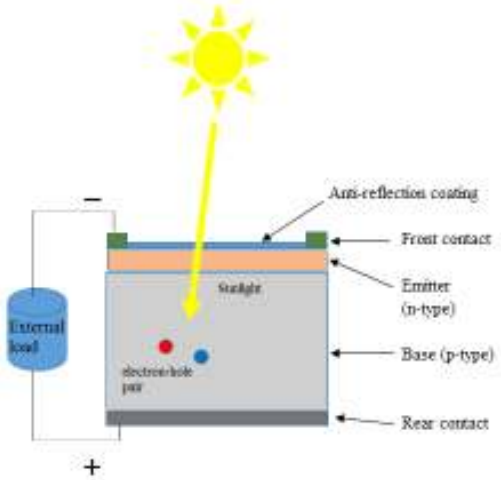

Figure 17: Scheme of a solar cell

The proper choice of the thickness of the anti-reflective coatings is important for the metallization process of electrical contact. Excessively thick ARC makes the process of pad metallization more difficult and decreases efficiency and optical parameters of the solar cell [72].

2.2.5.9. Anti-graffiti coatings

Graffiti is recognized as vandalism in most countries and it costs a lot to clean them off surfaces, walls or building. Anti-graffiti coatings are the best solution for solving this problem. Principally, anti-graffiti coatings are transparent and invisible to the naked eyes. There are two kinds of anti-graffiti coatings: the first one is a layer of anti-graffiti coating which prevents graffiti to adhere on the surface and the second one is a coating with the ability of easy cleaning which allow for easy removal of graffiti from the surfaces [73].

2.2.6. Nanoparticles in environment protection

Nanoparticles have become very interesting because of their various application and multi-purpose properties. The surface to mass ratio of nanoparticles is very large because of the small particle size and these materials demonstrate various properties which may not be present in the bulk material of same chemical composition [74].

Since nanocoatings are applied on the surface in thin layers, the overall mass of the applied material is decreased which affects the total mass of the coated sections [74]. For example, the total mass of a vessel in the marine industry is very important. The more coating material is applied on vessel parts the larger will be the total weight of the vessel which will make the transportation slower. The same reasoning may be extended to automotive industries, aircrafts and railway.

Due to their improved properties, some of the maintenance will be avoided with applying nanocoatings on surfaces. Obviously, the volume of the chemical materials that are necessary to clean or repair surfaces will be reduced. Consequently, the release and spread of chemicals in the environment will be decreased.

Reducing the volume of chemicals emission due to the use of nanoscale materials, the improvement of product quality due to the lack of utilization of a large number of raw materials to achieve the desired properties and prevent of unrequired maintenance services or duplication due to the high durability of these materials can be a major reason for the positive impact of

using nanomaterials [75].

2.2.7. Adverse health effects of nanomaterials

Potentially harmful effects of nanomaterials on health are the main concern of their usage. According to some results by the Scientific Committee on Emerging and Newly Identified Health Risks (SCENIHR), a number of nanomaterials may have adverse effects on human health. Nevertheless, it does not mean that all nanomaterials will surely be hazardous or toxic. The research is ongoing and every nano product is under intensive control and inspection. Generally, nanomaterials may affect the liver, cardiovascular system, kidneys, heart, brain, skeleton and soft tissues but the lungs are the most endangered organ. The toxic effect of nanomaterials can be expressed by inflammation, tissue damage, fibrosis, and tumors. On the other hand, flammable powder-shaped nanomaterials present an explosion risk because of their small size and large surface area.

There is no definite and accurate report database upon the nanocoatings that have a harmful effect on the environment or living beings. Here some nanomaterials which are most used in the coating industries will be pointed out such as TiO_2 and nano-silver. TiO_2 is one of the most important pigments in the coating industries. Regardless of its excellent function for improving the productivity of coating, it can affect the organisms in the aqueous systems because of producing free oxygen radicals. Silver can also produce some problems in the environment, especially in aqueous systems. The use of nanomaterials requires precise information on their life cycle. The manufacturers have mentioned that handling those materials may present a health risk for operators. In particular, there is more concern for operators when the nanocoatings will be applied on surfaces by spraying. Small particles of sprayed liquid coating (less than 10 microns in size) may deeply penetrate into lungs and eyes or may be absorbed through the skin into the operator body.

In most cases, the manufacturers of nanomaterials observe the rules of applying nanomaterials and take safety precautions of their usage. The problem will occur in cases when operators do not have information that they actually use a product containing nanomaterials. Consequently, they have contact with the materials continuously. The products containing nanomaterials may be processed and during the procedure, nanomaterials inhaled or come into contact with the workers' skin.

The conventional toxicity tests are not enough for controlling and predicting the toxic effect of

nanomaterials on the environment and the human body and this requires the use of new and elaborate approaches to determine the interaction of this materials. Unfortunately, the scientific community is still not convinced that nanomaterials are harmful to health. There is a wide range of nanomaterials with different effects and properties and this has made the general acceptance of the health hazard difficult. On the other hand, there are many gaps for selecting a suitable method of usage, handling, applying, packing and transportation of those materials [76-78].

2.2.8. Characterization of nanomaterials

It is very important to have complete information of nanomaterials before using them, and this information helps to understand better their chemical structure as well as their physical characteristics. If the person who applies nanomaterials has enough information on chemical and mechanical characterization of those materials, he will be able to determine how can use them safely. The manufacturers of nanomaterials are obligated to provide useful information in the technical data sheet and material safety data sheet. They also have to explain clearly the similarities and differences between the nanomaterials with the other materials. [79] Some important information which gives adequate knowledge of using and determining the hazardous potential of nanomaterials in given in the following sections.

2.2.9. Size of nanoparticles

In fact, there is no evidence that the size of nanomaterials affects their hazardous properties. Yet, there are reports that show that nanoparticles with a dimension less than 30 nm are not stable and their crystalline structure differs from that of larger particles of the same chemical composition. Thus, it is very difficult to predict the toxicological behavior of nanoparticles based on data obtained with large size particles.

There are many effects that are specific for nanoparticles only, i.e. for particles of the sizes from 1 to 100 nm. However, that does not mean that particles with the size above 100 nm are not hazardous or nanoparticles with one dimension below 100 nm (Figure 18) are toxic and risky. Regardless of the huge difference in properties, the hazard potential of nanosized particles is the same as of the other materials [80, 81].

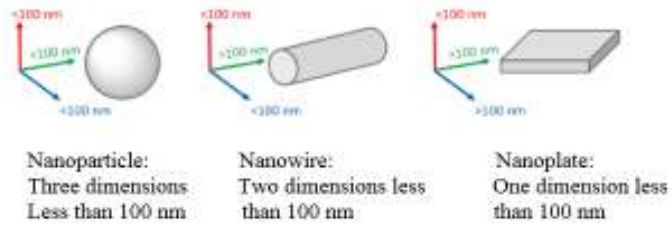

Figure 18: ISO definition of nanoparticles, nanowires, and nanoplates [82]

2.2.10. Agglomeration of nanomaterials

Intrinsically, in all situations nanomaterials after releasing rapidly form agglomerates. Those clusters of nanoparticles have a larger size in comparison with primary nanoparticles. Therefore they have the lower potential of inhalation in the workplace. Agglomeration behavior is under influence of the environment and side effects (for example mixing); that means that agglomeration state of nanoparticles is not stable and can be changed. The agglomeration state should be mentioned in the health hazard reporting because it has direct effect on risk assessment of nanoparticles (Figure 19) [83].

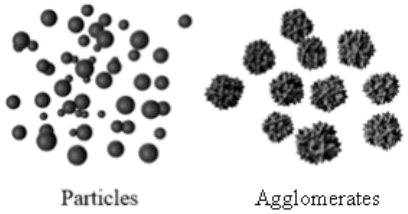

Figure 19: Schematic of nanoparticles agglomeration

2.2.11. Surface area of nanoparticles

Many toxic properties of nanoparticles depend on the surface of the particle. When the particle size of nanomaterials is reduced, the surface area will increase (Figure 20). Small particles may have completely different properties. For example, bulk silver intrinsically has a shiny silver color whereas silver nanoparticles have a various color that depends on their size and shape. The spherical silver nanoparticle with the size of below 20 nm is yellow or amber-colored. The difference in surface area is the main reason for explaining the potentially higher toxicity of nanoparticles in comparison to the larger particles [84].

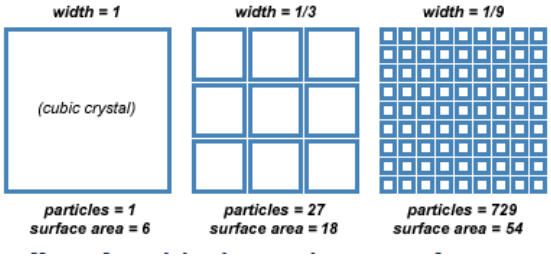

Figure 20: Effect of particle size on pigment surface area

2.2.12. Shape of nanoparticles

There is some evidence that the shape of nanomaterials can directly influence its toxic potential. By controlling size and shape of nanoparticles many properties of nanomaterials can be controlled. The examples of the possible shapes of nanoparticles are shown in Figure 21 [85-87].

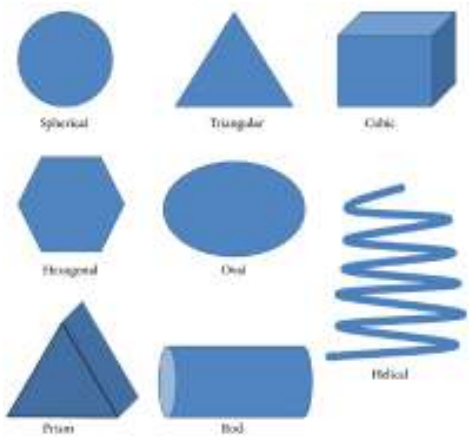

Figure 21: Different shapes of nanoparticles [87]

2.2.13. Application of nanoparticles in coatings

It is well-known that alumina and silica nanoparticles can improve especially corrosion, wear and scratch resistance. In addition, they can provide better adhesion and anti-staining in solvent-based coatings because they create a more compact film. It is essential to disperse nanoparticles in the coating uniformly.

Practically, the sufficient amount of nanoparticles is 0.5 – 2% of the total formulation. The type of nanoparticles to be used in the coating relies on the type and functionality of coating. They can be blended in the vehicles as previously stabilized particles in a dispersion/suspension or as powders [88].

The method of dispersion of nanoparticles depends on their type and surface properties. One of the practical methods is the synthesis of nanoparticles in solution to form a type of colloid solution which is then added into the coating formulation. The dissolved nanoparticles have to be integrated into the coating by some type of efficient mixing, e.g. by ultrasonic mixers which are capable to create adequate cavities in the resin matrix to embed the nanoparticles. This will very often produce intensive foaming of the coating vehicle which has to be suppressed by using sufficient dosage of anti-foaming agent. For achieving excellent dispersing and stabilizing it is essential to wet the nanoparticles properly [89].

2.2.14. Nanomechanical testing

In order to understand the basics of nanomaterials properties and their behavior, nanomechanical testing has been used which improve the information about these materials. The nanomechanical tests are commonly done in laboratories. Nevertheless, the operating conditions of nanomaterials should be simulated while performing nanomechanical in order to get reliable results for their nanomechanical and tribological properties. The manufacturers of nanomaterials are then able to use that information to improve the design of their products. In the mid-1970s the so-called nanoindentation technique was developed for testing small volume of materials and measuring their mechanical properties. The principle of this technique is related to a combination of determining the contact between an indenter and the sample, measuring the result of displacement and the application of low loads. From that information it is possible to determine the mechanical properties of nanomaterials. The conventional tests just are able to give general information of mechanical properties but nanoindentation technique is used for indication of local properties of nanomaterials [90].

3. MATERIALS AND METHODS

3.1. Materials

The manufacturer of Polyaspartic resin and its hardener, which were used in this research, is Covestro (Leverkusen, Germany, formerly Bayer Material Science).

The binder that was used was of polyisocyanate type with amino functional co-reactant because it has the ability to form a high solid, solvent-free, topcoat polyurethane coating. The hardener was solvent-free aliphatic polyisocyanate. This resin is fast-curing even at ambient temperature and possesses high durability and chemical resistance. Those two components may provide coatings with high film build, ultra-high solid content, and excellent resistance against mechanical damage. [91]

The important property of the aspartic acid esters is that water speeds up the reaction with polyisocyanates. The mixed coating can be quickly dried and hardened on the surface in a humid environment and, unexpectedly, the pot life of coating in this situation is relatively long. These coatings after drying and completing the curing procedure exhibit excellent corrosion resistance, durability and weathering resistance so they are primarily used as a topcoat. The reaction between diamine as an initiator with polyisocyanates gives a possibility to access the products with different reactivity and viscosity. Covestro presented three types of polyaspartic acid ester co-reactants, including Desmophen NH 1220, Desmophen NH 1420 and Desmophen NH 1520. The polyaspartic ester based polyurea coatings may upgrade the painting projects because of their fast curing time. The big concern in the painting projects is curing time of a coating because before there is a risk of contaminating the wet film of the coating by dust or blast grit before the complete curing of the coating. On the other hand, aliphatic polyaspartic ester coatings may be formulated to apply directly to metal (DTM) [92]. As the coating is aliphatic, it can be applied directly to steel surfaces which are properly prepared and there is a possibility to achieve high performance protection in a thick and single layer of the coating. A long time of pot life (approximately 4 h at 25 °C), besides superior color and gloss retention, caused this technology to be taken into consideration. The development of polyaspartic esters started in 1990s as a new technology [93]. Zwiener et al. indicated for the first time that polyaspartic esters are applicable as co-reactants for polyisocyanates.

Because the polyaspartic esters are suitable reactive diluent for high solid polyurethane coatings, at first this new technology was used in polyurethane solvent-based coating

formulation [94].

In order to reduce the amount of VOC, the polyaspartic esters may be blended with polyacrylate co-reactants and hydroxyl functional polyesters. Recently, all research is concentrated to improve the formulation of the coating in the direction of zero or near-to-zero VOC.

The co-reactants of the improved polyurea coatings are the polyaspartic esters which are necessary for reaction with a polyisocyanate. The fast curing time of polyaspartic coatings can influence many properties such as abrasion and corrosion resistance and gives ability to apply them in high build form as well as at low curing temperature and consequently to improve productivity.

The chemical structure of polyaspartic esters makes them capable to react with polyisocyanates. Those secondary aliphatic diamines can be produced by Michael addition reaction of different primary aliphatic diamines and dialkyl maleates [95].

Therefore, based on differences in chemical composition a whole group of products may be provided with different reactivity with polyisocyanates (Figure 22).

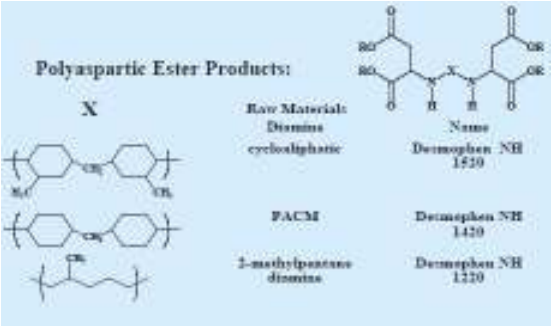

Figure 22: Structures of polyaspartic esters [96]

The polyaspartic ester structure has a sterically crowded environment around the nitrogen. This feature causes the decreased rate of reaction between the isocyanate group of polyisocyanate and the amino group of the polyaspartic. A slower reaction will obviously result in a longer gelling time and pot life. By changing the structure of the polyaspartic ester there is a possibility to improve the reaction rate of the polyisocyanate and the polyaspartic ester compound.

As it is shown in figure 22, by decreasing the steric crowding the reaction rate will increase. Therefore, Desmophen® NH 1520 reacts more slowly with polyisocyanate than Desmophen® NH 1420 and Desmophen® NH 1220.

Table 2 illustrates the difference between the gelling times of various kind of polyaspartic ester.

Table 2: Gel time reactivity data for aliphatic polyaspartics

Polyaspartic ester	Gel time at 38 °C	Gel time at 22 °C	Gel time at 08 °C
Desmophen ® NH 1520	Not tested	40 min	Not tested
Desmophen ® NH 1420	15 min	20 min	23 min
Desmophen ® NH 1220	1 min	1 – 2 min	2 min

In Table 3 it is indicated that water as a catalyst has a significant effect on the gel time of polyaspartic/aliphatic polyisocyanate mixture.

Table 3: The Catalytic Effect of Water on Reactivity

Polyaspartic ester	Water content (%)	Gel time at 22 °C
Desmophen ® NH 1420	0.08	65 min
Desmophen ® NH 1420	0.12	31 min
Desmophen ® NH 1420	0.17	11 min

According to the data in Table 3, the pot life will decrease in the humid atmosphere and consequently, the surface will be dried longer.

The coating film formed by the reaction between the polyaspartic ester and an aliphatic polyisocyanate as a crosslinker is highly stable, hard and extremely resistant against weathering and abrasion (Figure 23). Additionally, the polyaspartic ester is a good choice for formulating high performance protective coating on steel surfaces.

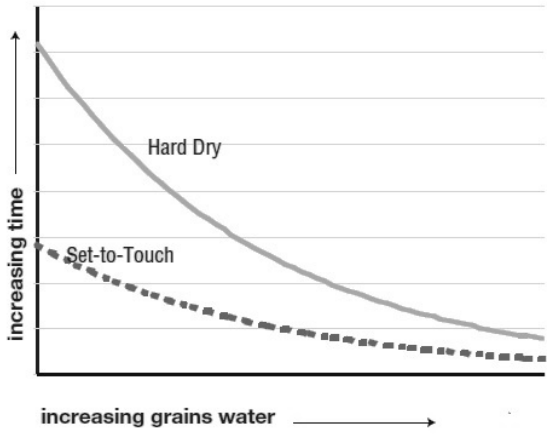

Figure 23: Effect of ambient moisture on dry times of fast curing aliphatic polyaspartic topcoat [96]

The data in table 4 show at these coatings have high tensile strength and very low elongations.

Table 4: Property data for aliphatic polyaspartic clear films

Polyaspartic ester	Tensile strength	Elongation
Desmophen ® NH 1520	6875	4%
Desmophen ® NH 1420	6650	4%
Desmophen ® NH 1220	2290	23%

There is a big difference between the aliphatic polyaspartic ester-based polyureas and classical aromatic polyureas based on MDI prepolymers and polyether backbones, in particular and in their curing time. The curing time of polyaspartic ester-based polyurea coatings depends on the temperature as well as on the humidity. Higher temperature and moisture as a catalyst accelerate the curing process in the aliphatic polyaspartic ester-based polyurea coatings. The temperature increases the kinetics of curing or drying processes as well.

According to the mentioned properties, fast cure coatings with long pot life [96] can be formulated.

The aliphatic diisocyanates are divided into three common types:

- ✓ hexamethylene diisocyanate (HDI) (Figure 24)
- ✓ methylene dicyclohexyl diisocyanate or hydrogenated MDI (HMDI)
- ✓ isophorone diisocyanate (IPDI)

The most broadly used of the aliphatic diisocyanates (ADI) is hexamethylene-1, 6-diisocyanate (HDI) which is used to produce HDI-based products. Wherever a high-performance coating in industries is required HDI is used [97].

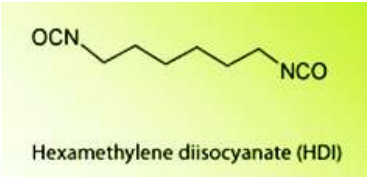

Figure 24: Aliphatic diisocyanate HDI (OCN—(CH2)6—NCO)

There are two main forms of raw materials:

- Monomeric diisocyanates – HDI, IPDI and HMDI (and several others)

- Blocked polyisocyanates – (mainly based on HDI)

Blocked polyisocyanates are produced as solvent-free and/or dissolved partially in different solvents. In this research the low-viscosity HDI trimer (Figure 25) is used a hardener or crosslinker.

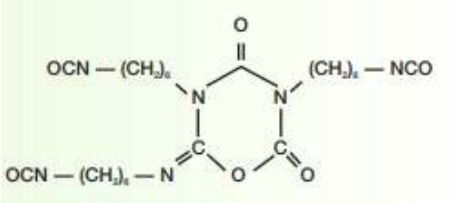

Figure 25: HDI Trimer

Polyisocyanates that have more than two functional groups are required for dimensional crosslinking. HDI is a polyisocyanate based on linear diisocyanates. It is used for the formation of flexible films and can be modified with polyols to improve different properties such as flexibility and hardness. Type of NCO bond (primary, secondary or tertiary) can influence the film coating properties by steric effects.

The main structure of the resin is built by the reaction between an aliphatic isocyanate and an aspartic acid ester to create a polyaspartic resin with urea-like structure (Figure 26).

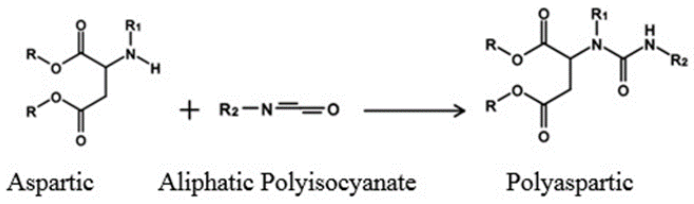

Figure 26: Chemical structure of a polyaspartic coating

The most important factor in the start formulation was the choice of suitable raw materials with regard to the desired coating properties. The start formulation of the coating is shown in Tables 5 and 6.

Table 5: Detailed start formulation of the anti-corrosive polyaspartic coating

	Component	Mass fraction (%)
Component A	Desmophen® NH 1420	43.00
	Dispersing agent	2.10
	Defoamer	0.50
	Synthetic iron oxide alpha-FeOOH	1.35
	TiO_2 rutile	10.89
	Fumed silica	0.98
	Rheology modifier	0.50
	Leveling agent	0.47
	Stabilizer	0.62
	NH_2-modified Nano SiO_2	2.00
	Adhesion promoter	1.41
	MPA (Methoxy propyl acetate)	2.60
	MOLSIV adsorbent	2.80
	Extenders	10.58
Component B	Desmodur® N 3600	20.20
Sum		100.00

Table 6: General start formulation of the anti-corrosive polyaspartic coating

Binder	63.2%
Solvent	3.9%
Additives (defoamer, rheology modifier, leveling agent, adhesion promoter, UV stabilizer, dispersing agent, anti-sedimentation agents)	5.6%
Pigments/Extenders	27.3%
	100.0%

The other important factor in the formulation of the polyaspartic coating were nanosilica particles (nano SiO_2) modified with the amino groups. The diameter of SiO_2 nanoparticles was 10–20 nm, with a specific surface area of 90–130 $m^2\ g^{-1}$, obtained from IoLiTec Ionic Liquids Technologies GmbH (Heilbronn, Germany).

Table 7: Characterization of nano SiO2

Ingredient name	Silicon dioxide (silica)
Empirical formula	SiO_2
Surface modification	amino group, dispersible
Loss on drying	< 3% (105 °C, 2h)
Loss on ignition	< 10% (950 °C, 2h)
Contents of SiO_2	> 85% (dry basis)
Contents of SiO_2	> 99.8% (950 °C, 2h)
Contents of carbon	> 0.3%
Average particle size	10–20 nm
Specific surface area	90–130 $m^2 g^{-1}$
Color	white
True density	2.2–2.6 g cm^{-3}
Bulk density	0.15 g cm^{-3}
Melting point	1610–1728 °C
Boiling point	2230 °C
pH	6.0–7.5

Nano silicon dioxide (Figure 27) is among the most versatile nanoparticles which are used in coating industries. The versatility is increased by surface modification. This material is also known as silica and it is divided into two types based on their structure:

- Porous P-type silica
- Spherical S-type silica

Each of the types has its unique properties and is used for and special applications. Nano silicon dioxide can be modified via a number of surfaces modification process. Currently, nanosilica may be modified in order to get hydrophobic and/or oleophobic particles. Nanosilica can be surface-modified with epoxy or amino groups as well; the materials are obtained by treating the nanosilica particles with suitable coupling agents. The modified nano silicon dioxide as a nanopowder is used especially in medical applications, alloys, ceramics, plastics, concretes, rubbers, glasses, and paints. The silica nanoparticles are used as a key component in the coating formulation that affects many properties, e.g. mechanical properties such as scratch resistance or opacity. Silica nanoparticles were used in this research for increasing adhesion of the film coating on metal surfaces [98, 99].

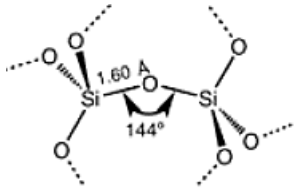

Figure 27: Chemical structure of silicon dioxide

The refractive index of silica nanoparticles is in a desirable match with many organic polymers and for this reason silica nanoparticles are considered for use in coatings. However, the surface of silica nanoparticles should be modified to obtain active particles which may incorporated into organic matrices. For SiO_2 particles to be dispersed completely and perfectly within the coating, and for those coatings to stay stable, the surface of silica nanoparticles has to be modified. The way of modification of nanoparticles should take into account all the components of the coating formulation, since silica nanoparticles are very sensitive to their environment.

Additives are other materials that have a significant effect on the properties of the coating but are used in low amounts. The selection of additives is governed by the desired result of the coating application. Some additives are used to improve the influence of each ingredient of the coating on the others.

The additives which were used in the coating formulation were carefully selected in order to improve the quality of the coating. One of the important issues was to increase adhesion at the metal/coating interface. For this reason, the adhesion promoter BYK-4510 (solution of a hydroxy-functional copolymer with acidic groups, Table 8) produced by the BYK company was used and the concentration of BYK-4510 was 1.41% based on the total formulation.

Table 8: Typical properties of BYK-4510

Acid value	30 mg KOH g^{-1}
Density (20 °C)	1.12 g ml^{-1}
Non-volatile matter	80%
(10 min., 150 °C)	
Solvents	Methoxypropanol
Flash point	48 °C

The acidic groups of this silicone-free adhesion promoter can improve adhesion on steel, galvanized steel, aluminum and non-ferrous metals because it has a strong affinity to metallic substrates.

BYK-4510 is compatible with polyisocyanate resins and reacts with them and merges in the polymer matrix. The additive is capable to improve the flexibility of coatings without decreasing their hardness. Beside the mentioned properties, this adhesion promoter may reduce the settling of fillers and inorganic pigments (TiO_2 in this research). This additive does not cause yellowing of the dried film coating and it has no negative effect on the other properties of the coating film. The positive effects of this additive on the properties of the coatings prepared in this research will be explained later.

When using inorganic pigments, the gloss of the coat may be reduced if the pigments have not been sufficiently stabilized with a suitable wetting and dispersing additive before adding the adhesion promoter.

Some other additives were used in order to improve the impact, bending, and scratch resistant as well as to increase flexibility.

According to the recommendation by the manufacturer of nano silicon dioxide, the quantity to be added is between 0.1–2.0 percent by mass of the total coating formulation (Table 9).

Table 9: The samples differing in the amount of the nanosilica added

No.	Sample label	Amount of nano silicon dioxide (per mass of the total formulation)
1	PA1	0.1%
2	PA2	0.5%
3	PA3	0.9%
4	PA4	1.2%
5	PA5	1.6%
6	PA6	1.9%
7	PA7	2.0%

In this coating, nanosilica particles were used (silicon dioxide, SiO_2) to increase and improve the adhesion. It was important to assure compatibility between the extenders, pigments, and the binder. A combination of anticorrosive pigments improved by nanosilica and additives was used in the coating. The surface of nanosilica was modified with amino groups. This amino group modified nanosilica was selected based on the fact that the coating formulation contained alpha amino acid groups as well. Besides, it was hoped that the use of nanosilica modified with amino

groups would increase the adhesion at the coating/metal interface.

The first step was to make a coating sample based on the initial formula (Figure 28). For this purpose, a sufficient amount of polyaspartic acid ester resin was weighed and different additives were admixed to the resin.

Figure 28: Admixing of the first sample of the polyaspartic coating in 2013

In this formulation method it was important to add these additives sequentially. The second essential thing was to select the proper additives based on the chemical structure because the chemical structure and compatibility of the selected additives were the significant issues. Those factors had a major influence on the characteristics of the coating in order to reach the main target, which was to enhance adhesion at the coating/metal interface. The next major properties were wettability and contact surface. Enhancing degree of wetting is in a direct relation with suitable and complete distribution of the pigment and extender particles. Therefore it was necessary, at this stage, to improve the dispersing and wetting of the solid particles in the resin.

There were many problems to disperse a combination of pigments into the binder. For solving those problems a small amount of the binder (NH 1420) was weighed and the pigments were added one by one to form a paste. The paste was processed by a pearl mill (Figure 29) to grind and disperse the pigments completely. The milling process was continued until the fineness of particles according to ASTM D1210 test method was less than 15 microns. In the second step, SiO_2 nanoparticles were dispersed in the rest of the binder by an ultrasonic disperser (Hielscher). Then, the two parts were mixed together (Figure 30) and passed through a roll mill (Figure 31) to make the final dispersion uniform.

Figure 29: The laboratory pearl mill PS-C, 3.5 liters, variable rotational speed

Figure 30: Mixing all ingredients of the coating in the final step

Figure 31: roll mill machine for grinding particles and homogenization of coating vehicle

The samples were produced based on the formulation shown in Table 5 by increasing the nanosilica percentage as mentioned in Table 9. Then, the quality and properties of the samples were evaluated by laboratory testing [100].

The 2 mm thick mild steel sheets were prepared by the surface preparation method Sa 2.5 (Figure 32) and cut into panels with dimensions 15 x 10 cm.

Figure 32: The panel prepared by the surface preparation method Sa 2.5

The panels were coated with PA1 and the other samples from Table 9 by airless spraying. The wet film thickness of the coating on the panel was 100 microns whereas the thickness of the dried film was 85 microns (according to the standard test methods ASTM D1212 and ISO 2808). Every time after applying the sample the panels were put in a place free of dust, wind, and contamination. The dried film coating on the metal panel was ready for laboratory testing after 160 h (as advised by the manufacturer of binder, hardening time = 160 h). There were two types of test methods: mechanical tests and analytical tests. The mechanical tests were applied on all seven samples of the coating and the analytical tests were applied to the final coating sample only (PA7). The mechanical tests results indicated the final formulation of the coating. The tests performed were: fineness, adhesion, film flexibility, impact, surface drying time, drying time, dry to handle, hardness, pot life at 25 °C, volume of solids, density, VOC, theoretical coverage, settling, dry film thickness, sag resistance, wet film thickness, weathering resistance, UVA 340 nm, corrosion resistance (salt spray chamber) and gloss (Figure 33). Some of the tests were defined as visual tests and the results were depending on visual observations only.

Figure 33: Some of the equipment used in mechanical testing

All the results of the mechanical tests were recorded for the final decision. The sample PA7 as a final formulation passed all the demanded and expected mechanical test results. The PA7 panel after seven days of drying the coating film was ready to set in a salt spray cabinet SF/100 CW (5% NaCl 99.8% and 38 °C).

Three coated samples with PA7 were considered: 1) PA7-N without any cut on surface 2) PA7-1 with a 7 cm cut in the center of panels 3) PA7-2 with an x-cut (7 cm per each cut) in the center of the panel. The impedance of the samples PA7-N, PA7-1, and PA7-2 was measured (by EG&G Princeton Applied Research, model 5210) before exposure in the salt spray cabinet.

In addition, the degradation of the sample PA7 was studied by Fourier transform infrared (FTIR) spectroscopy (PerkinElmer spectrometer Spectrum One, USA) before starting the corrosion resistance test. The spectra were recorded in the range of 650 to 4000 cm^{-1} and in compliance with the standard ASTM E1252-98(2007).

Finally, the polyaspartic coating (the sample PA7) was applied on the low carbon steel panel with dimensions 22 cm and analyzed by scanning electron microscopy (SEM) with energy dispersive X-ray spectroscopy (EDX) probe in order to examine the eventual existence of agglomerates of the nanoparticles in the coating structure. Scanning electron microscopy was conducted with the use of the Tescan Vega III apparatus equipped with SBU Easyprobe device, with a tungsten filament, at the charging voltage of 10 kV (for obtaining the image) and 20 kV (for obtained the X-ray spectrum). Before testing, the sample was stained with a conductive layer of gold and palladium [101].

3.2. Methods

3.2.1. Electrochemical Impedance Spectroscopy (EIS)

Almost everyone knows about the concept of electrical resistance. It is the ability of a circuit element to resist the flow of electrical current. A technique that measures the dielectric characteristics and properties of a medium as a function of frequency is EIS.

EIS is a non-destructive analysis that specifies properties between the layers of all kind of substances such as conductors, semiconductors, and insulators. Many electric parameters of the system may be checked and tested in a single EIS test with an additional advantage that the signal can be averaged over long periods to achieve higher accuracy. Choosing the proper form of the equivalent circuit used in modeling the EIS curves is the main difficulty of obtaining consistent results with the EIS technique. Depending on the specific form of the equivalent circuit, the real resistance of the coating will be one of the parameters of the model. So if an incorrect model is selected, or some of the model parameters are fixed at inappropriate values, the calculated coating resistance can be incorrect. For example, in studying self-healing coating systems, as the self-healing layer develops, the model may need to be adjusted to the new coating structure. Electrochemical impedance spectroscopy is nowadays a method that is present in almost every corrosion laboratory. The instruments have gradually decreased in size and became portable [102].

The advantages of EIS method are as follows: it is a suitable method for studying paints and coatings of high electrical resistance, the data are collected as functions of time, it is a non-destructive technique, it provides quantitative information, it is suitable method for studying corrosion in real environments. The electrochemical impedance spectroscopy is capable to separate the different steps involved in the process whose kinetics is being analyzed. Thus the electrochemical impedance has the unique possibility to separate the kinetics of the different steps involved in the total process under investigation, because as a transfer function it gives a local, linear and full description of the system under study [103].

The disadvantages of EIS include its high costs and complicated analysis used in transformation of collected information into quantitative results.

Because impedance is not a physical reality, but rather the information property of the object under investigation, the explanation of the experimental information is primarily based on the

construction of a working model, following a preliminary working theory, which must be either confirmed or discarded.

The capacitance of the coating is one of the most often studied parameters obtained by EIS measurements for characterizing the protective properties of organic coatings. For example, by analyzing this parameter it is possible to measure the water uptake phenomena which are very important in barrier coatings. The ideal trend described in many cases is not representative of the actual evolution measured on coatings. Often one phase is missing or a reduction of the coating capacitance is measured [103].

The coating capacitance is described by the following equation:

$$C = A\varepsilon_r\varepsilon_0 / d \quad , \tag{13}$$

where C is the coating capacitance, ε_r is the relative permittivity, ε_0 is the permittivity (dielectric constant) of vacuum (8.85410^{-14} F cm^{-1}), A is the area of the capacitor, and d is the distance between the two plates of the capacitor.

The relative permittivity of a coating is between 3 and 8 ambient temperatures (i.e., 293 – 298 K), and that of water is much higher, 80.2 – 82.2 in the same temperature range (the value for vacuum is 1, of course, values for other materials are given in Table 10). Therefore, water absorption by the coating will create a significant increase in its dielectric constant, with the resultant increase of the coating capacitance.

Table 10: Dielectric constants of some materials

Material	Relative permittivity, ε
Vacuum	1
Water	80.2 – 82.2
Barrier Coating	3 – 8
Teflon	2
Aluminum oxide	7
Ceramic	1200
Glass	7.5

If a coating layer absorbs water, the capacitance of the coating layer will change. EIS may be utilized to determine that change. There is an indirect relation between the thickness of a coating and its capacitance. Decreasing the coating thickness will increase the capacitance of a coating consequently. If the area of the coating increases, the capacitance of a coating increases as well [102, 103].

A coated metal with a coating which is not damaged usually has a very high impedance (Figure 34).

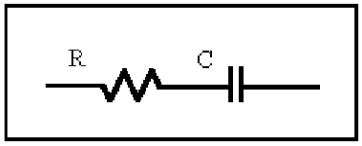

Figure 34: An equivalent electrical circuit representation of purely capacitive coating

EIS system used in this work was based on three electrodes, and included a potentiostat PalmSens 3, a frequency response analyzer and a computer with PSTrace software (Figure 35). All the impedance calculations are run by the software.

Figure 35: EIS instrument

Figure 36 shows the scheme of EIS measurements. In the first step, AC potential is applied to the sample via a reference electrode (RE). In the second step, the amount of current passed through the sample plate (or working electrode – WE) to the counter electrode (CE) is measured. For collecting the current and applying the potential the potentiostat is used. The frequency response analyzer (FRA) is responsible for calculating the impedance. The process is controlled by the computer software.

Figure 36: Scheme of electrochemical impedance spectroscopy (EIS) measurements

It is necessary to use a Faraday shield surrounding the cell for a very low level of noise in measurements. A Faraday shield reduces not only the current noise on the working electrode but also the voltage noise by the reference electrode. It is a conductive cage around the cell. Faraday shields are made of metal, conductive plastic or fine mesh wire screen. All the cell area should be surrounded with the Faraday shield entirely and permanently. The cage should be connected to potentiostat's ground terminal.

A spectrum is created by sweeping the AC potential frequency and measuring impedance over a wide frequency range. Besides, the amplitude of the AC potential disturbance remains small to limit the system to the linear region, so that the applied potential should not be a reason of irreversible change of the sample condition. As shown in Figure 37, the current response to a sinusoidal potential is the same frequency sinusoid which is shifted in phase in the linear region.

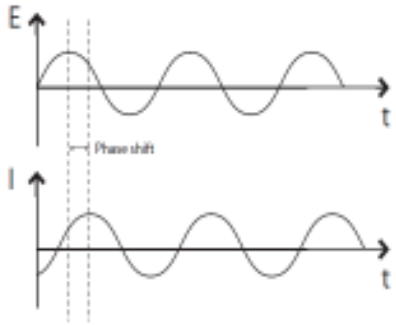

Figure 37: Sinusoidal current response in a linear system

The impedance of the sample is calculated by the simultaneous analysis of the current and potential signals. The AC potential signal is:

$$E(t) = E_{\mathrm{m}} \sin(\omega t), \tag{14}$$

where E is the potential at time t, E_{m} is the amplitude of the potential signal, $\omega = 2\pi f$ is the

angular frequency in radians per second and f is the frequency.

As it is demonstrated in Figure 31, the current response $I(t)$, of the system is at the same frequency but shifted in phase (ϕ):

$$I(t) = I_{\mathrm{m}} \sin(\omega t + \phi), \tag{15}$$

where I_{m} is the amplitude of the current signal.

According to the Ohms law, the impedance is expressed by dividing the potential by the current in the polar coordinate as:

$$\mathbf{Z}(\omega) = \mathbf{E}(t)/\mathbf{I}(t), \tag{16}$$

Actually, the impedance is a resultant of the two effects: the imaginary part and the real part. The phase angle is $\phi(\omega)$ whereas the modulus of the impedance is $|\mathbf{Z}| = E_{\mathrm{m}} / I_{\mathrm{m}}$ and by using the complex number $\mathbf{Z} = Z' + jZ''$, the impedance relationship can be exhibited in Cartesian coordinates. The imaginary number j is the square root of -1. The following relations are valid:

$$Z' = |\mathbf{Z}| \cos\phi, \tag{17}$$

$$Z'' = |\mathbf{Z}| \sin\phi, \tag{18}$$

$$\phi = \tan^{-1}(Z''/Z'), \tag{19}$$

$$|\mathbf{Z}| = \sqrt{Z''^2 + Z'^2}. \tag{20}$$

The EIS spectra are displayed in different ways. In a Nyquist plot the imaginary part of the impedance (Z''), is drawn against the real part of the impedance (Z'). The impedance magnitude $|\mathbf{Z}|$ and impedance phase angle ϕ are drawn versus frequency in a Bode and phase plot, respectively. EIS spectra are analyzed by using appropriate equivalent circuits (EC) whose components reveal physical or electrochemical properties of the system [104-112].

3.2.2. Fourier-transform infrared spectroscopy (FTIR)

Since the 1940s, dispersive IR spectroscopy instruments were commonly applied to acquire IR spectra. In recent decades, the dispersive instruments were replaced by other types of IR spectrometers using different methods of acquiring spectral data. Fourier-transform infrared spectrometers are now broadly available and they have greatly improved the quality of the

spectra collected. FTIR is relatively easily used for obtaining spectra of gaseous, liquid and solid samples. FTIR is based on IR irradiation of the samples. Some of the IR radiation passed through the sample, and the other part is absorbed by the sample.

The spectrum of the radiation absorbed by the sample molecules, or transmitted through the sample creates its "fingerprint". The infrared spectra of two molecules will differ just like the fingerprints.

Fourier-transform infrared spectroscopy (Figure 38) is based on the interference of radiation of the two beams. The difference of path length of the two beams creates a signal – an interferogram. The interferogram is then converted into frequencies by the Fourier transformation of the signal [113-115].

Figure 38: Fourier-transform infrared spectroscopy apparatus (FTIR)

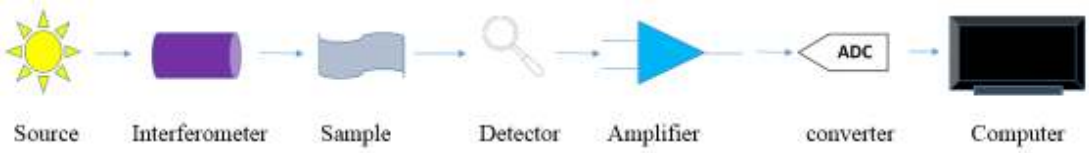

Figure 39: Main components of an FTIR spectrometer

Main components of FTIR spectrometers are shown schematically in Figure 39. The radiation emerging from the source passes through an interferometer onto the sample and then to a detector. The signal is then amplified, high-frequency contributions are removed by a filter, the data are converted into digital form by an analog-to-digital converter and then transferred to a computer for performing Fourier transformation [115]. There are two sources of radiation used in FTIR spectrometers: Globar source and Nernst source, for providing a continuous source of

infrared radiation in the mid-infrared region [115]. Nernst source is made of rare earth oxides, it has a diameter of 1–2 mm, length of 20 mm and working temperature of 1200–2200 K. Globar source is made of silicon carbide, it has a diameter of 5 mm, length of 50 mm and working temperature of 1300–1500 K. Nevertheless, high-pressure mercury lamps will be used in the far-infrared region and tungsten-halogen lamps in the near-infrared region. The resolution for an FTIR instrument is determined by the maximum path difference between the two beams. The limiting resolution in wavenumbers (cm^{-1}) is the inverse value of the path length difference (cm). In the typical FTIR the spectra are presented with the wavenumbers decreasing from left to right.

There are three main regions of the infrared spectrum (Figure 40):

- The far-infrared (<400 cm^{-1})
- The mid-infrared (4000–400 cm^{-1})
- The near-infrared (13000–4000 cm^{-1})

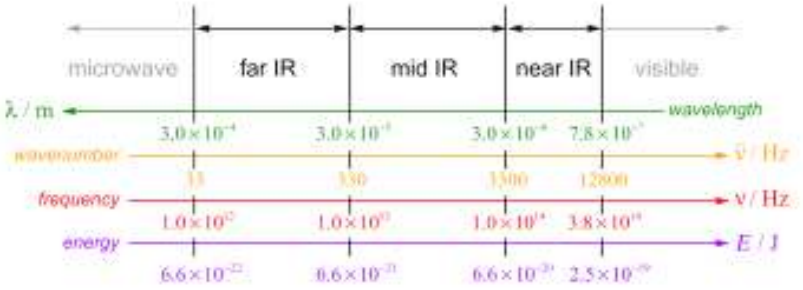

Figure 40: The infrared spectral regions [115]

There is some important information about materials provided by near and far-infrared regions, although that mid-infrared region is easier to study. Usually, there are more infrared bands in the region between 1800 and 400 cm^{-1} than in the region from 4000 and 1800 cm^{-1}.

After recording an infrared spectrum, the next important step is its interpretation. The characteristic frequencies are produced by particular parts of a molecule (structural groups) and this information can give a possibility to interpret the spectra. There are four main regions of the mid-infrared spectrum (4000–400 cm^{-1}) that include:

- X–H stretching region (4000–2500 cm^{-1})

- triple-bond region (2500–2000 cm^{-1})
- double-bond region (2000–1500 cm^{-1})
- fingerprint region (1500–600 cm^{-1})

Each band can be related to the specific bending or stretching of a bond, the movement of atoms or some special deformation of the molecule.

In the region from 4000 to 2500 cm^{-1} stretching vibrations originating from excited O–H, C–H and N–H bonds are observed. A wide band appearing in the range 3700–3600 cm^{-1} belongs to O–H stretching, whereas the range between 3400 and 3300 cm^{-1} attributed to N–H stretching is sharper than O–H stretching. Aliphatic compounds create C–H stretching bands in the range from 3000 to 2850 cm^{-1}. The wavenumber of C–H stretching increases to fall within the range from 3100 and 3000 cm^{-1} in case of C-H bonds situated near to an aromatic ring or a double bond.

In the range between 2500 and 2000 cm^{-1} absorptions by triple-bond are found. There are differences between absorption of C≡C bonds in the range between 2300 and 2050 cm^{-1} and C≡N bonds in the range between 2300 and 2200 cm^{-1} because of the high force constants of those bonds. The C≡C stretching bands are typically very weak but C≡N stretching has medium intensity. There are other absorptions in this region as well, for example characteristic absorptions of phosphorus or silicon bonds are commonly found between 2400 and 2200 cm^{-1}. The region between 2000 and 1500 cm^{-1} belongs to C=C and C=O stretching. Carbonyl stretching depends on the type of C=O bond and exists in the range between 1830 and 1650 cm^{-1}. It is easy to recognize it because it is the most intense band in the spectrum. On the other hand, the metal carbonyl stretching generally absorbs above 2000 cm^{-1}, but because of the symmetry of dipole moment those bands either do not exist or they are very weak. Their stretching occurs at 1650 cm^{-1} and in this region there is a stronger absorption which belongs to C=N stretching.

In the near-infrared region (13000–4000 cm^{-1}) there are bands of C–H, N–H or O–H stretching which are typically weak in intensity and frequently mutually overlapped so they are less useful for the analysis.

The far-infrared region (400–100 cm^{-1}) gives useful information about the vibrations of molecules including heavy atoms, molecular skeleton vibrations, molecular torsions and crystal lattice vibrations, but this region in comparison with mid-infrared region is less useful in expressing the correlations between spectra and the molecular structure.

The stretching of small groups which are bonded to a large group is dependent on the heavier group. The range where various characteristic bands (peaks) are expected to occur is shown in Figure 41.

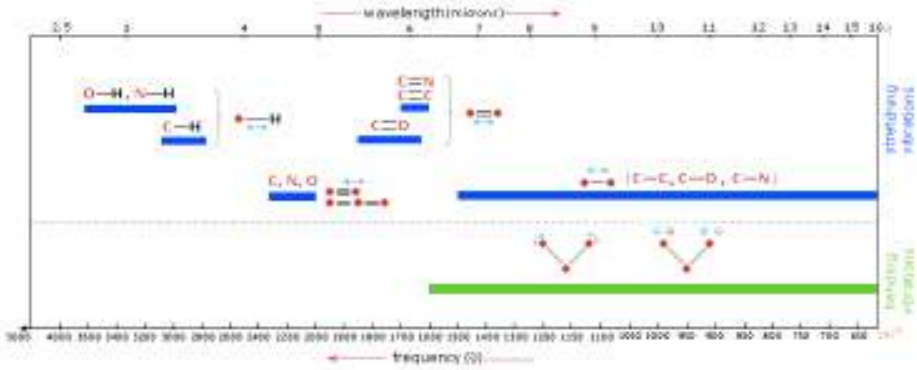

Figure 41: Characteristic wavenumbers of the peaks of various functional groups;

(The figure designed by Eric Hernandez) [116]

When using mid-infrared spectrum to assign a molecular structure some strategies should be considered:

- The high wavenumber end of the spectrum should be considered first (>1500 cm^{-1}) where major bands are to be identified
- The correlation table should be used to prepare a list of the options for all of the major bands.
- The low wavenumber end of the spectrum should be used for confirming or elaborating the possible structural elements.
- It is not possible to assign all the bands in the spectrum.
- Cross-checking should be used whenever possible.
- If there is no band in the characteristic region, this should be considered as a negative evidence, which is equally important result as any positive evidence.
- Band intensities can vary considerably for the same group.
- Solvent (if existing) can affect the position of some peaks.
- Bands characteristic for the solvent have to be subtracted from the spectrum wherever possible.

Infrared spectroscopy is used to analyze a wide variety of samples, but it cannot solve every chemical analysis problem. When used in conjunction with other methods such as mass spectroscopy, nuclear magnetic resonance, and elemental analysis, infrared spectroscopy usually makes possible the positive identification of a sample.

In modern FTIR, the spectra are compared with the ones recorded in the database. The software will find a match or close similarity of wavenumbers of absorption bands and indicate the names of the found compounds [114-119].

3.2.3. Scanning electron microscopy (SEM)

The first commercial scanning electron microscope was produced in 1966 by Cambridge Scientific Instruments, with a resolution of around 100 nm. A scanning electron microscope (Figure 42) is scanning a sample with a focused electron beam and collects an image of the sample at very high magnifications with information about sample topography and composition. The image of the surface of a material produced by SEM at high magnifications appears to be quite "realistic" and consistent with the images "expected" by human brain.

Figure 42: Scanning Electron Microscope (SEM)

Three-dimensional, high resolution images scanned by SEM give information on composition, topography, and morphology of the surface of materials.

Figure 42 shows a schematic of SEM. The electron source is located at the top of the column and produces electrons. The column is under vacuum which prevents interaction between any existing atoms and molecules with the electron beam and enables the production of high-quality images (Figure 43) [120].

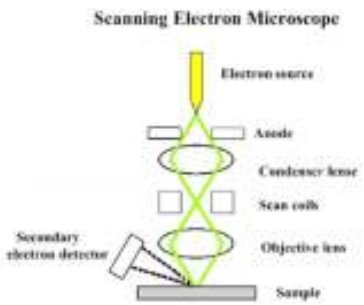

Figure 43: The schematic of SEM

The electromagnetic lenses are used for controlling the electron beam. The objective lens focuses the beam onto the sample whereas the condenser lens determines the size of the electron beam. The scan coils are used for moving the electron beam across the sample. The apertures are used in conjunction with the lenses to control the beam size. Various electrons are emitted from samples upon interacting with the electron beam. There is a detector above the sample used for the detection of backscattered electrons – BackScattered Electron (BSE) detector (Figure 44).

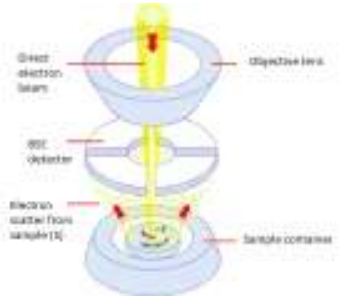

Figure 44: The location of the BSE detector

In order to enhance the efficiency of detecting secondary electrons, the secondary electron (SE) detector at the side and an angle of electron chamber are located, so it can provide more details of surface information.

The parts of SEM include the electron source – thermionic gun or field emission gun, electromagnetic lenses, vacuum chamber, sample chamber and stage, computer, detectors, secondary electron detector (SED), backscatter detector, diffracted backscatter detector (EBSD), X-ray detector (EDS). Moreover, SEM needs a permanent supplier of power, vacuum and cooling system, and vibration-free space and needs to be set in an isolated area where the instrument will be isolated from ambient magnetic and electric fields. SEM can exhibit the

details of surface information by drawing a sample in a raster pattern with an electron beam.

SEM is applicable wherever there is an interest in the characterization of solid materials. SEM indicates and determines topographical, morphological and compositional information of the surface sample. It can provide information in microstructures, examine surface contaminations, display spatial conversions in chemical compositions, make qualitative chemical analyses and recognize crystalline structures.

Advantages of a SEM include its wide field of applications, the detailed three-dimensional and topographical imaging and the multipurpose information collected from different detectors. It is easy to work with SEM if the operators are properly trained and with the use of modern software. SEM works quickly and is able to complete scanning electron imaging, BSE and EDS analyses in less than five minutes. The advanced SEM can provide data in a digital form.

The disadvantages of SEM are its size and cost. SEM instrument is very expensive as well as large, and it has to be located in an area free of any possible electric, magnetic or vibration interference. It has a special maintenance procedure which includes keeping a steady voltage and currents to electromagnetic coils and providing circulation of cool water. Moreover, for working with SEM and preparation of the samples a particular training for operators is required. All the samples have to be prepared before setting in the vacuum chamber and the preparation of samples may result in artifacts. There is no certain way to remove or recognize all potential artifacts. The researchers experienced in sample preparation can reduce the negative impact because they are able to recognize the artifacts from real data. On the other hand, there is a limitation posed on sample size – in the vacuum chamber of SEM only small solid samples can be placed (Figure 45). There is a small risk to exposure to radiation with the electrons which are scattered from below the sample surface. The operators should duly observe and handle the manufacturer's safety recommendations [121, 122].

Figure 45: the polyaspartic sample PA7 in the SEM vacuum chamber under the test

3.2.4. Contact angle goniometer

The optical contact angle (OCA) evaluating and contour analysis systems of the OCA series merge high resolution optics, exact liquid dosing, and precise sample positioning into powerful and valid measuring systems (Figure 46).

Figure 46: Goniometer DataPhysics OCA 20, Instrument for measuring the contact angle

The surfaces and hidden interfaces of polymers play an important role in the properties and applications of polymers. The analysis of polymer surfaces and interfaces in many cases requires quite special techniques, and often only a combination of different techniques can help [123]. Many interfacial phenomena appear in situations where three phases meet. The most common situation is contact between solid, liquid and gas. The three phases meet at the so-called three-phase contact line. [123].

When a system is in equilibrium, the three-phase contact line does not move as there is a balance of the tangential forces caused by the interfacial and surface tension. If a liquid is in contact with a solid and a gas, it forms the equilibrium contact angle, θ_C, at the three-phase contact line. As shown in figure 47, a vector projection on the contact plane between liquid and solid yields the Young equation:

$$\gamma_L \cos\Theta_C = \gamma_S - \gamma_{SL}, \tag{21}$$

where θ_C is the equilibrium contact angle, γ_L is surface tension of the liquid, γ_S is the surface energy of the solid and γ_{SL} is interfacial energy between solid and liquid [124].

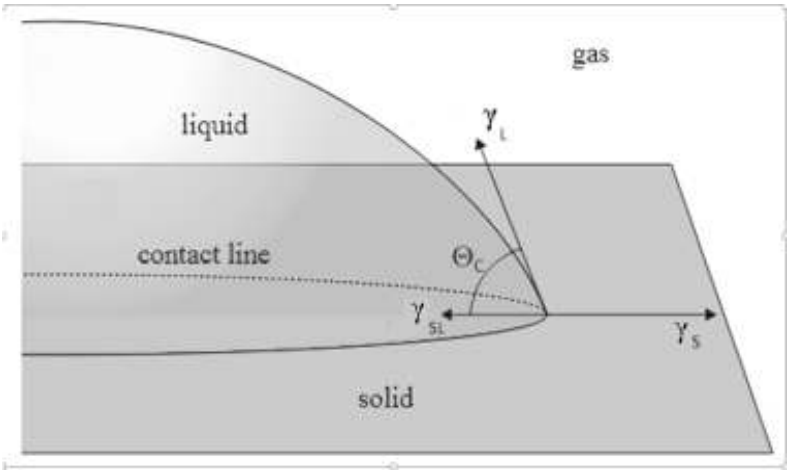

Figure 47: Contact angle at a solid-liquid-gas contact line [124]

The surface energy of the solid and the solid/liquid interfacial tension are usually unknown. Various types of interaction models between the liquid and solid are used to assess these values. There are two extreme of the equilibrium contact angle. First, the drop of liquid at 0° is uniformly and totally spread and makes a thin film of liquid on the surface which is known as a complete wetting. Second, the drop makes a sphere and touches the solid in only one single point at an angle of 180° which is known as a complete dewetting (Figure 48) [125].

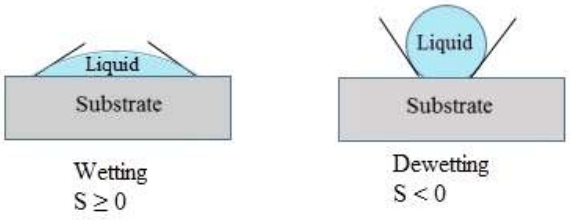

Figure 48: Difference between wetting and dewetting [125]

The contact angle is very high in some materials and liquid droplets can roll off very easily. In other words they exhibit the "lotus effect". On the other hand, there are materials with small contact angle which form a thin film layer on the surfaces, for instance paints. The equilibrium contact angle and its receding supplement may be measured optically.

The interface is the contact between two different phases; there are five different types of interfaces: liquid-gas, solid-gas, solid-liquid, solid-solid and liquid-liquid. The surface is formed at the solid-gas and liquid-gas interfaces.

The atoms/molecules of a solid or a liquid are kept together by interaction forces, which is opposite to the ideal gas situation.

Measuring contact angle and interfacial tension in order to achieve some important information is performed with the OCA systems. Some of the applications where contact angle is of importance include:

- Painting, printing and coating of metals, plastics and papers
- The progress of high efficiency composites
- The definition of the surface cleanliness of semiconductor wafers and video screen glass substrates
- The improvement of cosmetic and pharmaceutical products, e.g. pastes and creams or powder coatings
- The surface finish and textile cleaning
- The progress of surface-active plant protective
- The optimization of the adsorption behavior of absorbent papers

The measurement of the accurate temperature is significant for all thermodynamic values. Data-Physics has merged temperature evaluation and the range of display is from -10 to 400 °C in all OCA systems. The sample stage adjustable in three degrees of freedom permits a comfortable adjustment of the measuring positions on the sample body. The hollow dosing needles for the test liquids can be adjusted vertically and horizontally to the optical axis. DataPhysics of the version OCA 20L presents solutions even for uncommon sample shapes and sizes. There is the ability of the automation liquid handling and measuring in the OCA 20 by the micro-controller module. Up to four motor-driven dosing units are easily connected to the OCA 20 and the control software. The static contact angles and the dynamic wetting angles i.e. advancing and receding angles, can be measured with these devices using a fixed dosing volume. Regardless of the type of material measured, including polymers, surfactants or molten metals etc., the OCA 20 will measure the surface and interfacial tension from the contours of a pendant and sessile drops as well as of liquid layers on plates, bars and fibers [125-127].

4. RESULTS AND DISCUSSION

There were two main parts in this research: formulating a polyaspartic coating based on nanosilica to improve adhesion of the coating on the metal surface and checking the results of the polyaspartic coating with the mechanical and analytical test methods.

The dried coating film on the metal surface was expected to play a protective role against mechanical and chemical damage. The mechanical tests were performed firstly.

The hardness of the dried coating film is important as much as its flexibility. Both of those properties are indirectly related to the coating adhesion. If the dried coating film is very hard, the first severe impact on the coated metal surface will create a lot of microcracks, which causes penetration of humidity, dust, grease, and contamination to the coating/metal interface. The consequence of this penetration is loss of adhesion in this area and separation of the dried coating film from the substrate.

The samples PA1 and PA2 with the nano SiO_2 content of 0.1% and 0.5%, respectively, were rejected because flocculation was observed, the pigment was not stabilized within the vehicle, blushing and pinholes had occurred in the applied film. After 24 hours sedimentation started within the cans and created a sticky layer on the bottom of the coating cans (Figures 49 and 50) [128-130]. The problems in the sample PA1 were attributed to the small amount of dispersing agent (0.53 % by wt. total formulation). In this phase of the research, the sample preparation was performed by adding gradually and continuously the pigments and additives to the binder. The results showed that an impenetrable mass of pigments was formed within the vehicle, due to the high solid content of pigments having large particle size (which is common in high build coatings). In the presence of such a mass, the nanoparticles of SiO_2 did not have any chance to find a suitable place for setting there. The solution was found in: 1) increasing the amount of dispersing agent to form a stable coating and 2) changing the way of adding raw materials to the formulation.

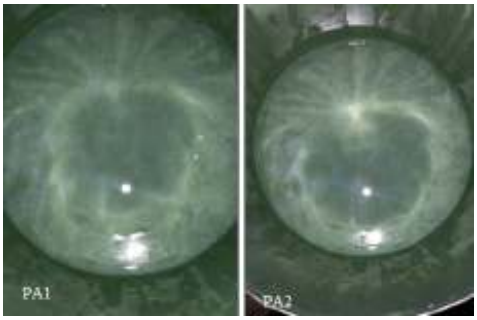

Figure 49: Samples PA1 and PA2 in the can with defects such as flocculation, lack of stabilization of pigments in the coating vehicle and blushing

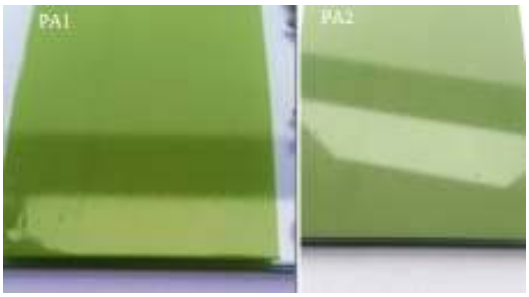

Figure 50: Too many pinholes were found in the dried film coating of PA1 and PA2

The problems were present in the samples PA3 and PA4 as well, although the amount of dispersing agent was increased to 1.00% by wt. of total formulation, a change in the order of adding raw materials was effected and the amount of nano SiO_2 was increased to 0.9%. The wet film thickness was 100 m on the low carbon steel plate. The problems did not appear immediately in the samples PA3 and PA4. There were no visual defects in the liquid coatings, but their particle size was unacceptable and they were rejected based on the result of impact test (Figure 51). The standard impact test was applied as recommended by ASTM D2794. The film rupture was caused by two main factors: lack of adhesion and insufficient flexibility of the coating film.

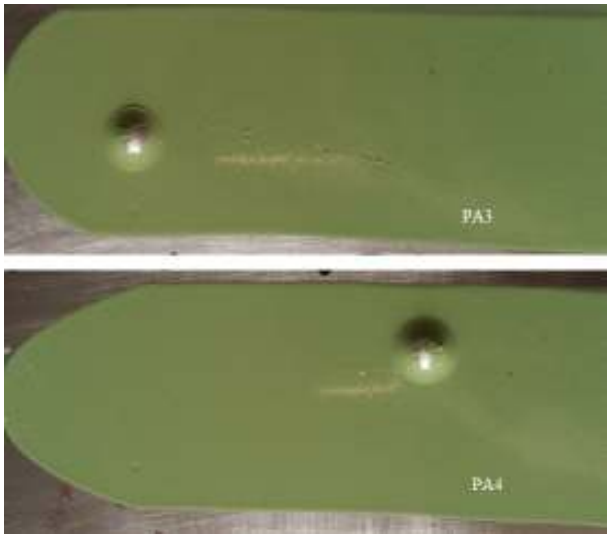

Figure 51: The result of impact test were unsatisfactory for the samples PA3 and PA4

The problems were present too with the sample PA5 with 1.6% of nanoparticles (Figure 52). It was rejected because of the results of impact and bending tests. Direct and indirect impact test results were 35 cm and 15 cm, respectively, according to ASTM D2794. The results of bending (coating flexibility) test according to ASTM D1737 were 18 mm/180° whereas the sufficient result is >4 mm/180°. After intensive study of raw materials characterization it was realized that the amounts of dispersing agent and leveling agent should be increased. Their manufacturer recommended using their maximum allowed amount [131].

Figure 52: The sample PA5 with a lot of pinholes and particle agglomerates in the dried coating film

The amount of nano SiO_2 was gradually increased with each following sample due to the failure in the adhesion test. But, as the quantity of nanoparticles increased, weak results of hardness

and flexibility tests were exhibited. Therefore, in the sample PA6 the amounts of dispersing agent and leveling agent were increased to 2.1% by and 0.47% by wt., respectively. Nevertheless, the obtained coating film showed evidences of incompatibility with increased quantities of dispersing agent as well as nanosilica (Figure 53) [132].

Figure 53: Incompatibility in the sample PA6

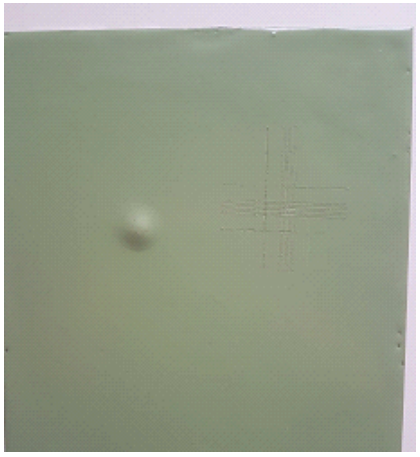

Figure 54: Weak adhesion test result (3B) and unacceptable Impact test result (50 cm)

Figure 55: The sample PA6, the results of testing in a salt spray cabinet

After careful consideration it was realized that chromium oxide (Cr_2O_3) is a cause of incompatibility with the increased amount of nanosilica (Figures 53–55).

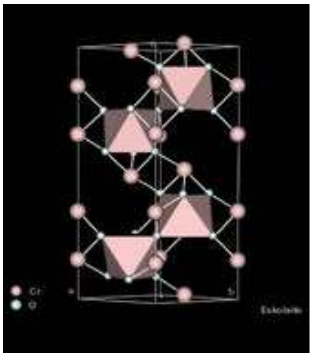

Figure 56: Chemical structure of Cr2O3

Chromium oxide has a tendency to react with the silica and form a hard mineral which causes volume instability (Figure 56). Technical information on the chromium oxide filler is presented in Table 11.

Table 11: Technical information on the chromium oxide filler (Cr2O3)

Technical data	**Approx.**
Cr_2O_3 content [%]	99
Water-soluble content [%]	0.3
Sieve residue (0.045 mm sieve) [%]	0.005
pH value [-]	5.0–7.0
Bulk density [g cm^{-3}]	1.0–1.3
Particle shape	Spherical
Predominant size [µm]	0.3
Density [g cm^{-3}]	5.2
Oil absorption [g (100 g)$^{-1}$]	11

Finally, the sample PA7 with 2.0% of the nanosilica was formulated. Consequently, the quantity of the additives was changed proportionally. The main coating formulation in this phase was changed in terms of eliminating chromium oxide (Cr_2O_3). Chromium oxide was replaced by zinc aluminum orthophosphate hydrate ZPA (Figure 57) with chemical formula $ZnAl_2(PO_4)_2(OH)_23H_2O$ (manufactured by Heubach GmbH) [133].

Actually, zinc orthophosphate is commonly used as an anticorrosive pigment to protect steel from corrosion. The attempts were done to increase the efficiency of zinc orthophosphate by its modification. Double orthophosphates were used where one of the cations is zinc.

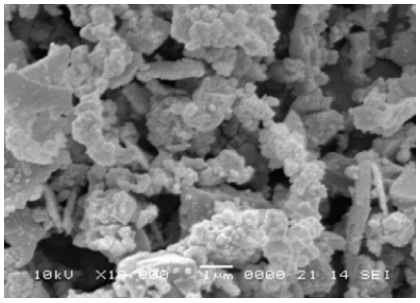

Figure 57: Hydrated zinc aluminum phosphate (ZnO 40%, Al2O3 4.5%, PO4 55.5%) (By David Veselý in the Journal Transfer inovácií)

Table 12 shows the chemical and physical characterization of zinc aluminum orthophosphate hydrate, ZPA.

Table 12: Technical information on the zinc aluminum orthophosphate hydrate (ZPA) filler

Technical data	**Approx.**
Zinc as Zn [%]	38.5–40.5
Aluminum as Al [%]	4.0–5.5
Phosphorus as PO_4^{3-} [%]	53.0–56.0
Loss on ignition 600 °C [%]	9.0–12.5
Water soluble chloride [%]	Max. 0.025
Water soluble sulfate [%]	Max. 0.05
Conductivity [S cm^{-1}]	Max. 300
pH value [-]	5.5–6.5
Density [g cm^{-3}]	2.8
Bulk density, untamped [g cm^{-3}]	0.3
Bulk density, tamped [g cm^{-3}]	0.6
Oil absorption [g $(100\ g)^{-1}$]	40
Sieve residue (32 m sieve) [%]	Max. 0.01
Average particle size [μm]	2.0–3.5

The improved impenetrability properties of the coating were obtained by combining micronized rutile titanium dioxide pigment treated with alumina and zirconia compounds and fumed silica which has been surface treated with poly dimethyl siloxane (PDMS). Those pigments were

responsible for providing a well-balanced combination of high durability and very good optical properties and stable rheological performance over time [134].

The result was excellent with remarkable improvement in adhesion at the coating/metal interface.

4.1. Mechanical testing

The important mechanical test results of PA6 are given in Table 13. According to the tests, film flexibility increased due to poor adhesion at the PA6/metal interface. On the other hand, the poor adhesion demonstrated that the PA6 surface tension is higher than the metal substrate surface free energy which caused the contact angle of PA6 on substrate to depart from the value of 0°. The result of impact resistance was in the same direction and was not satisfactory enough.

The adhesion should be improved as much as possible to reach a value appropriate to extend elongation of the coating and heal the related imperfections [133].

Hence, some pigments in the main coating formulation were changed to increase wetting and consequently to reduce the surface tension which was responsible for the sufficient and spontaneous spreading of the coating on the metal surface.

Table 13: The mechanical test results of the sample PA6

No.	Name of the test	Result	Acceptable result	Standard method
1	Fineness	15 micron	OK	ASTM D1210
2	Adhesion	4B	5B	ASTM D3359
3	Film flexibility	10 mm/180°	4 mm/180°	ASTM D522
4	Impact	Direct 55cm	Direct 80cm	ASTM D2794
		Reverse 70cm	Reverse 90 cm	
5	Surface drying time 20 °C	48 min	30 min	ASTM D1640
6	Drying time 20 °C	1 h and 53 min	1 h	ASTM D1640
7	Dry to handle 20 °C	11 h	5 h	ASTM D1640
8	Hardness by Konig after 7 days	181 s	250 s	ASTM D4366
9	Pot life	1 h and 17 min	2 h	ASTM D2196-15

As indicated by the data in Table 14 the sample PA7 prove that desirable mechanical properties of the coating film were obtained.

The final formulation was based on 2% of nanosilica particles (purity of 99.8%, surface modified with amino groups. The main concern was the dispersion of nanoparticles in the coating, which may exhibit a tendency to behave as an elastomer. In that case the wetting properties of coating are expected to decrease. For solving that problem two important additives were added: wetting and dispersing agent [135-137].

The final state of dispersion of solid particles within the liquid vehicle is governed by three aspects: 1) wetting, 2) mechanical dispersion process and 3) stabilization. It is important to achieve complete wetting of the pigment particles to spread them perfectly within the liquid phase of the coating vehicle to. According to the Young equation:

$$\cos\Theta_c = \left(\gamma_S - \gamma_{SL}\right)/\gamma_L , \tag{22}$$

or

$$\gamma_S = \gamma_{SL} + \gamma_L \cos\Theta_c , \tag{23}$$

where γ_S is the free surface energy of the solid substrate, γ_{SL} is the interfacial tension between the solid and the liquid, γ_L is the surface tension of the liquid and θ_c is the contact angle between the solid and the liquid. In the case of complete wetting θ_c is zero and consequently:

$$\gamma_L = \gamma_S - \gamma_{SL} . \tag{24}$$

This means that if the purpose is to spread the solid particles in the liquid phase, the liquid surface tension should be lower than the free surface energy of the solid. The lower surface tension of liquid results in a better wetting of pigments.

The molecular size of additives is important issue, too. For instant, there is a possibility that large molecule of additives for instant keep the nanoparticles inside their bulk volume and trap them. Therefore it was considered to select a nanosized dispersing agent for dispersing nanosilica [137].

The role of mechanical dispersion process is to break up the large particles agglomerates into primary particles and smaller agglomerates by grinding or some other suitable mechanical action. This process increases the contact surface of pigment particles.

For sufficient stabilization, the molecules of an additive should be adsorbed strongly in contact

with the surface of pigment particles. The adsorption of additive molecules is achieved by ionic bonding, hydrogen bonding or dipole interaction between the groups or segments of additive molecules and the pigment surface.

Commonly, the structures of wetting and dispersing agents are amphiphilic which means that they possess both hydrophilic and lipophilic properties. The difference between wetting and dispersing agents is merely in their molecular weight; wetting agents have smaller molecules than dispersing additives [138].

One of the methods for checking if the pigments in the vehicle are sufficiently wet or dispersed is by measuring the particle size distribution by Grindometer. As shown in Table 14, the fineness of particles in the sample PA7 was 15 m, as measured by the Grindometer gauge (VF2110, ASTM D 1210). This is an excellent result because the fineness of conventional high build coatings is not less than 40 m. The pigment particles were therefore wetted and dispersed very efficiently.

Generally, nanosilica may provide a high level of scratch and wear resistance that will indirectly affect the adhesion. The results of gloss test are also shown in Table 14. Common protective coatings will show 10% reduction of gloss after 1000 h of exposure to UVA radiation, but the investigated PA7 film put into the UVA cabinet showed a reduction of just 12% after 2000 h of exposure. Gloss reduction points to a start of chalking process which later results in a decrease of scratch resistance and adhesion. The result shows that the PA7 nanocoating may be a better option to use on metal surfaces, which improves and extends the lifecycle of the protective coating.

Obtaining adhesion in the coating/metal interface is a big concern of all protective coating manufacturers. Adhesion is molecular attraction between dissimilar materials. The adhesion in the interface is promoted primarily by increasing the potential of a coating to wet and the substrate and spread over it and consequently to create maximum molecular contact. The other factors are time, pressure, and temperature, chemical compatibility of the material, surface roughness etc. [139].

The work of adhesion between metal (solid, S) and coating (liquid, L), W_{SL}, may be expressed by the following equation:

$$W_{SL} = \Lambda\gamma = \gamma_S + \gamma_L - \gamma_{SL}. \quad (25)$$

The larger the work, the better the adhesion, which means that low values of the interfacial

tension γ_{SL} will promote the adhesion. By combining Equation (25) with Young equation (23) the work of adhesion is:

$$W_{SL} = \gamma_L \left(1 + \cos \Theta_c\right) \quad (26)$$

The work of adhesion is a thermodynamic quantity and related to the contact angle. Low values of contact angle give higher values of work of adhesion will be high [138-140].

The first experiments on the sample PA7 indicated a lack of adhesion after 1000 h in a salt spray chamber. The same was true for PA7-2, which exhibited a lot of blisters over the whole panel as shown in Figure 58.

Figure 58: PA7-2 after 1000 h under the salt spray test before adding more adhesion promoter and surface agent

This result showed that the amount of adhesion promoter and surface agent additives should be increased to enhance adhesion of PA7 in harsh atmosphere and under mechanical stress [141, 142]. Unsatisfactory adhesion of PA7 is illustrated in Figure 59.

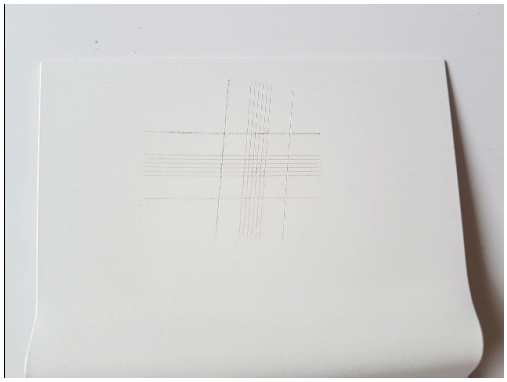

Figure 59: Adhesion test result of the sample PA7 before adding adhesion promoter (BYK-4510); the result is B4

The adhesion promoter (BYK-4510) which was used is a hydroxy-functional copolymer with acidic groups. This type of silicone-free adhesion promoter with acidic groups promotes the

chemical affinity of a coating to metallic surfaces in particular. BYK-4510 reacts with polyisocyanates and is consequently merged with the polymer matrix. The adhesion promoter may improve the flexibility of the coating without reducing hardness, but it depends on the coating system.

Adhesion test results are included in Table 14, which shows that the complete wetting and low surface tension of the PA7 sample (after adding the adhesion promoter) are the two main factors to improve the adhesion. The result according to the cross-cut test was excellent (5B, Figure 60).

Figure 60: Adhesion test result of the sample PA7 after adding adhesion promoter (BYK-4510); the result is 5B

The result of the impact test shown in Figure 61 proved that the flexibility of the sample PA7 is excellent both in direct impact and reverse impact; the coating sample withstood significant elongation without suffering damage.

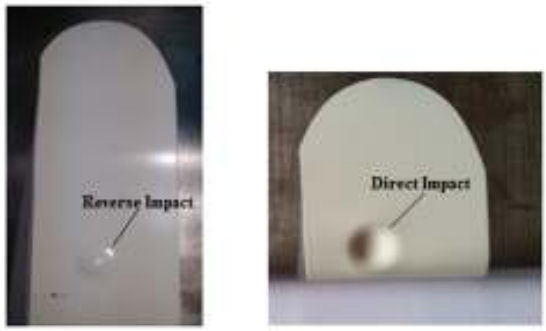

Figure 61: Impact test result of the sample PA7

Figure 62 indicates that the elasticity under Mandrel bending test, adhesion, and elongation

ability of the dried film PA7 had a perfect result. There were no cracks or microcracks in the dried film PA7 after bending of 180° on a 2 mm cylinder.

Figure 62: Bending test results of the sample PA7

The samples PA7-N, PA7-1, and PA7-2 exposed in the neutral salt spray test cabinet (5% NaCl, 38 °C) revealed excellent results after exposure of 2556 h. Figure 63 shows the surface of PA7-1 (horizontal cut), and PA7-2 (x-cut) samples after exposure – PA7 seems to be protective enough in those cases as well.

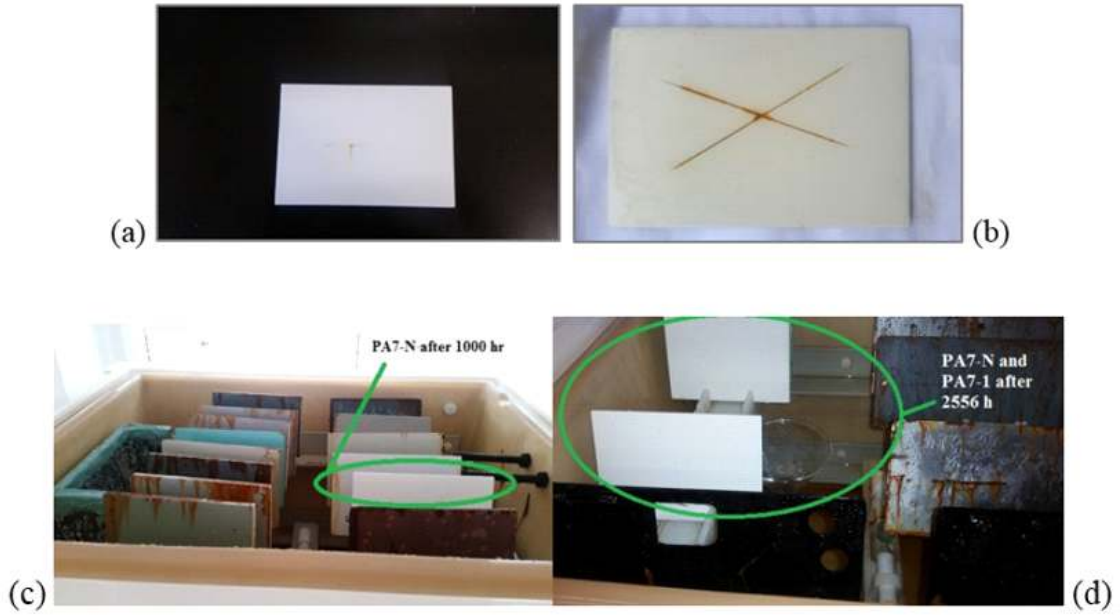

Figure 63: (a) Coated panel with the polyaspartic coating PA7-1 with horizontal cut and (b) coated panel with the polyaspartic coating PA7-2 with x-cut after exposure to 2500 hours of ASTM B117 salt spray test and (c, d) coated panel with the polyaspartic coating PA7-N without cut and PA7-1 with horizontal cut after exposure to 1000 and 2556 hours of ASTM B117 salt spray test.

Table 14 shows the results of different test methods performed in this study on the sample PA7.

Table 14: The mechanical results of the sample PA7 as a final formulation

No.	Name of the test	Result	Acceptable result	Standard method	Remark
1	Fineness	15 µm	OK	ASTM D1210	
2	Adhesion	5B	5B	ASTM D3359	
3	Film flexibility	2 mm/180°	4 mm/180°	ASTM D522	
4	Impact	direct 100 cm	direct 80 cm	ASTM D2794	
		reverse 100 cm	reverse 90 cm		
5	Surface drying time	20 min	30 min	ASTM D1640	20 °C
6	Drying time	45 min	1h	ASTM D1640	20 °C
7	Dry to handle	5 h	5 h	ASTM D1640	20 °C
8	Hardness	261 s	250 s	ASTM D4366	by Konig after 7 days, Test method A
9	Pot life at 25 °C	3h	2h	ASTM D2196-15	
10	Volume of solids	86%	87%	ASTM D5201-05a	may vary by color
11	Density	1.47 g L^{-1}	1.5 g L^{-1}	ASTM D 1475	
12	VOC	114 g L^{-1}	120 g L^{-1}	ASTM D2369-10	
13	Theoretical coverage	16 m^2 L^{-1}	12 m^2 L^{-1}	ASTM D2697-03(2014)	
14	Settling	10	10	ASTM D869	10 → perfect suspension and 0 → fail
15	Dry film thickness	85 µm	N/A	ISO 2808	
16	Sag resistance	No sag	N/A	ASTM D4400	(75 – 300 µm)
17	Wet film thickness	100 µm	N/A	ASTM D1212	
18	Weathering resistance UVA 340 nm	< 2100 h No chalking	N/A	ASTM D4587	cycle: 8 h UV / 4 h condensation, 60±5 °C
19	Corrosion resistance (salt spray)	2500 h, no rust and blisters (on cut panel)	N/A	ASTM B117	Dry film thickness of the tested panel was 200 µm. On x-cut panel the result was different.
20	Gloss	60° – 98 (before UV test) 60° – (after 2000 h UV test)	N/A	ASTM D523	After 2000 h in UVA cabinet, the reduction was approximately 12%

4.2. Scanning electron microscopy (SEM) results

The polyaspartic coating (sample PA7) was applied on the panel with dimensions 22 cm made of low carbon steel and analyzed by SEM and EDX (Tescan Vega III, SBU EasyProbe scanning electron microscope) in order to examine the existence of agglomeration of the nanoparticles in the coating structure. The evaluation was under accelerating voltage of electron beam (10 kV) and at different magnifications [143].

An analysis of the protective coating on the metal substrate via scanning electron microscopy

(SEM) with the energy dispersive X-ray spectrometry (EDX) was performed. The analysis should determine the possibility of the presence of any agglomerates of the SiO_2 nanoparticles in the dried coating film structure (Figure 64).

In the dried film of sample PA7, larger particles were noticed, but the EDX analysis showed that they were pigment particles or some filler in all cases. The EDX results of the individual particles are shown in Table 15. No sign of agglomerates of the SiO_2 nanofiller was detected (Figure 65) [144].

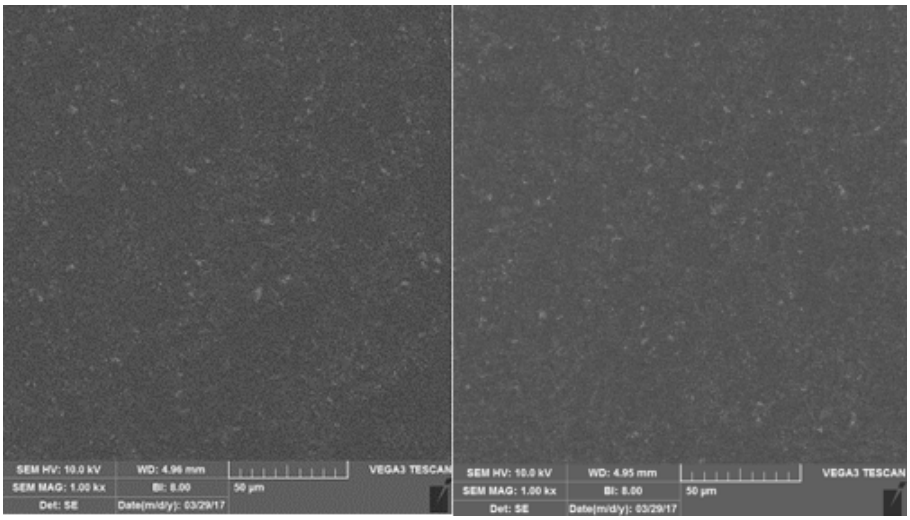

Figure 64: Particles in the sample PA7 as shown by SEM

Table 15: Composition of individual particles of PA7 tested by EDX (accuracy ± 2%)

Particle	Composition, wt. %
#1	41% Ba, 7% S, 2% Au
#2	36% Ba, 6% S, 3% Au
#3	21% Ca, 13% Mg, 5% Au, 2% Cr
#4	14% Ba, 9% Cr, 5% Au, 3% Ti, 1% S
#5	35% Cr, 16% Ba, 12% Ti, 8% Au, 2% Pd
#6	7% Cr, 4% Au, 3% Ba, 2% Si, 2% Ti
#7	21% Ba, 17% Cr, 16% Ti, 11% Au, 5% Si, 2% Pd

The difference to the sum of 100% is attributed to carbon, nitrogen, and hydrogen. Gold and palladium originate from the fragments of conductive coating used in the sample preparation.

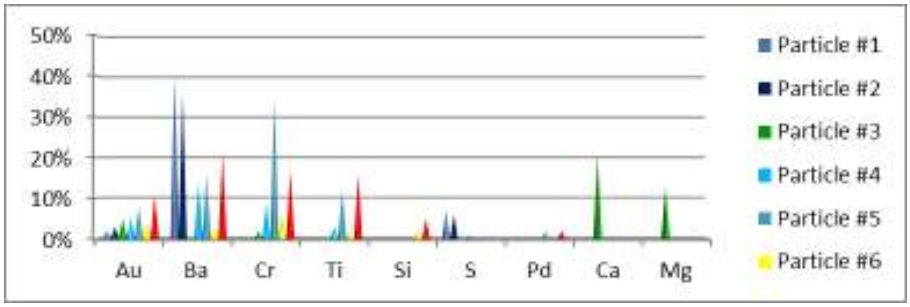

Figure 65: Compositions of individual particles of PA7 tested by EDX (accuracy ± 2%)

4.3. Electrochemical impedance spectroscopy (EIS) results

In impedance spectroscopy, a small sinusoidal potential was applied on the sample over a wide frequency range, from 10^4 to 10^{-2} Hz. The controlling computer system recorded the current response induced by the potential and in addition the phase angle between the maxima of potential and current [145]. The high-performance sample PA7 was exposed to 5% NaCl at 38 °C for 446 days and the impedance was measured continuously. Figure 66 shows Nyquist plots for different times of exposure. The sample PA7 had very high impedance in the beginning, but its impedance slowly decreased in time and then rose again.

The impedance of protective coatings at 0.1 Hz may be taken as an indicator of the protective properties of the coating. High quality coatings are excellent electrical insulators with electrical resistivity typically higher than 10^9 Ωcm^2. Good quality coatings have a resistivity between 10^8 and 10^9 Ωcm^2, fair quality coatings have a resistivity between $10^{6.5}$ and 10^8 Ωcm^2, and poor coatings have a resistivity lower than $10^{6.5}$ Ωcm^2 [142]. Figure 66 shows the variation of impedance at 0.1 Hz with time. As it can be seen, after 446 days the result demonstrated impedance higher than 10 Ωcm^2, which meant excellent corrosion protection. The average logarithm of impedance was 9.50±0.44.

From the impedance recorded at 100 Hz, capacitance, dielectric constant and water uptake of the coating (shown in Figure 67) could be calculated by the following formulae [146]:

$$C = 1 \Big/ \left(2\pi f \left| Z \right|_{@100\,\mathrm{Hz}} \right), \tag{27}$$

$$\varepsilon_{\mathrm{r}} = Cd \big/ \varepsilon_0 A, \tag{28}$$

$$\varphi = \frac{\log_{10}\left(C_t / C_0 \right)}{d \log_{10} \varepsilon_{\mathrm{W}}}, \tag{29}$$

where C is the coating capacitance, C_0 is the initial coating capacitance, C_t is the coating

capacitance at time t, ε_0 is the permittivity of vacuum, ε_r is the relative permittivity of the coating, is the water uptake, A is the area of the panel, and d is the coating thickness.

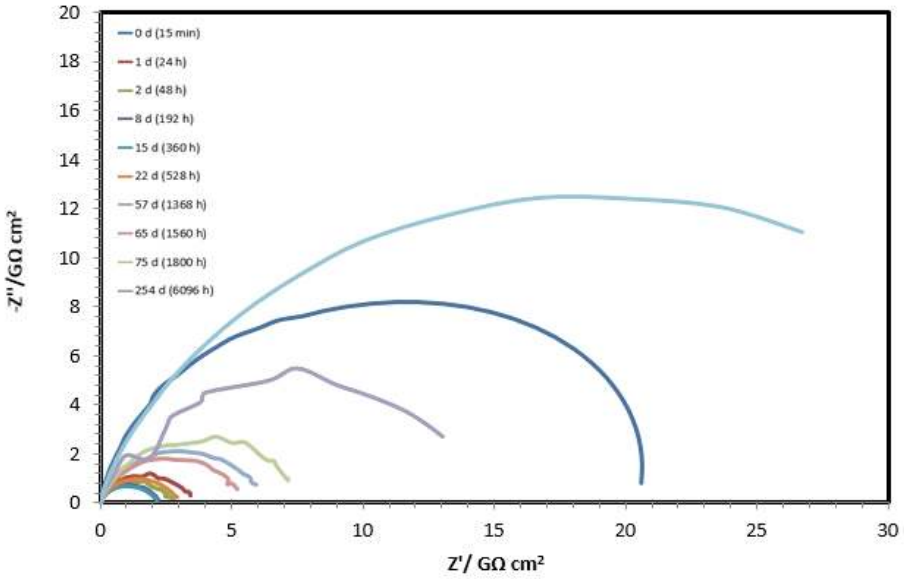

Figure 66: EIS spectra of the test PA7 panel as a function of immersion time

(Nyquist plot – log IZ'I vs. log IZ˝I) during 466 d

The average value of capacitance equals 1.30±0.13 nF cm^{-2}, of the dielectric constant equals 4.43±0.45 and of the water uptake equals 7.12±1.41%. These values indicate that the coating has retained its protective properties throughout the period of exposure [147].

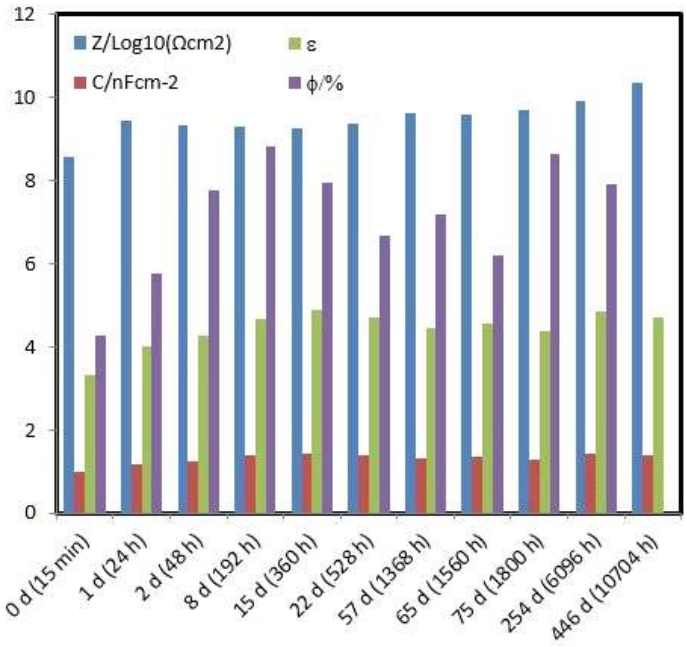

Figure 67: PA7 coating parameters calculated from EIS measurements for different times of exposure to 3.5% NaCl

There are many studies on water uptake, water absorption and anticorrosive properties of protective coatings. Based on information similar to that shown in Figures 66 and 67, some coating properties may be predicted as well as its durability on metal surfaces. The coating deterioration and corrosion rate are commonly calculated from the two main factors – coating capacitance *C* and impedance *Z*, both obtained by EIS.

As the results of many studies in this field have proved, the type of resin, coating thickness and temperature all influence the coating capacitance. Chemical nature of the resin strongly affects dielectric and water uptake properties of the coating. Polyurethane-based coatings are characterized by the low water uptake, because of the functional groups present in the polyurethane backbone. The polyurethane-based coatings exhibit good corrosion protection performance.

On the other hand, the dielectric properties of a coating are also influenced by the thickness of the coating film. Commonly, the coating capacitance increases with time until the saturation of the coating film with water and then it remains constant. The constant value for the thicker coating film is reached in a longer time in comparison with the thinner coating film and the coating capacitance for thicker coating film is smaller than for the thinner film. When the saturation is attained and the constant value of the coating resistance is reached, the thicker coating films exhibit higher resistance. The value of water uptake is related to the coating film

thickness as well, so higher water uptake values are found in thicker films. Water penetrates gradually into the coating film and eventually forms a new liquid/metal interface under the coating film which initiates corrosion.

In addition to the mentioned factors, ambient temperature is important, too. Water uptake of the polymer increases with rising temperature.

Commonly, high solid polyurethane coatings are able to prevent corrosion on metal surfaces in harsh conditions such as buried pipelines or undersea constructions. In the presented experiments, the high solid polyaspartic coating (PA7) was applied to mild steel. The experiments showed that despite of the low thickness of the film the water uptake did not increase in time. The PA7 sample displayed the ability to decrease the corrosion rate even when applied as thin (dry) coating film; the impedance results in Figure 66 showed that the coating resistance to water penetration increased over time moderately [148-153].

4.4. Fourier-transform infrared spectroscopy (FTIR) results

The degradation of the sample PA7 was studied by Fourier-transform infrared spectroscopy (FTIR), a practical technique for evaluating and diagnosing the reason of decreasing adhesion in organic coatings. The spectra were recorded in the range of 650 to 4000 cm^{-1} according to the standard ASTM E1252-98(2007). The sample was characterized before starting the corrosion resistance test and after 1 day, 700 h, 1500 h and 2500 h. The results are shown in Figure 68.

Main absorption bands were found at ~3356 cm^{-1}, ~2927 cm^{-1}, ~2856 cm^{-1}, ~1713cm^{-1}, ~1519 cm^{-1}, ~1453 cm^{-1}, ~1361 cm^{-1}, ~1218 cm^{-1}, and ~1016 cm^{-1}, which may be attributed to the vibration of N–H, C–H, C=O (ester), C=O (amide), CH_2, and CH_3 groups. Therefore, these graphs indicate the presence of esters and amines groups. The band at 3356 cm^{-1} is attributed to N–H group of polyurethane. The absorption bands at ~1218 cm^{-1}, ~1016 cm^{-1} may be due to the vibration of the Si–O groups. The absorbance values of all the bands remained unchanged during the research, which means that there was practically no degradation during the period of 2500 h exposure in the salt spray cabinet. The absence of degradation points to the high adhesion at the coating/metal interface in harsh conditions and the coating may be predicted to have a long service life. [154-156].

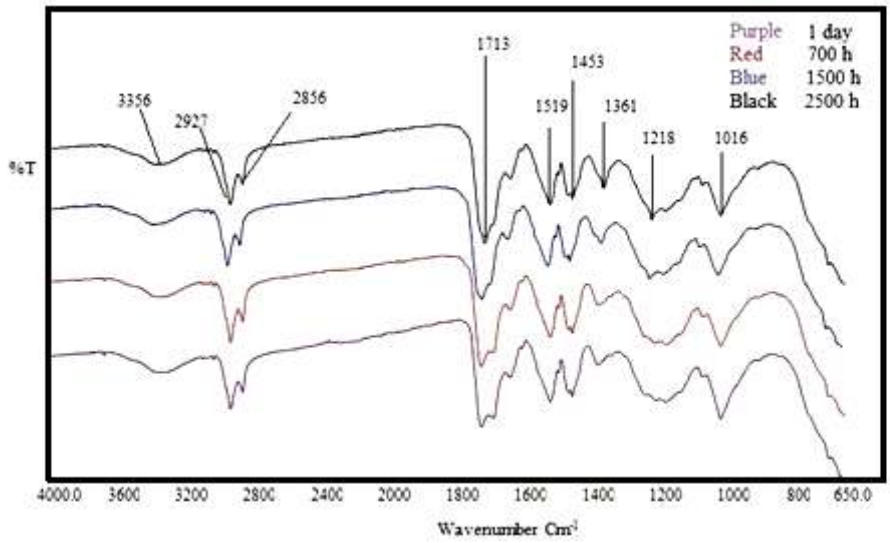

Figure 68: FTIR spectra of the sample PA7 as a function of time of exposure in the salt spray cabinet

4.5. Contact angle measurement results

Contact angle measurements were performed on an OCA 20 goniometer by DataPhysics Instruments GmbH (Figure 69).

Mild steel sample plates were prepared according to surface preparation standard Sa 2.5 (ASTM D7127, roughness of 45 μm). The sample plates were degreased with xylene before contact angle measurements, as well as before applying the coatings.

Contact angle measurements were performed on a bare mild steel sample plate, as well as on sample plates covered with protective coating samples PA6 and PA7. The following test fluids were used with the known free surface energy values: water (redistilled water), diiodomethane (99%, Aldrich), formamide (99.5%, Fluka). The measurements were carried out at the temperature of 23±1 °C with a 4 μl drop. Five measurements were carried out at different locations of the same sample and the mean values of the contact angles were calculated. The standard deviation of the measured data was max. ±2.0. The obtained values of free surface energy were used for the calculation of the system adhesion parameters: thermodynamic adhesion work, W = [N m^{-1}], free interface energy, γ = [N m^{-1}], and the spreading parameter, S.

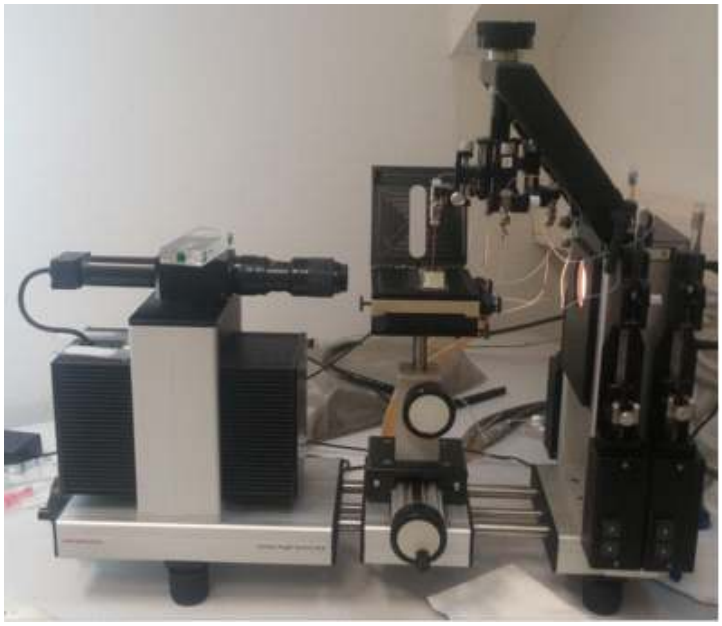

Figure 69: Goniometer DataPhysics OCA 20 for measuring the contact angle

Owens-Wendt-Kaelble method was used for calculating the surface free energy of a metal from the contact angle with a coating. In this method, the surface free energy is divided into polar and disperse part. According to Young's equation, there is a relationship between the contact angle γ_C, the surface tension of the coating, γ_C, the interfacial tension between the metal and coating, γ_{MC} and the surface free energy, γ_M, of the metal. This is in fact Eq. (23) written with different indices:

$$\gamma_M = \gamma_{MC} + \gamma_C \cos\Theta_C \,, \tag{30}$$

γ_{MC} is an unknown variable which has to be determined. The interfacial tension $_{MC}$ is calculated from γ_M and γ_C and the similar interactions between the phases. These interactions are interpreted as the geometric mean of a disperse part, γ^d, and a polar part, γ^p, of the surface tension or surface free energy:

$$\gamma_{MC} = \gamma_M + \gamma_C - 2\sqrt{\gamma_M^d \cdot \gamma_C^d} - 2\sqrt{\gamma_M^p \cdot \gamma_C^p} \,, \tag{31}$$

d denotes the dispersion forces and p stands for the polar forces. At least two liquids with known disperse and polar parts of the surface tension are required to determine the surface free energy of the solid, wherein at least one of the liquids must have a polar part larger than zero.

Generally, the contact angle is determined by the surface energy. There are many factors which influence the surface tension at the metal/coating interface and consequently the contact angle.

They will determine the wetting and the adhesion strength. One of the factors is the roughness of the metal surface. If the surface roughness is of the same order of magnitude as the molecular size, then the surface roughness can influence the surface energy. The surface roughness profile and the bonding at the coating layer interface are not related directly. The surface energy matching will be positive for wetting of the coating which means good adhesion.

In case of sufficient roughness of the surface, the coating layer can create an appropriate mechanical link with the surface, which leads to a strong adhesion. However, if the surface roughness profile is not well-developed, the adhesion will be weak. So, wetting alone is necessary but not sufficient for good adhesion.

In order to achieve a proper adhesion, strong interaction is needed. The strongest adhesion is achieved by covalent bonding at the interface. In case of the presence of water molecules, van der Waals bonding will not be sufficient so the surface should be very dry to achieve adequate adhesion.

The smaller is the interfacial tension at the coating/metal interface the better will be the wetting of the surface. The increase in wetting is accompanied by the reduction of the contact angle, γ_c, and $\theta_c = 0$ means complete wetting. Thus, a high free surface energy of coating causes a low surface tension in the interface.

The obtained results of surface free energy calculated by the Owens-Wendt-Kaelble method (OW) are shown in Table 16.

Table 16: Contact angles and surface free energy calculated by the Owens, Wendt and Kaelble method (OW)

Sample	Contact Angle (degree)			Surface Energy (N m^{-1})		
	H_2O	formamide	diiodomethane	γ	γ^d	γ^p
Metal	51.3±1.2	50.8±2.1	36.6±1.9	37.54	33.08	4.46
PA6	50.2±3.0	33.8±0.4	5.1±1.0	58.71	44.64	14.07
PA7	72.1±2.3	59.5±0.3	39.5±0.3	41.71	35.08	6.63

The results show that γ for PA7 is larger than γ for the metal surface.

Regarding the γ, γ^d, γ^p of the coating samples (PA6, PA7) and metal surface in table 16, the adhesion parameters were calculated by the following equations.

$$W = \gamma_M + \gamma_C - \gamma_{MC}, \tag{32}$$

$$S = \gamma_M - \gamma_C - \gamma_{MC} . \quad (33)$$

The results are shown in Table 17.

Table 17: Calculation of Adhesion Parameter by the Owens-Wendt& Kaelble model (OW)

Sample	Adhesion Parameter (N m^{-1})		
	γ_{MC}	W_{MC}	S
M/PA6	3.56	33.98	30.98
M/PA7	0.25	120.71	37.29

Contact angle γ_c, is calculated by Eq. 30. $\cos\theta_c$ for PA6 and PA7 are 0.58 and 0.98 which gives γ_c of 55° and 27°, respectively. Therefore, better wetting of the metal surface is achieved by PA7.

The work of adhesion for PA7 is 120.71 N m^{-1}m which illustrates excellent contact and stronger intermolecular interaction of the sample PA7 in comparison with the sample PA6.

Based on Eq. 33, the coating wets the metal substrate partially if $S < 0$. If $S > 0$, the coating completely wets the metal substrate. Both PA6 and PA7 samples have $S > 0$ and both of them are able to completely wet the metal surface. Their adhesion strength is determined by other adhesion parameters [157-159].

4.6. Optical microscopy images

Using a Dino-Lite digital microscope and the corresponding Dino Capture 2.0 software, the images of the samples of the PA7 nano coating at the magnification of 65 were obtained, as shown in Figure 70. The figure shows no creep or rust in the coating film. On the edge of crack of the panel there are no blisters and swelling observed. Therefore, it may be concluded that the rate of corrosion is reduced drastically by using the PA7 on the metal surface.

Intrinsically, the coating chemical structure should be deteriorated with elapse of time due to polymer aging. The coating is in good state at the cut despite of the harsh atmosphere conditions in the salt spray cabin. This is yet another evidence that PA7 provides excellent protection against corrosion and corrosive situation in long exposure times.

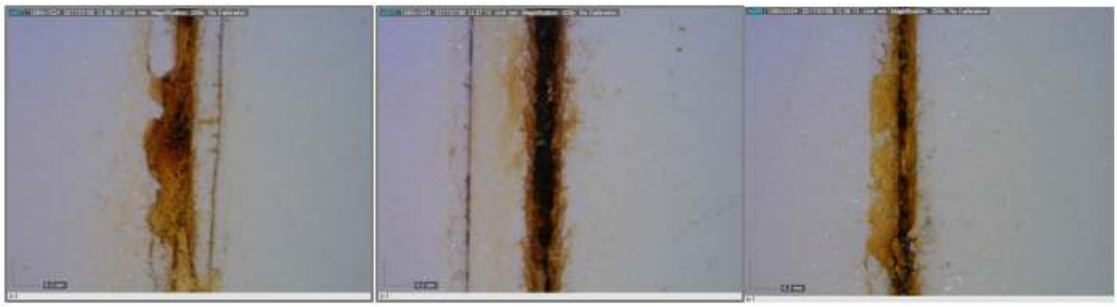

Figure 70: Microscopic picture of cutting on the panel coated by the PA7 sample after 2500 hours in salt spray cabin

4.7. Comparison with other coatings

Table 18 demonstrates the results of the comparison pf improved polyaspartic coating PA7 and the conventional protective coating systems for highly corrosive environments such as marine splash zones. As it can be seen, there is a huge difference in results. The VOC decreased significantly. In addition, the coverage of the coating was practically doubled comparing to other coating samples. The result of the immersion test after 10704 h and high impedance prove that the adhesion did not deteriorate, as the coating capacitance was almost constant, which is shown in Figure 68. The impedance range (log*Z*) was higher than 10 Ω cm^2 proving that PA7 is a high performance coating in comparison with other samples.

Table 18: Comparison of some properties of the improved polyaspartic coating and conventional anti-corrosive coating systems

Property in corrosivity category C5-M Very high (Marine)	**Sample A**	**Sample B**	**Sample C**	**Sample D**
VOC (g L^{-1})	114	250	442	276
Coverage (m^2 L^{-1})	16	8	7–9	10
Immersion test, Method A (h)	> 10704	< 2500	> 2500	> 2500
Impedance after 10000 h (Ω cm^2)	> 10	≥ 8	< 8	< 8
Dry to handle time at 25 °C (h)	8	12	24	24

Sample A = The improved polyaspartic coating PA7 (DTM)
Sample B = Polyaspartic coating (Conventional, DTM)
Sample C = Zn-rich Epoxy/Epoxy/PU
Sample D = Epoxy/Epoxy/PU

5. CONCLUSION

The polyaspartic coating polymer base was improved by adding nanosilica. The coating film formed by reaction between the polyaspartic ester and an aliphatic polyisocyanate as a crosslinker is highly stable, hard and extremely resistant against weathering and abrasion. Additionally, the polyaspartic ester was a good choice for formulating high performance protective coating on steel surfaces. One of the important materials in the chemical structure of the polyaspartic coating was nano SiO_2 modified with amino groups, with diameter of 10–20 nm. The refractive index of silica nanoparticles is in a desirable match with many organic polymers, and for this reason silica nanoparticles were considered to be used in the coating.

The adhesion promoter BYK-4510 was compatible with polyisocyanate resin NH 1420, reacted with it and merged in the polymer matrix. The adhesion promoter acted interestingly because it improved the flexibility of coating without decreasing its hardness. Beside the mentioned properties, this adhesion promoter reduced the settling of fillers and inorganic pigments in the coating vehicle.

The formulated coating applied directly to the carbon steel surface in a thin layer of 85 microns of dry film thickness showed excellent protection against chemical and mechanical damage. According to the test results, this coating reduces the number of layers to be applied compared to the conventional coating systems, has high resistance, ultra-low volatile organic compound (VOC) content (114 g L^{-1}), and consequently reduces maintenance costs and environmental impact of the coating process.

Various coating characteristics indicate that it retained its protective properties throughout the period of exposure of 2500 hours in the salt spray cabinet, showing no signs of degradation, as confirmed by FTIR measurements. Additionally, SEM and EDX analysis results showed no signs of agglomeration of nanosilica filler. High coating impedance (> 10^9 Ωcm^2) was retained throughout the period of 10704 h of exposure to 3% NaCl solution, while the coating capacitance remained practically constant, and water uptake remained < 9%. The results of OCA 20 for measuring contact angle confirmed that the coating sample PA7 has strong adhesion on the metal surface due to complete wetting and very small contact angle. The surface tension of the coating is very low and, subsequently, the intermolecular interaction is very strong. So, the results indicate that using nanosilica with other suitable pigments and additives in the coating formulation provides a resilient coating with good prospects of attaining a long service

lifetime. According to these results, the investigated nanosilica polyaspartic coating shows outstanding properties and presents a significant progress in formulating nanocomposite protective coating systems.

6. REFERENCES

1. R. Lambourne, T. A. Strivens, Paint and Surface Coatings; Theory and Practice, 2nd ed., William Andrew Publishing, Norwich, NY, USA, 1999, pp. 1-4.
2. Z. W. Wicks Jr., F. N. Jones, S. P. Pappas, Organic Coatings: Science and Technology, 2nd ed., Wiley Interscience Publication, Hoboken, NJ, USA, 1999, pp. 1-6.
3. M. Moses, Understanding Color: Creative Techniques in Watercolor, Sterling Publishing Company, New York, NY, USA, 2007, pp. 1-8.
4. G. H. Koch, M. P. H. Brongers, N. G. Thompson, Y. P. Virmani, J. H. Payer, Corrosion Costs and Preventive Strategies in the United States, FHWA, NACE, USA, 2001.
5. A. R. Marrion, The Chemistry and Physics of Coatings, 2nd ed., RSC Publishing, Cambridge, UK, 2004, pp. 1-7.
6. L. L. Shreir (ed.), Corrosion: Corrosion Control, Newnes, Boston, MA, USA, 2013, pp. 1-7.
7. R R. Lambourne, T. A. Strivens, Paint and Surface Coatings; Theory and Practice, 2nd ed., William Andrew Publishing, Norwich, NY, USA, 1999, pp. 5-7.
8. W. M. Bos, Prediction of Coating Durability – Early Detection Using Electrochemical Methods, Doctoral Dissertation, Technical University Delft, the Netherlands, 2008, pp. 1-139.
9. J. R. Davis, Corrosion: Understanding the Basics, ASM International, Materials Park, OH, USA, 2000, pp. 1-49.
10. Chemical Economics Handbook, Paint and Coatings Industry Overview, IHS Markit, London, UK, 2017.
11. B. N. Popov, Corrosion Engineering: Principles and Solved Problems, Elsevier, Technology & Engineering, Amsterdam, the Netherlands, 2015, pp. 558.
12. Kusumgar, Nerlfi & Growney's multiclient study, Global Paint & Coatings https://www.coatingsworld.com/issues/2017-09-01/view_market-research/kusumgar-nerlfi-amp-growney-publish-third-global-p (accessed on October 21, 2018)
13. K. B. Tator, Nanotechnology: The future of coatings – Part 1, Materials Performance 53 (2014) 34-36.
14. C. Buzea, I. I. Pacheco, K. Robbie, Nanomaterials and nanoparticles: Sources and toxicity, Biointerphases 2 (2007) MR17-MR71.
15. K. R. Sharma, Process Considerations for Nanostructured Coatings, in Anti-Abrasive Nanocoatings Current and Future Applications, M. Aliofkhazraei (ed.), Woodhead Publishing,

Cambridge, UK, 2015, pp. 137-153.

16. https://www.nanowerk.com/how_nanoparticles_are_made.php (accessed on October 12, 2018)

17. E. E. Stansbury, R. A. Buchanan, Fundamentals of Electrochemical Corrosion, Chapter 1, ASM International, Materials Park, OH, USA, 2000, pp. 1-20.

18. Z. Ahmad, Principles of Corrosion Engineering and Corrosion Control, Elsevier, Amsterdam, the Netherlands, 2006, pp. 1-13.

19. J. G. N. Thomas, The Electrochemistry of Corrosion, G. Hinds (ed.), http://www.npl.co.uk/upload/pdf/electrochemistry-of-corrosion.pdf (accessed on October 12, 2018)

20. D. A. Snow, M. J. Schofield, Definitions of Corrosion, Plant Engineer's Reference Book 2nd ed., Butterworth-Heinemann, Oxford, UK, 2003, pp. 1-25.

21. W. S. Tait, Corrosion Prevention and Control of Chemical Processing Equipment, in Handbook of Environmental Degradation of Materials 2nd ed., M. Kutz (ed.), Elsevier, Amsterdam, the Netherlands, 2012, pp. 863-886.

22. I. Kartsonakis, I. Danilidis, G. Pappas, G. Kordas, Encapsulation and Rrelease of corrosion inhibitors into titania nanocontainers, J. Nanosci. Nanotechnol. 10 (2010) 1-9.

23. Z. Ahmad, Principles of Corrosion Engineering and Corrosion Control, Elsevier, Amsterdam, the Netherlands, 2006, pp. 271-274.

24. A. Augustyniak, Smart Epoxy Coatings for Early Detection of Corrosion in Steel and Aluminum, in Handbook of Smart Coatings for Materials Protection, A. S. H. Makhlouf, Woodhead Publishing, Cambridge, UK, 2014, pp. 560-585.

25. R. Lewarchik, Understanding corrosion inhibitive pigments, Prospector, July 2014, https://knowledge.ulprospector.com/744/pc-corrosion-inhibitive-pigments/ (accessed on October 12, 2018)

26. V. E. Carter, Metallic Coatings for Corrosion Control: Corrosion Control Series, Newnes-Butterworths, Oxford, UK, 2013, pp. 1-108.

27. E. M. Fayyad, M. A. Almaadeed, A. Jones, A. M. Abdullah, Evaluation techniques for the corrosion resistance of self-healing coatings, Int. J. Electrochem. Sci. 9 (2014) 4989-5011.

28. W. Freitag, D. Stoye, Paints, Coatings and Solvents, John Wiley & Sons, Hoboken, NJ, USA, 2008, pp. 1-7.

29. R. Talbert, Paint Technology Handbook, CRC Press, Boca Raton, FL, USA, 2007, pp. 55-61.

30. I. Hamerton, Recent Developments in Epoxy Resins, Rapra Technology, Shawbury, UK, 1996, pp. 1-8.

31. http://www.pslc.ws/macrog/epoxy.htm (accessed on October 12, 2018)

32. B. Ellis, Introduction to the Chemistry, Synthesis, Manufacture and Characterization of Epoxy Resins in Chemistry and Technology of Epoxy Resins, B. Ellis (ed.), Springer Science & Business Media, Berlin, Germany, 2012, pp. 1-30.

33. P. A. Schweitzer, Paint and Coatings; Applications and Corrosion Resistance, CRC Press, Boca Raton, FL, USA, 2006, pp. 111-112.

34. C. G. Munger, Causes and Prevention of Paint Failure in Good Painting Practice, Steel Structures Paint Manual, Steel Structures Painting Council, Pittsburgh, PA, USA, 1994.

35. R. Lewarchik, Acrylic Resin Fundamentals, Prospector, April 2016, https://knowledge.ulprospector.com/4320/pc-acrylic-resin-fundamentals/ (accessed on October 12, 2018)

36. L. L. Shreir (ed.), Corrosion: Corrosion Control, Newnes, Boston, MA, USA, 2013, pp. 43.

37. D. G. Weldon, Failure Analysis of Paints and Coatings, John Wiley & Sons, Hoboken, NJ, USA, 2009, pp. 90-96.

38. Z. Czech, A. Butwin, E. Herko, B. Hefczyc, J. Zawadiak, Novel azo-peresters radical initiators used for the synthesis of acrylic pressure-sensitive adhesives, Express Polym. Lett. 2 (2008) 277-283.

39. E. Sharmin, F. Zafar, Polyurethane: An Introduction, Chapter 1, Intech, 2012, https://www.intechopen.com/books/polyurethane/polyurethane-an-introduction, (accessed on October 13, 2018)

40. M. Gibril, R. El-Jazwi, F. M. Shuaeib, Recent advances in protective coating of crude oil storage tanks, The 6th Libyan Corrosion Conference, Tripoli, Libya, 2007, pp. 460-472, https://www.researchgate.net/publication/234311546_Recent_Advances_in_Protective_Coating_of_Crude_Oil_Storage_Tanks (accessed on October 13, 2018)

41. M. Bock, Polyurethanes for Coatings, Vincentz, Hannover, Germany, 2001, pp. 11-59.

42. http://www.coatings.covestro.com (accessed on October 13, 2018)

43. M. Jeffries, Polyaspartic Coatings – High-profile Protective and Marine Applications, Webinars of the Coatings Society, https://www.paintsquare.com/education/branding_images/12-18-13Polyaspartic%20Webinar%20Protective%20and%20Marine.pdf (accessed on October 13, 2018)

44. P. A. Sørensen, S. Kiil, K. Dam-Johansen, C. E. Weinell, Anticorrosive coatings: A review, J. Coat. Technol. Res. 6 (2009) 135-176.

45. A. R. Marrion, A. Guy, Coatings Components Beyond Binders, in The Chemistry and Physics

of Coatings, A. R. Marrion (ed.), RSC Publishing, Cambridge, UK, 2004, pp. 267-291.

46. M. J. Austin, Anti-Corrosive Inorganic Pigments, in Surface Coatings: Volume 1, Raw Materials and Their Usage, Oil and Colour Chemists' Association (ed.), Springer Science & Business Media, Berlin, Germany, 2012, pp. 409-530.

47. J. Repp, J. P. Ault, A. Sheetz, Zinc-rich coatings – how they work and how to check if they'll work, Elzly Technology Corporation, Ocean City, NJ, USA, http://elzly.com/wordpress/wp-content/uploads/2018/05/Paper_20435_final.pdf (accessed on October 13, 2018)

48. G. Buxbaum, G. Pfaff, Industrial Inorganic Pigments, John Wiley & Sons, Hoboken, NJ, USA, 2006, pp. 195-228.

49. H. A. H. Gundersen, High Temperature Cathodic Disbonding of Organic Coatings on Submerged Steel Structures, Master Thesis, Norwegian University of Science and Technology, Department of Materials Science and Engineering, 2011.

50. L. Isaksen, The effect of barrier pigments in coatings, https://www.linkedin.com/pulse/effect-barrier-pigments-coatings-lasse-isaksen/ (accessed on October 13, 2018)

51. J. M. D. Lane, G. S. Grest Spontaneous asymmetry of coated spherical nanoparticles in solution and at liquid-vapor interfaces, Phys. Rev. Lett. 104 (2010) 235501.

52. J. V. Koleske, R. Springate, D. Brezinski, Additives reference guide, Paints & Coating Industry 30 (2014) 38-90.

53. L. W. McKeen, Fluorinated Coatings and Finishes Handbook, William Andrew Publishing, Norwich, NY, USA, 2006, pp. 89-97.

54. A. Forsgren, Corrosion Control through Organic Coatings, CRC Press, Boca Raton, FL, USA, 2006, pp. 50-51.

55. International Maritime Organization, Anti-fouling Systems, 2002, http://www.imo.org/en/OurWork/Environment/Anti-foulingSystems/Documents/FOULING2003.pdf (accessed on October 13, 2018)

56. https://www.coatingsworld.com/issues/2016-07-01/view_market-research/world-paint-amp-coatings-demand-to-reach-54-7-mill/ (accessed on October 13, 2018)

57. J. Baghdachi, Smart Coatings, ACS Symp. Ser. 1002 (2009) 3-24.

58. I. Khana, Kh. Saeed, I. Khan, Nanoparticles: Properties, applications and toxicities, Arab. J. Chem., DOI:10.1016/j.arabjc.2017.05.011

59. W. Dubbert, K. Schwirn, D. Völker, P. Apel, Use of Nanomaterials in Coatings, Fact Sheet, Federal Environment Agency, Germany, 2014,

https://www.umweltbundesamt.de/sites/default/files/medien/378/publikationen/use_of_nanomaterials_in_coatings_0.pdf (accessed on October 13, 2018)

60. AZO Materials, Nanomaterials and Their Applications, 2001, https://www.azom.com/article.aspx?ArticleID=1066 (accessed on October 13, 2018).

61. http://agencia.fapesp.br/nanoparticles-coated-with-antibiotic-eliminate-drug-resistant-bacteria/25473/ (Image: M. Borba Cardoso, accessed on October 21, 2018)

62. B. S. Murty, P. Shankar, B. Raj, B. B. Rath, J. Murday, Applications of Nanomaterials, Springer, Berlin, Germany, 2013, pp. 107-148.

63. F. Presuel-Moreno, M. A. Jakab, N. Tailleart, M. Goldman, J. R. Scully, Corrosion-resistant metallic coatings, Materials Today 11, (2008) 14-23.

64. P. J. Rivero, J. A. Garcia, I. Quintana, R. Rodriguez, Design of nanostructured functional coatings by using wet-chemistry methods, Coatings 8 (2018) 76.

65. N. Nuraje, W. S. Khan, Y. Lei, M. Ceylan, R. Asmatulu, Superhydrophobic Electrospun Nanofibers, J. Mater. Chem. A 1 (2013) 1929-1946.

66. M. Cloutier, D. Mantovani, F. Rosei, Antibacterial coatings: challenges, perspectives, and opportunities, Trends Biotechnol. 33 (2015) 637-652.

67. K. Saini, D. Das, M. K. Pathak, Thermal barrier coatings -applications, stability and longevity aspects, Procedia Eng. 38 (2012) 3173-3179.

68. L. Wu, X. Guo, J. Zhang, Abrasive resistant coatings – A review, Lubricants 2 (2014) 66-89.

69. Y. C. Yuan, T. Yin, M. Z. Rong, M. Q. Zhang, Self-healing in polymers and polymer composites. Concepts, realization and outlook: A review, Express Polym. Lett. 2 (2008) 238-250.

70. S. K. Ghosh, Self-healing Materials: Fundamentals, Design Strategies, and Applications, Wiley-VCH, Weinheim, Njemačka, 2008, pp. 1-28.

71. B. Swatowska, T. Stapinski, K. Drabczyk, P. Panek, The role of antireflective coatings in silicon solar cells – the influence on their electrical parameters, Opt. Appl. 41 (2011) 487-492.

72. P. M. Carmona-Quiroga, R. M. J. Jacobs, S. Martinez-Ramirez, H. A. Viles, Durability of anti-graffiti coatings on stone: natural vs accelerated weathering, PLOS ONE (2017), doi:10.1371/journal.pone.0172347.

73. M. J. Pitkethly, Nanomaterials – the driving force, Mater. Today 7 (2004) 20-29.

74. C. Soma, P. Wick, H. Krug, B. Nowack, Environmental and health effects of nanomaterials in nanotextiles and facade coatings, Environ. Int. 37 (2011)1131-1142.

75. I. J. Yu, M. Gulumian, S. Shin, T. H. Yoon, V. Murashov, Occupational and Environmental

Health Effects of Nanomaterials, Biomed. Res. Int. 2015 (2015) 789312, doi:10.1155/2015/789312

76. A. Pietroiusti, H. Stockmann-Juvala, F. Lucaroni, K. Savolainen, Nanomaterial exposure, toxicity, and impact on human health, WIREs Nanomed Nanobiotechnol. (2018), doi:10.1002/wnan.1513.

77. R. D. Handy, B. J. Show, Toxic Effects of nanoparticles and nanomaterials: Implications for public health, risk assessment and the public perception of nanotechnology, Health Risk Soc. 9 (2007) 125-144.

78. Sh. J. Ikhmayies, Characterization of nanomaterials, JOM 66 (2014) 28-29.

79. D. Guo, G. Xie, J. Luo, Mechanical properties of nanoparticles: basics and applications, J. Phys. D Appl. Phys. 47 (2013) 013001.

80. Sh. Chaturvedi, P. N. Dave, N. K. Shah, Applications of nano-catalyst in new era, J. Saudi Chem. Soc. 16 (2012) 307-325.

81. M. McCully, M. Sanchez-Navarro, M. Teixido, E. Giralt, Peptide mediated brain delivery of nano- and submicroparticles: a synergistic approach, Curr. Pharm. Des., 24 (2018) 1366-1376.

82. B. Halamoda-Kenzaoui, M. Ceridono, P. Urbán, A. Bogni, J. Ponti, S. Gioria, A. Kinsner-Ovaskainen, The agglomeration state of nanoparticles can influence the mechanism of their cellular internalization, J. Nanobiotechnology 15 (2017):48.

83. B. MacEvoy, The material attributes of paints, https://www.handprint.com/HP/WCL/pigmt3.html (accessed on October 14, 2018).

84. M. Caldorera-Moore, N. Guimard, L. Shi, K. Roy, Designer nanoparticles: Incorporating size, shape, and triggered release into nanoscale drug carriers, Expert Opin. Drug. Deliv. 7 (2010) 479-495.

85. J. D. Robertson, L. Rizzello, M. Avila-Olias, J. Gaitzsch, C. Contini, M. S. Magoń, S. A. Renshaw, G. Battaglia, Purification of nanoparticles by size and shape, Sci. Rep. 6 (2016) 27494

86. M. A. Gatoo, S. Naseem, M. Y. Arfat, A. M. Dar, Kh. Qasim, S. Zubair, Physicochemical properties of nanomaterials: implication in associated toxic manifestations, BioMed Res. Int. 2014 (2014) 2014, 498420.

87. P. van Broekhuizen, F. van Broekhuizen, R. Cornelissen, L. Reijnders, Use of nanomaterials in the European construction industry and some occupational health aspects thereof, J. Nanopart. Res. 13 (2011) 447-462.

88. S. K. Kulkarni, Nanotechnology: Principles and Practices, Springer, Berlin, Germany, 2014, pp. 55-76.

89. P. Maier, A. Richter, R.G. Faulkner, R. Ries, Application of nanoindentation technique for structural characterisation of weld materials, Mater. Charact. 48 (2002) 329-339.

90. K. H. Wuehrer, Bringing polyaspartic technology to the next level: low viscous solvent-free floor coatings, Bayer Material Science, 2014, https://docplayer.net/48869088-Bringing-polyaspartic-technology-to-the-next-level-low-viscous-solvent-free-floor-coatings-envvt-2014-karl-h.html (accessed on October 14, 2018).

91. E. P. Squiller, T. D. Wayt, J. Forsythe, K. E. Best, A. Olson, A. Ekin, Polyaspartic coating compositions, Covestro LLC, EP2970556A4, 2016-10-26.

92. D. J. Primeau, L. Hanson, R. V. Scott, The true polyurea spray elastomer story: chemistry, advances and applications, Meeting of the Thermoset Resin Formulators Association, Montreal, Quebec, Canada, 2006, https://www.trfa.org/erc/docretrieval/uploadedfiles/Technical%20Papers/2006%20Meeting/Primeaux_paper.pdf (accessed on October 14, 2018)

93. C. Angeloff, E. P. Squiller, K. E. Best, Two-component aliphatic polyurea coatings for high productivity applications, Journal of Protective Coatings & Linings, August 2002, 42-47, https://www.paintsquare.com/library/articles/Two_Component_Aliphatic_Polyurea_Coatings_for_High_Productivity_Applications.pdf (accessed on October 14, 2018)

94. J. F. Dormish, Polyaspartic Coatings, Adhesives & Sealants Industry, March 2016, https://www.adhesivesmag.com/articles/94477-polyaspartic-coatings (accessed on October 14, 2018).

95. E. P. Squiller, C. Angeloff, K. E. Best, Polyaspartics: An aliphatic coating technology for high productivity applications, SSPC (The Society for Protective Coatings) 2006 Conference Proceedings, January 2006, 1-21.

96. I. Shimoyama, Thermoset Polyurethanes, in Handbook of Thermoset Plastics, 2nd edition, S, H. Goodman (ed.), William Andrew Publishing, Norwich, NY, USA, 1998, pp. 269–301.

97. A. Goldschmidt, H. J. Streitberger, BASF Handbook on Basics of Coating Technology, Vincentz, Hannover, Germany, 2003, pp. 27-253.

98. I. Kuli, M. Abu-Lebdeh, E. H. Fini, S. A. Hamoush, The use of nanosilica for improving mechanical properties of hardened cement paste, Am. J. Eng. Appl. Sci 9 (2016) 146-154.

99. G. Gündüz, Chemistry, Materials, and Properties of Surface Coatings: Traditional and Evolving Technologies, DEStech Publications, Lancaster, PA, USA, 2015, pp. 641-701.

100. X. J. Raj, T. Nishimura, Electrochemical investigation into the effect of nano-titania on the protective properties of epoxy coatings on mild steel in natural seawater, Int. J. Petrochem. Sci. Eng.

2 (2017) 29-37.

101. A. Amirudin, D. Thierry, Application of electrochemical impedance spectroscopy to study the degradation of polymer-coated metals, Prog. Org. Coat. 26 (1995) 1-28.

102. D. Vladikova, The technique of the differential impedance analysis, Part I: basics of the impedance spectroscopy, Proceedings of the International Workshop "Advanced Techniques for Energy Sources Investigation and Testing", Sofia, Bulgaria, 2004, https://pdfs.semanticscholar.org/b6ac/e8d1aba6e3e917b590045eacdc6352746b38.pdf (accessed on October 21, 2018).

103. F. Deflorian, L. Fedrizzi, S. Rossi, P. L. Bonora, Organic coating capacitance measurement by EIS: ideal and actual trends, Electrochim. Acta 44 (1999) 4243-4249.

104. Gamry Instruments, EIS of Organic Coatings and Paints, Application note, https://www.gamry.com/assets/Application-Notes/EIS-of-Organic-Coatings-and-Paints.pdf (accessed on October 14, 2018).

105. S. Amand, M. Musiani, M.E. Orazem, N. Pebere, B. Tribollet, V. Vivier, Constant-phase-element behavior caused by inhomogeneous water uptake in anti-corrosion coatings, Electrochim. Acta, 87 (2013) 693-700.

106. R. Cabrera-Sierra, M. Miranda-Hernández, E. Sosa, T. Oropeza, I. González, Electrochemical characterization of the different surface states formed in the corrosion of carbon steel in alkaline sour medium, Corros. Sci., 43 (2001) 2305-2324.

107. M. E. Orazem, B. Tribollet, Electrochemical impedance spectroscopy, Wiley, Hoboken, N.J., USA, 2008.

108. M. Sánchez, N. Aouina, D. Rose, P. Rousseau, H. Takenouti, V. Vivier, Assessment of the electrochemical microcell geometry by local electrochemical impedance spectroscopy of copper corrosion, Electrochim. Acta, 62 (2012), pp. 276-281.

109. F. Mansfeld, Concerning the display of impedance data, Corrosion 44 (1988) 558-559.

110. W.J. Lorenz, F. Mansfeld, Determination of corrosion rates by electrochemical DC and AC methods, Corros. Sci. 21 (1981) 647-672.

111. F. Mansfeld, M.W. Kendig, S. Tsai, Evaluation of corrosion behavior of coated metals with ac impedance measurements, Corrosion 38 (1982) 478-485.

112. F. Mansfeld, M.W. Kendig, Impedance spectroscopy as quality-control and corrosion test for anodized Al-alloys, Corrosion 41 (1985) 490-492.

113. A. A. Ismail, Frederick R.van de Voort, J. Sedman, Fourier transform infrared spectroscopy:

Principles and applications, in Techniques and Instrumentation in Analytical Chemistry, Vol. 18, J. R. J. Paré, J. M. R. Bélanger (eds.), Elsevier, Amsterdam, the Netherlands, 1997, pp. 93-139.

114. A. Stuart, Infrared Spectroscopy: Fundamentals and Applications, Wiley, Hoboken, NJ, USA, 2004, pp. 1-135.

115. http://www.benjamin-mills.com/chemistry/A-level/IR/ (accessed on October 14, 2018).

116. T. Woods, C. Reid, Fourier Transform Infrared Spectroscopy, Industrial Sample Analysis Polymer, Research Centre School of Physics, https://www.tcd.ie/CMA/misc/ftir.pdf (accessed on October 14, 2018).

117. S. A. Perusich, Fourier transform infrared spectroscopy of perfluorocarboxylate polymers, Macromolecules 33 (2000) 3431-3440.

118. F. Deflorian, L. Fedrizzi, S. Rossi, Electrochemical impedance spectroscopy and Fourier transform infrared spectroscopy of natural and accelerated weathering of organic coatings, Corr. Sci. 54 (1998) 598-605.

119. J. Coates, Interpretation of Infrared Spectra, A Practical Approach, Encyclopedia of Analytical Chemistry, John Wiley & Sons, Hoboken, NJ, USA, 2000, pp. 10815–10837.

120. F. Krumeich, Properties of electrons, their interactions with matter and applications in electron microscopy, http://www.microscopy.ethz.ch/downloads/Interactions.pdf, (accessed on October 15, 2018)

121. A. V. Crewe, P. S. D. Lin, The use of backscattered electrons for imaging purposes in a scanning electron microscope, Ultramicroscopy 1 (1976) 231-238.

122. J. B. Bindell, Scanning Electron Microscopy, in Encyclopedia of Materials Characterization, C. R. Brundle, C. A. Evans, Jr., S. Wilson (eds.), Butterworth-Heinemann, Oxford, UK, 1992, pp. 70-84.

123. M. Stamm, Polymer Surface and Interface Characterization Techniques, in Polymer Surfaces and Interfaces, M. Stamm (ed.). Springer, Berlin, Germany, 2008.

124. Y. Yuan, T. R. Lee, Contact Angle and Wetting Properties, in Surface Science Techniques, Vol. 51, G. Bracco, B. Holst (eds.), Springer-Verlag, Berlin, Germany, 2013, pp. 3-34.

125. DataPhysics, Contact angle, https://www.dataphysics-instruments.com/knowledge/understanding-interfaces/contact-angle/ (accessed on October 15, 2018)

126. D. Gentili, G. Foschi, F. Valle, M. Cavallini, F. Biscarini, Applications of dewetting in micro and nanotechnology, Chem. Soc. Rev. 41 (2012) 4430-4443.

127. D. P. Subedi, Contact angle measurement for the surface characterization of solids, Himalayan Phys. 2 (2011) 1-4.

128. Y. Yonemoto, T. Kunugi, Discussion on a mechanical equilibrium condition of a sessile drop on a smooth solid surface, J. Chem. Phys. 130 (2009) 144106

129. R R. Lambourne, T. A. Strivens, Paint and Surface Coatings; Theory and Practice, 2nd ed., William Andrew Publishing, Norwich, NY, USA, 1999, pp. 185-283.

130. J. Bieleman, Additives for Coatings, Wiley-Vch Press, Weinheim, Germany, 2000, pp. 65-224.

131. A. S. Khanna, High-Performance Organic Coatings, CRC Press, Boca Raton, FL, USA, 2008, pp. 56-120.

132. G. T. Bayer, M. Zamanzadeh, Failure Analysis of Paints and Coatings, http://www.plant-maintenance.com/articles/failure_analysis_paint_coating.pdf (accessed on October 15, 2018)

133. Z. W. Wicks Jr., F. N. Jones, S. P. Pappas, Organic Coatings: Science and Technology, 2nd ed., Wiley Interscience Publication, Hoboken, NJ, USA, 1999, pp. 675-680.

134. G. Gündüz, Chemistry, Materials, and Properties of Surface Coatings: Traditional and Evolving Technologies, DEStech Publications, Lancaster, PA, USA, 2015, pp. 343-515.

135. D. Veselý, P. Veselý, Anticorrosive coatings with content of non toxic Ca-titanate pigment, Transfer inovácií 15 (2009) 99-106, https://www.sjf.tuke.sk/transferinovacii/pages/archiv/transfer/15-2009/pdf/099-106.pdf (accessed on October 21, 2018)

136. M. M. Mirza, E. Rasu, A. Desilva, Influence of Nano Additives on Protective Coatings for Oil Pipe Lines of Oman, Int. J. Chem. Eng. Appl. 7 (2016) 221-225.

137. P. A. Schweitzer, Paint and Coatings; Applications and Corrosion Resistance, CRC Press, Boca Raton, FL, USA, 2006, pp. 19-245.

138. S. Pilotek, F. Tabellion, Nanoparticles in coatings. Tailoring properties to applications. Eur. Coat. J. 4 (2005) 170+17

139. E. M. Petrie, Handbook of Adhesives and Sealants, McGraw-Hill, New York, NY, USA, 2000, pp. 49-89, 253-273.

140. M. A. Butt, A. Chughtai, J. Ahmad, R. Ahmad, U. Majeed, I. H. Khan, Theory of adhesion and its practical implications: A critical review, J. Fac. Eng. Technol. 15 (2008) 21-45.

141. A. Jarray, V. Gerbaud, M. Hémati, Prediction of solid–binder affinity in dry and aqueous systems: Work of adhesion approach vs. ideal tensile strength approach, Powder Technol. 271 (2015) 61-75.

142. American National Standards Institute, Test Procedure and Acceptance Criteria for Factory Applied Finish Coatings for Steel Doors and Frames, Steel Door Institute, USA, 2012.

143. H. L. Lee, Fundamentals of Adhesion, Springer Science & Business Media, Berlin, Germany, 2013, p. 14.

144. X. Shi, T. A. Nguyen, Z. Suo, Y. Liu, R. Avci, Effect of nanoparticles on the anticorrosion and mechanical properties of epoxy coating, Surf. Coat. Technol. 204 (2009) 237-245.

145. E. Barsoukov, J. R. Macdonald, Impedance Spectroscopy: Theory, Experiment, and Applications Wiley-Interscience, Hoboken, NJ, USA, 2005, pp. 129-205.

146. C. Moreno, S. Hernandez, J. J. Santana, J. Gonzalez-Guzman, R. M. Souto, S. Gonzalez, Characterization of water uptake by organic coatings used for the corrosion protection of steel as determined from capacitance measurements, Int. J. Electrochem. Sci. 7 (2012) 8444-8457.

147. X. F. Yang, C. Vang, D. E. Tallman, G. P. Bierwagen, S. G. Croll, S. Rohlik, Weathering degradation of a polyurethane coating, Polym. Degrad. Stab. 74 (2001) 341-351.

148. X. Yuan, Z. F. Yue, X. Chen, S. F. Wen, L. Li, T. Feng, EIS study of effective capacitance and water uptake behaviors of silicone-epoxy hybrid coatings on mild steel, Progr. Org. Coat. 86 (2015) 41-48.

149. F. Rezaei, F. Sharif, A. A. Sarabi, S. M. Kasiriha, M. Rahmanian, E. Akbarinezhad, Evaluating water transport through high solid polyurethane coating using the EIS method, J. Coat. Technol. Res. 7 (2010) 209-217.

150. D. Loveday, P. Peterson, B. Rodgers, Evaluation of organic coatings with electrochemical impedance spectroscopy Part 2: Application of EIS to coatings, JCT CoatingsTech. (2004) 88-93, http://www.consultrsr.net/files/jct/JCT200410.pdf (accessed on October 15, 2018)

151. J. Mojica, F. J. Rodriguez, E. Garcia-Ochoa, J. Genesca, Evaluation of thick industrial coating films by EIS and EN, Corr. Eng. Sci. Technol. 39 (2004) 131-136.

152. D. Loveday, P. Peterson, B. Rodgers, Evaluation of organic coatings with electrochemical impedance spectroscopy Protocols for testing Coatings with EIS, JCT CoatingsTech. (2004) 22-27, http://www.consultrsr.net/files/jct/JCT200502.pdf (accessed on October 15, 2018)

153. S. Shreepathi, S. M. Naik, M. R. Vattipalli, Water transportation through organic coatings: correlation between electrochemical impedance measurements, gravimetry, and water vapor permeability, J. Coat. Technol. Res. 9 (2012) 411-422.

154. R. Curbelo, Fourier Transformation and Sampling Theory, in Encyclopedia of Spectroscopy and Spectrometry, 3rd ed., J. C. Lindon, G. E. Tranter, D. W. Koppenaal, Elsevier, Amsterdam, the Netherlands, 2017, pp. 720-724.

155. A. Munajad, C. Subroto, Suwarno, Fourier transform infrared (FTIR) spectroscopy analysis of transformer paper in mineral oil-paper composite insulation under accelerated thermal aging, Energies 11 (2018) 364.

156. J. J. Ojeda, M. Dittrich, Fourier Transform Infrared Spectroscopy for Molecular Analysis of Microbial Cells, in Microbial Systems Biology, Methods and Protocols, A. Navid (ed.), Springer, Berlin, Germany, 2012, pp. 187-211.

157. C. W. Extrand, Work of Wetting Associated with the Spreading of Sessile Drops, in Contact Angle, Wettability and Adhesion, vol. 6 (K. L. Mittal, ed.), CRC Press, Boca Raton, FL, USA, 2009, pp. 81-94.

158. K. Y. Law, H. Zhao, Surface Wetting: Characterization, Contact Angle, and Fundamentals, Springer, Berlin, Germany, 2015, pp. 1-135.

159. S. Wu, Polymer Interface and Adhesion, CRC Press, Boca Raton, FL, USA, 1982, pp. 133-257.

7. List of Symbols and Abbreviations

7.1. List of symbols

a	Activity [-]
A	Area [cm^2]
C	Capacitance [nF cm^{-2}]
d	Distance between capacitor plates [cm]
d	Dispersion forces (as superscript)
E	Electrical potential [V]
E	Complex electrical potential [V]
$E°$	Standard potential [V]
E_m	Amplitude of the potential signal [V]
E_r	Reversible potential [V]
F	Faraday constant, 96485.33289(59) [C mol^{-1}]
f	Frequency [Hz]
I	Current response [A]
I	Complex current response [I]
I_m	Amplitude of the current signal [A]
j	Imaginary number, $(-1)^{0.5}$ [-]
n	number of electrons transferred per ion [-]
p	Partial pressure [bar]
p	Standard pressure [bar]
p	Polar forces (as superscript)
R	Gas constant, 8.314 [J K^{-1} mol^{-1}]
S	Spreading parameter [N m^{-1}]
T	Absolute temperature [K]

t	Time [s]
W	Work of adhesion [N m^{-1}]
W	Work of adhesion between solid metal and liquid coating [N m^{-1}]
$\mathbf{Z}$	Complex impedance [Ω cm^2]
Z''	Imaginary part of impedance [Ω cm^2]
Z'	Real part of impedance [Ω cm^2]
$_C$	Surface tension of the liquid coating [N m^{-1}]
$_L$	Surface tension of the liquid [N m^{-1}]
$_M$	Surface tension of the solid metal [N m^{-1}]
$_{MC}$	Interfacial energy between solid metal and liquid coating [N m^{-1}]
$_S$	Surface tension of the solid [N m^{-1}]
$_{SL}$	Interfacial energy between solid and liquid [N m^{-1}]
$_C$	Contact angle [°]
ε_0	Electrical permittivity of vaccum, 8.85410^{-14} [F cm^{-1}]
ε_r	Relative electrical permittivity [-]
	Impedance phase angle [rad]
	Water uptake [-]
ω	Angular frequency [rad s^{-1}]

7.2. List of abbreviations

AC	Alternating current
ADI	Aliphatic diisocyanates
AIBN	Azobisisobutyronitrile
AIDS	Acquired immune deficiency syndrome
ARC	Anti-reflective coating
ASTM	American Standard Test Method
BSE	Backscattered electrons
CE	Counter electrode
CIP	Coating inspector program
CPDP	Cyclic potentiodynamic polarization
DGEBA	Diglycidyl ether of bisphenol A
DGEBF	Diglycidyl ether of bisphenol F
DIN	Deutsche Institut für Normung
DTM	(Applying) directly to metal
EBSD	Diffracted backscatter detector
EDS	X-ray detector
EDX	Energy dispersive X-ray spectroscopy
EIS	Electrochemical impedance spectroscopy
EPMA	Electron probe microanalysis
FRA	Frequency response analyzer
FTIR	Fourier-transform infrared spectroscopy
HDI	Hexamethylene diisocyanate
HERT	Hydrogen evolution reaction tests
HIV	Human immunodeficiency virus
HMDI	Methylene dicyclohexyl diisocyanate (hydrogenated MDI)

IPDI	Isophorone diisocyanate
ISO	International Standard Organization
LEIS	Localized electrochemical impedance spectroscopy
LPR	Linear polarization resistance
MDI	Methylene diphenyl diisocyanate
MEK	Methyl ethyl ketone
MIBK	Methyl isobutyl ketone
MIO	Micaceous iron oxide
MOLSIV	Molecular sieve
MPA	Methoxy propyl acetate
NACE	National Association of Corrosion Engineers
OCA	Optical contact angle
OCP	Open circuit potential
PA	Polyaspartics
PDMS	poly dimethyl siloxane
PU	Polyurethane
RE	Reference electrode
Sa 2.5	Swedish sand blasting standard (Near white metal blast cleaning grade)
SCENIHR	Scientific Committee on Emerging and Newly Identified Health Risks
SE	Secondary electron
SECM	Scanning electrochemical microscope
SED	Secondary electron detector
SEM	Scanning electron microscopy
SIET	Scanning ion-selective electrode technique
SKP	Scanning Kelvin probe
TBT	Tributyltin

TWI	Training within industry
UV	Ultraviolet
UVA	Ultraviolet A
VOC	Volatile organic compounds [g/L]
WE	Working electrode
ZPA	zinc aluminum orthophosphate hydrate
ZRP	Zinc-rich paint

CURRICULUM VITAE (CV)

Arezoo Assarian [redacted] After completing the general gymnasium "Tazkiyyeh" in Arak, Iran, she enrolled in the Faculty of Applied Chemistry in Arak Azad University, in 1990 in Iran. She graduated in 1995 with the graduate thesis entitled "Analyzing of protective coatings properties and determination of their defects". She moved in Croatia in September 2007 and started studying in the Faculty of Chemical Engineering and Technology of the University of Zagreb in 2009 to obtain master degree in 2009 in the chemical engineering of materials. She graduated in 2012 with the master thesis entitled “Rheological evaluation of bitumen modified with Styrene Butadiene Styrene block copolymer". She enrolled the doctoral study program of engineering chemistry at the Faculty of Chemical Engineering and Technology of the University of Zagreb in October 2012 with the title of thesis “Development of polyaspartic coating with improved adhesion on metallic surfaces by using nanosilica”

.

She started working in Iranian paint and coating industries in October 1990 as a laboratory junior expert. She worked in Iran and UAE until 2007 as an expert in laboratory, coatings and corrosion inspector, product manager, project leader and protective coating formulator and consultant in different industries. Some of her key strengths include:

- ✓ Patent formulations in the field of nano smart coating for wood surfaces based on water and plastic surfaces based on solvent
- ✓ NACE certified coating inspector (CIP level 1 and 2, 38084) and TWI certified (CSWIP3.0, 68865)
- ✓ Significant technical expertise in the development of protective coatings based on acrylics, alkyd, fluoropolymers, polyaspartics
- ✓ Extensively experienced in coating and corrosion in the marine industry
- ✓ Skilled in utilizing quality control standards of ASTM, DIN, BS, ISO 9001
- ✓ Proven ability to successfully analyze and capture an organization’s critical business requirement and provide innovation and cost-effective services and solutions

Since 2007 until present, she has worked in Croatia as a protective coating and corrosion specialist in private companies.

All of these experiences are the result of her constant 22 years long activities in the paint and coating industry. During these years she has held the following positions in Iran, the United Arab Emirates and Croatia:

- Quality control laboratory expert
- Paint manufacturer
- Paint manufacture facility manager
- Paint manufacture facility manager for shipyard industry and oil platforms
- International technical coating and welding inspector

She has established an R&D laboratory in Croatia and she has conducted many research projects and formulated some improved coatings.

She is a member of NACE International and the Croatian Society for Materials Protection (HDZaMa).

The results of the research have been published as a paper in the journal Acta Chimica Slovenica: A. Assarian, S. Martinez, Improving polyaspartic anti-corrosion coating protective properties with the use of nanosilica, Acta Chim. Slov. 65 (2018) 569–577.

She has actively participated in several conferences with poster presentations VIII. , IX. and X. Meeting of Young Chemical Engineers in 2012, 2014 and 2016, respectively, in Zagreb, Croatia, the Seminar of Structural Materials and their Influence on Quality of Potable Water in 2012, in Zagreb, Croatia, 7th Croatian Meeting on Road Maintenance, in 2013 in Šibenik, Croatia, 28th International Conference on Surface Modification Technologies in 2014, in Tampere, Finland., and Eurocorr 2015, in Graz, Austria.